Improving patient selection for complex cardiac implantable electronic devices Pathophysiological insights, biomarkers and cost effectiveness

Claridge, Simon Braham Leo

Awarding institution:
King's College London

IMPROVING PATIENT SELECTION FOR COMPLEX CARDIAC IMPLANTABLE ELECTRONIC DEVICES:

PATHOPHYSIOLOGICAL INSIGHTS, BIOMARKERS AND COST EFFECTIVENESS

Simon Claridge

LLB (Hons), MBBS (Hons), MRCP (UK)

Department of Imaging Sciences & Biomedical Engineering

King's College London

This dissertation is submitted for the degree of Doctor of Philosophy

June 2018

Abstract

Cardiac resynchronisation Therapy Devices (CRT) and Implantable Cardioverter Defibrillators (ICDs) are routinely implanted in heart failure patients and patients at risk of ventricular arrhythmias (VA). Not all patients with CRT experience an improvement with symptoms and not all patients with an ICD receive an appropriate shock or therapy. Improved patient selection for these devices would be beneficial and is the focus of this thesis with my investigations focusing on the underlying pathophysiological mechanisms of dyssynchronous heart failure, potential novel imaging biomarkers to predict outcomes from complex cardiac devices and also an analysis of the cost-effectiveness implications of improved patient selection.

Recent research has suggested a role of improved coronary flow in patients who respond to CRT and also an improved haemodynamic response to left ventricular endocardial pacing. We performed a prospective clinical study to assess whether left ventricular endocardial pacing improved coronary flow and a further sub-study to investigate the relationship between coronary flow and acute contractility.

Our understanding of the role of myocardial fibrosis and scar in the pathogenesis of VA is evolving and it is now possible to assess both of these entities using cardiac magnetic resonance imaging (CMR). We performed a prospective study to determine whether CMR identification of fibrosis and scar could be used to predict VA in an ICD population specifically focusing of measures of myocardial fibrosis in patients with non-ischemic cardiomyopathy and measure of myocardial scar and peri-infarct heterogeneity (grayzone) in patients with ischemic cardiomyopathy. This study demonstrated for the first time that T1 mapping (a marker of fibrosis) was a specific

markers of risk in the non-ischemic group whereas grayzone predicted risk in the ischemic group.

Finally, I used published data to demonstrate the cost-effectiveness of a risk stratification tool which determines whether CRT defibrillator patients should be offered a further CRT defibrillator or a CRT pacemaker at the time of generator change.

Key words:

Endocardial pacing, coronary flow, cardiac resynchronisation therapy, defibrillator, T1 mapping, cost-effectiveness, NICE.

Table of Contents

Table of Figures

Table of Tables

Acknowledgements

I'd like to thank all the patients who took part in the studies presented in this thesis. For some studies the procedural burden was very high but in spite of this, so many patients were very willing to help and be involved with the studies- thank you.

I'd like to thank all the staff at GSTT and KCL who helped me to complete these studies and analyses, assisted in solving all sort of problems encountered during the three years and whose wide area of expertise led to me investigate aspects of complex device therapy I hadn't even been aware of at the start of the PhD project.

I would specifically like to thank Dr Zhong Chen, Dr Thomas Jackson, Dr Bradley Porter, Dr Jessica Webb, Dr Silvia Mennuni, Dr Christopher Rajkumar, Dr Gerald Carr-White, Dr Amedeo Chiribiri and Professor Reza Razavi. Gratitude and thanks to Professor Fritz Prinzen and Dr Uyen Nguyen- I look forward to further explorations of the relationship between CMR and VCG!

Enormous thanks to Professor Aldo Rinaldi for patiently putting up with me and being forever armed with a crack idea to move things forward.

Finally to my "wife"/ girlfriend/ partner, Emily in respect for her patience with this endeavour- I love you and thanks… again. Izzie, Hana, Ben and Ellie (who was born during this period of study), thanks for the numerous fun distractions! Lots of love x

Abbreviations

CRT	Cardiac Resynchronisation Therapy
CRTD	Cardiac Resynchronisation Therapy with a Defibrillator
CRTP	Cardiac Resynchronisation Therapy with a Pacemaker
ICD	Implantable Cardioverter Defibrillator
VA	Ventricular Arrhythymia
CMR	Cardiac Magnetic Resonance Imaging
LBBB	Left Bundle Branch Block
LVESV	Left Ventricular End Systolic Volume
LV	Left ventricle
RV	Right ventricle
LAD	Left Anterior Descending Artery
CFR	Coronary Flow reserve
VCG	Vectorcardiography
NCM	Non-ischemic cardiomyopathy
ICM	Ischemic cardiomyopathy
LGE	Late gadolinium enhancement
fQRS	Fragmented QRS

Chapter 1 Background

1.1 Cardiovascular disease and heart failure

Cardiovascular disease is the second most common cause of death in the United Kingdom (UK) accounting for over 150,000 deaths in 2015 with a total cost to the UK of >4,000,000,000 pounds per year.[1] Cardiovascular disease can manifest in many ways including coronary artery disease, cerebrovascular disease, valvular heart disease, electrophysiological abnormalities and intrinsic heart muscle problems.

The endpoint of many of these conditions is heart failure or "the heart failure syndrome". Heart failure can be described as a defect in heart function, which leads to a rise in atrial pressure leading to symptoms of breathlessness (if the left side of the heart is affected) or swelling in the legs and abdomen (if the right side of the heart is affected). Breathlessness is typically assessed using the New York Heart Association Classification (see Figure 1).

Figure 1- New York Heart Association Classification of Symptoms in Heart Failure (NYHA class)

Class I	No limitation on physical activity. Ordinary physical activity does not cause breathlessness fatigue or palpitations
Class II	Slight limitation of physical activity. Comfortable at rest but ordinary physical activity results in undue breathlessness,

	fatigue or palpitations
Class III	Marked limitation of physical activity. Comfortable at rest but less than ordinary physical activity results in undue breathlessness, fatigue or palpitations
Class IV	Unable to carry on physical activity without discomfort. Symptoms at rest can be present. If any physical activity is undertaken, discomfort is increased.

The syndrome can be further classified into patients with a reduction in the left ventricular pumping function of the heart- Heart failure with reduced ejection fraction-"HF-REF" and patients with preserved contraction but in whom increased pressures are required to fill the left ventricle- Heart failure with preserved ejection fraction- "HF-PEF".

It is estimated that over 900,000 people in the UK suffer from heart failure.[2] With optimum treatment, the annual mortality from HF-REF is estimated to be in the region of 5-10%.[2] Targets for the treatment of heart failure have been identified as our understanding of the pathophysiology has evolved with ACE inhibitors, aldosterone receptor antagonists, cardioselective betablockers, If channel blockers and most recently neprilysin inhibitors all forming part of an evidence-based medical armamentarium used for the treatment of patients with HF-REF (see Figure 2). [3-7]

Figure 2- Pathophysiology of heart failure and targets for medical therapy

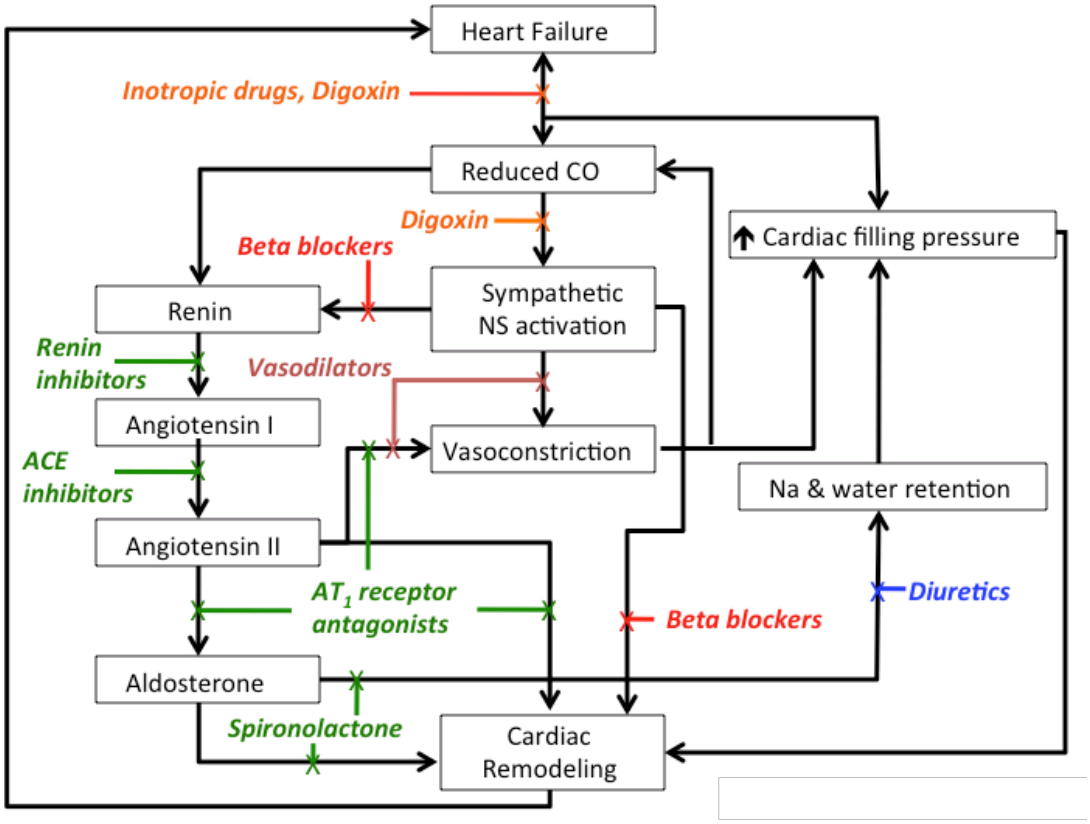

Despite the undoubted role these medications play in improving mortality and morbidity in HF-REF patients, there remains significant mortality associated with the heart failure syndrome. The two commonest modes of death are sudden cardiac death as a result of ventricular arrhythmia (VA)) and chronic cardiogenic shock as a result of pump failure. Alongside, this evolution in medical therapy for HF-REF, two medical devices have been developed in the last 30 years which have also demonstrated mortality benefits, targeting the risk of sudden death and pump failure separately although they are often prescribed together in patients and can be implanted in a single device. The two devices are Implantable Cardioverter Defibrillators (ICDs) and Cardiac Resynchronisation Therapy (CRT).

1.1.1 Development of CRT and evidence base

Heart failure patients particularly those with HFREF often have abnormal electrical activation of the heart. This can manifest as atrial arrhythmias such as atrial fibrillation and atrial flutter, conduction abnormalities across the atrio-ventricular node, ventricular ectopy and ventricular dyssynchrony. Each of these abnormalities has the potential to cause unco-ordinated contraction of the heart resulting in impaired cardiac output and worsening heart failure. This reduced cardiac output results in upregulation of neurohumoral activation, adverse remodelling and creates a vicious, downward spiralling circle.

Ventricular dyssynchrony specifically results in the contraction of different parts of the ventricle at different times, typically resulting in the prolongation of electrical activation across the ventricle to >120ms. Three typical forms of ventricular dyssynchrony are described, left bundle branch block (LBBB), right bundle branch block (RBBB) and non-specific interventricular conduction defects. This delay represents a potential target for therapy with the aim being to reduce electrical activation of the ventricles back to normal by stimulating the ventricles from different sites simultaneously. This was first attempted acutely by Cazeau et al and chronically by Daubert et al in 1998 who succeeded in obtaining permanent biventricular pacing in 35 patients using a normal right ventricular lead placed in the right ventricular endocardium and a left ventricular lead placed via the coronary sinus into a branch of the left sided coronary venous system. [8,9] From these first experimental uses, there have now been several large randomised controlled trials that have shown CRT reduces mortality in HFREF patients of different NYHA classes and is now

considered a standard treatment offered to patients with heart failure and abnormal electrical ventricular activation. [10,11]

1.1.2 CRT outcomes and non-response

Despite the positive results of the CRT trials, it was clear that not all patients in the study populations benefitted from CRT implantation.

With regard to those patients who did not seem to improve with CRT, the term 'non-responder' was coined which in turn led to a large volume of research into how to select likely non-responders prior to implant and how to turn non-responders into responders. The definition of response varies with some authors referring to an improvement in NYHA symptoms, others to a >15% reduction in Left Ventricular End Systolic Volume and others using a combination of these criteria or variations of these metrics. A reduction in LVESV has been shown to better predict long term outcome following CRT than reported changes in symptoms and is the metric used to determine response in this thesis.[12]

1.1.2.1 Selecting likely responders to CRT in advance

Research initially focused on whether advanced imaging (specifically transthoracic echocardiography measures) might be able to help predict responders to CRT and small, single centre studies initially suggested that echocardiography may be able to select patients with mechanical dyssynchrony who might better respond to CRT. [13-16]. Disappointingly however, the TARGET trial demonstrated that when these indices were examined in a large multi-centre cohort then the previously achieved results were not reproducible. [17,18]

This disappointment led in turn to further investigation of the pathophysiological effects of dyssynchronous heart failure and the physiological effects of CRT. It became clear that dyssynchronous heart failure led to changes in coronary flow, metabolism and even gene expression and that CRT had the potential to reverse some of these changes (see Figure 3).[19-22]

Figure 3- The vicious circle of dyssynchronous heart failure[23]

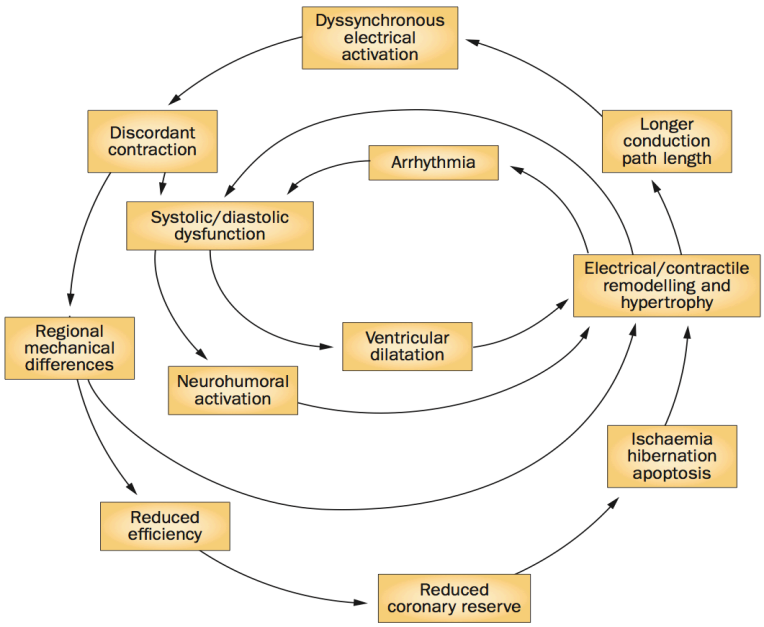

1.1.2.2 Turning non-responders into responders

Whilst it is evident that some patients do not get better with CRT, as noted above, the definition of non-response is variable and thus the proportion of patients who do not respond to CRT varies depending upon the definition employed. When using quality of life assessment scores the non-response rate has been shown to be approximately

30-35% whereas when a harder endpoint such as reduction in left ventricular end systolic volume >15% has been used as the measure the number of non-responders is nearer 50%.[24-26] Regardless of the definition used, the cohort of patients who do not benefit from CRT represents at least a significant minority of those who are implanted with the device. This has lead to the development of literature assessing the reasons for poor outcomes in CRT and suggested strategies for optimising non-responders (see **Error! Reference source not found.**).[27]

Figure 4- Reasons for "non-response" to CRT[27]

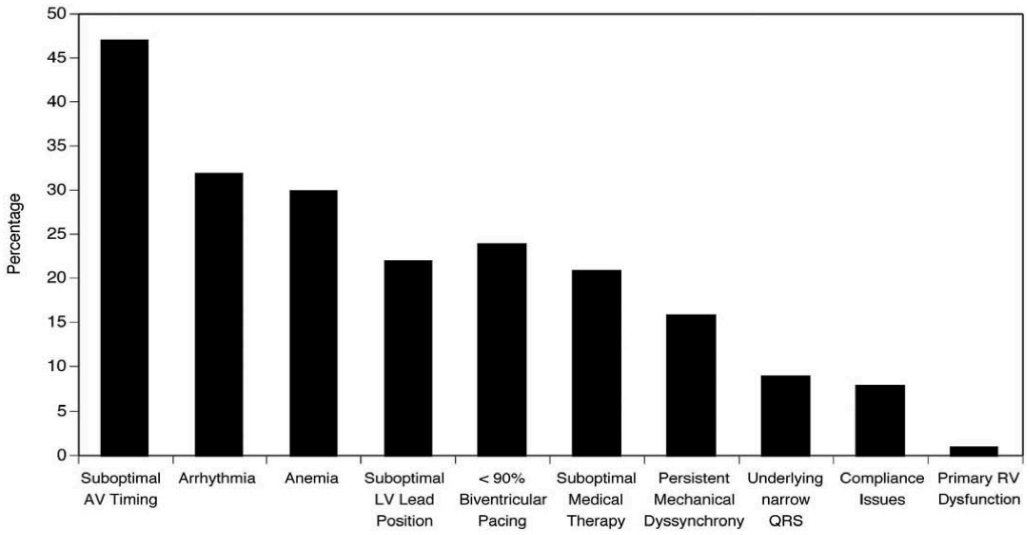

1.1.2.3 Left ventricular endocardial pacing

The identification of patients who fare poorly with CRT particularly those who may have either a “suboptimal lead position” as noted in **Error! Reference source not found.** has led investigators to consider different ways to deliver CRT in patients who are not responding.

Potential strategies that have been attempted include stimulation from several points in the ventricle –"multi site pacing" and pacing from inside the left ventricle rather than from the epicardial coronary veins – "endocardial" pacing. [28,29] Endocardial pacing is particularly attractive in that theoretically the left ventricular lead position is not constrained by the coronary venous anatomy allowing access to the latest activating segment of the heart, avoidance of myocardial scar and theoretical early access to the Purkinje network.[30,31] Acute improvements of ventricular function have been demonstrated with endocardial pacing over and above standard CRT and a large case series has reported positive findings in non-responders and patients in whom implantation of a conventional LV lead proved impossible.[29,32] Nonetheless the mechanism by which endocardial pacing exerts its apparent benefits is unclear.

1.1.3 Changes in coronary flow and perfusion with CRT

As noted above, this failure to easily identify non-responders has led to increasing interest in the pathophysiological mechanisms that underlie electrical and mechanical dyssynchrony in heart failure. One aspect of this has been a renewal in interest in the importance of myocardial perfusion to CRT response and its relationship with any concomitant metabolic abnormalities. Previous studies suggested CRT offered an increase in global contractility without an increase in overall myocardial work or oxygen consumption.[33] However a recent study has suggested that myocardial oxygen consumption does increase with CRT but that the corresponding increase in contractility is relatively much greater resulting in an improvement in overall myocardial efficiency. [34] Furthermore, experimental work in the canine model suggests that response to CRT is dependent on a minimal myocardial perfusion.

[35]Perfusion below this threshold, which lies within pathophysiological levels seen in the clinical setting, seems to preclude a favourable response to CRT.

Thus, the role of myocardial perfusion in CRT appears to be a relevant area of inquiry and one of the elements that needs to be understood in the search for accurate criteria to predict CRT response. Furthermore increasingly accurate descriptions of metabolic changes associated with heart failure and electromechanical dyssynchrony are beginning to show promise in the prediction of non-response.

1.1.3.1 Effect of ventricular dyssynchrony on myocardial perfusion and coronary flow

There has been a wealth of research into the assessment of the coronary circulation and myocardial perfusion in patients with LBBB. [36] This is due to the particularly marked positive response of these patients to CRT and also the significant historical interest in "false positive" non-invasive tests for inducible ischaemia in this cohort. LBBB represents a delay in electrical and accordingly mechanical activation of the left ventricle resulting in inter- and intraventricular dyssynchrony.

Early work by Delhaas et al in a canine model paced from different ventricular sites, demonstrated significantly reduced regional oxygen uptake and regional blood flow in early activated areas of myocardium compared with late activated areas. [37] This was refined in a canine model, where septal hypoperfusion was linked with a reduction in the systolic circumferential shortening following left bundle branch ablation.[38] The model also demonstrated an increase in myocardial blood flow to the lateral wall in conjunction with an increase in systolic circumferential shortening in that region.

These findings suggest that the reduction in myocardial blood flow to the septum may be a result of reduced septal workload and conversely that the increase in myocardial blood flow to the lateral wall is a result of an increased workload. Such findings suggest a physiological rather than pathological response. Further work by Vernooy et al demonstrated that these regional differences in myocardial bloodflow disappeared following the application of CRT.[39]

Studies that assessed the effects of ventricular electromechanical dyssynchrony on myocardial perfusion and metabolism in man have largely obtained data from nuclear imaging. Initial investigation of patients with LBBB suggested that there was relative hypoperfusion in the septum compared with the lateral wall of the left ventricle even in patients with normal coronary arteries and these findings have been replicated on many occasions. [40,41]

More recent quantitative research by Koefli et al has demonstrated an increase in global myocardial blood flow during rest and exercise in presumed non-ischaemic patients with LBBB when compared with patients without electrical dyssynchrony. [42] This increase in myocardial perfusion, particularly in the lateral wall during exercise, accords more with Delhaas' and Vernooy's findings in the canine model and may be a reflection of increased myocardial oxygen demand due to inefficient cardiac mechano-energetics induced by dyssynchronous electrical activation. The rationale for this is that, in a normal LV, all myocardial segments are activated almost simultaneously and contract synchronously. This results in both septal and lateral annuli being pulled towards the stationary LV apex. However, in LBBB, the septum is activated first and while it is developing a contractile force and shortening, the contralateral wall is passive. This exerts a pulling effect on the latent opposite wall.

The combination of unloaded contraction of the septum, stretching the lateral wall, followed by delayed lateral wall contraction, which then stretches the septum, leads to an overall greater workload, particularly for the lateral wall. This is reversed when CRT is applied resulting in homogenisation of work across the ventricle.

Koepfli's study also demonstrated reversible relative hyperperfusion in the lateral wall of patients with reversible LV dyssynchrony during right ventricular (RV) pacing compared with their intrinsic rhythm. Thus rather than LBBB causing septal hypoperfusion it is possible that LBBB causes lateral wall hyperperfusion.

Koepfli studied "spontaneous" LBBB patients and makes no reference to the patients' LV systolic function. This limits extrapolation of these findings to the CRT heart failure population. For patients who have developed LV impairment as a result of chronically high percentages of right ventricular pacing are likely to have undergone cellular and metabolic changes not found in those with LBBB without heart failure.[43] Indeed, longer term RV apical pacing has been shown to result in myocardial perfusion defects in variable locations within the ventricle. [44]The incidence and size of these perfusion defects increases with time. They are associated with apical wall motion abnormalities and a reduction in left ventricular ejection fraction.

Koepfli's work is alone in studies on man suggesting that there is lateral wall hyperperfusion rather than septal hypoperfusion. In spite of the above criticisms, this quantitative assessment of both coronary flow and myocardial perfusion suggesting lateral wall hyperperfusion on exertion offers a different explanation to the septal hypoperfusion hypothesis examined above.

The theory that dyssynchrony may alter regional myocardial work is supported by Masci et al. who found using Positron Emission Tomography (PET) that patients with LBBB and reduced ejection fraction had a higher myocardial glucose metabolism in the lateral wall compared with the septum when compared with a group of non-dyssynchronous patients with non-ischaemic cardiomyopathy.[45] This suggests that a heterogeneous shift in the LV regional workload due to dyssynchrony results in alterations in the regional myocardial metabolic demand. The extra metabolic load as a result of dyssynchronous LV contraction can in theory lead to higher demand on global myocardial perfusion. However, Masci found no consistent changes in myocardial perfusion to either confirm or refute this theory.

Skalidis et al. demonstrated, in an invasive setting, that the time to maximum peak diastolic flow velocity was significantly longer in the left anterior descending (LAD) coronary artery of patients with LBBB and perfusion defects compared with normal subjects. [46] This observation coupled with the associated reduction in coronary flow reserve (CFR) suggests that dyssynchrony can have a deleterious effect on the myocardial microvascular circulation. Interestingly, Koepfli also noted a reduction in the CFR in the septum of patients with LBBB. Skalidis et al postulated that an increase in early diastolic compressive resistance resulting from delayed ventricular relaxation in LV dyssynchrony resulted in an impairment of early diastolic blood flow in the LAD. The authors further demonstrated that CFR was similarly reduced in patients with LBBB induced by RV pacing. [47]This impairment of CFR seems to suggest that septal perfusion defects are not a physiological response to reduced demand but a pathophysiological adaptation.

Most recently Ogano et al have demonstrated in a non-ischaemic group of patients the presence of septal perfusion defects in 19/26 patients with LBBB. [41] Following the implant of a biventricular pacemaker, an improvement in the septal perfusion defect correlated with a reduction in left ventricular end systolic volume.

As noted above, much of the perfusion data is taken from semi-quantitative analysis of SPECT. This technique assumes that there is equal systolic wall thickening across the ventricle; however in LBBB there is reduced septal systolic wall thickening. This means that SPECT assessment of septal perfusion in LBBB should be interpreted cautiously as there is the risk of partial-volume effects mimicking hypoperfused myocardium. Nowak et al demonstrated this elegantly, comparing Single Photon Emission Computed Tomography (SPECT) with Positron Emission Tomography (PET) perfusion of LBBB patients.[48] They found that the corrected myocardial blood flow using PET was homogenous across the LBBB ventricle compared with the heterogenous perfusion found using SPECT. Of note, the heterogeneities tended to show septal hypoperfusion.

It is tempting to suggest that all the noted perfusion defects in LBBB are the result of this issue. However, soon after Nowak's study had been published, Vernooy et al reported experimental data using a canine model that had undergone LBBB ablation. Using microspheres, (the gold standard of perfusion quantification), the group demonstrated a 17 +/- 16% reduction in septal myocardial blood flow and a 18 +/- 12% increase in the lateral wall myocardial blood flow from baseline. This shift in blood flow was reversed following the application of CRT.

These data suggest that dyssynchronous electrical activation leads to altered coronary flow patterns and subsequent changes in perfusion and metabolism which may be deleterious to cardiac function. It is however unclear whether the well described heterogeneity in perfusion reflects hypoperfusion of the septum or hyperperfusion of the lateral wall (see Table 1). This assessment is further complicated by the possibility that the assumptions of SPECT imaging render it a poor modality to assess perfusion in LBBB patients (see Figure 5). It is suggested that the well-described reduction in CFR in the septum in man as noted by Skalidis et al reflects a pathological rather than physiological down regulation of septal coronary flow as one would expect a physiological adaptation to be overcome with the administration of adenosine. [46]

Table 1- Summary of studies investigating blood flow and perfusion with dyssynchronous heart failure

	N=	Study model	Method	FDG uptake	Global MBF	Regional MBF	MBFR	CFV/ CFR
Masci[13] **(2010)**	18	NICM: LBBB (11) vs non-LBBB (8)	CMR/ PET	Inhomogenous in LBBB-highest in lateral wall	Same in both groups	No clear pattern in either group	Same in both groups	N/A
Koepfli[10] **(2009)**	30	(10) LBBB vs (10) RV pacing (on and off) vs (10) healthy controls	PET	N/A	LBBB- global increased perfusion than controls at rest and with exercise	LBBB- increased throughout but particularly lateral wall hyperfusion with exercise. Similar reversible lateral hyperperfusion with RV pacing on	No obvious shift from septum to lateral wall with adenosine	No difference except reduced CFR to septum with RV pacing on vs off
Skalidis[14] **(1999)**	24	NICM (LBBB) (Group 1: 6pt ; Group 2: 7pt) vs Control group (11)	Thallium stress and Cardiac cath	N/A	Group 1: Septal reversible perfusion defect on exercise Group 2: No LAD distribution perfusion defects Control Group: NAD	N/A	N/A	Time to diastolic Vmax > in Group 1 than Group 2 and controls Group 1 lower CFR < Group 2 < Control group
Skalidis[15] **(2001)**	22	RV paced (14) vs Control (8)	Thallium stress and Cardiac cath	N/A	7/14 showed perfusion defects	Non-specific alerations in myocardial perfusion	N/A	CFV lower in paced patients. If perfusion defect, further reduction in CFR
Nielsen	30	AAI (15) vs	PET	N/A	DDD pacing	DDD pacing	N/A	N/A

(2000)		DDD (15)			reduced compared with AAI	reduced septal and inferior flow		

The above table summarises the findings of the key studies investigating myocardial perfusion and coronary physiology in CRT patients.

Abbreviations: CFR- coronary flow reserve, CFV- coronary flow velocity, CMR- cardiac magnetic resonance imaging, ICM- ischaemic cardiomyopathy, Inv,- Invasive study, MBF- myocardial blood flow, MBFR- myocardial blood flow reserve, NICM- non-ischaemic cardiomyopathy, N/A- not applicable

Figure 5- Panel A demonstrates SPECT imaging of LBBB. Panel B shows changes after 6 months of CRT

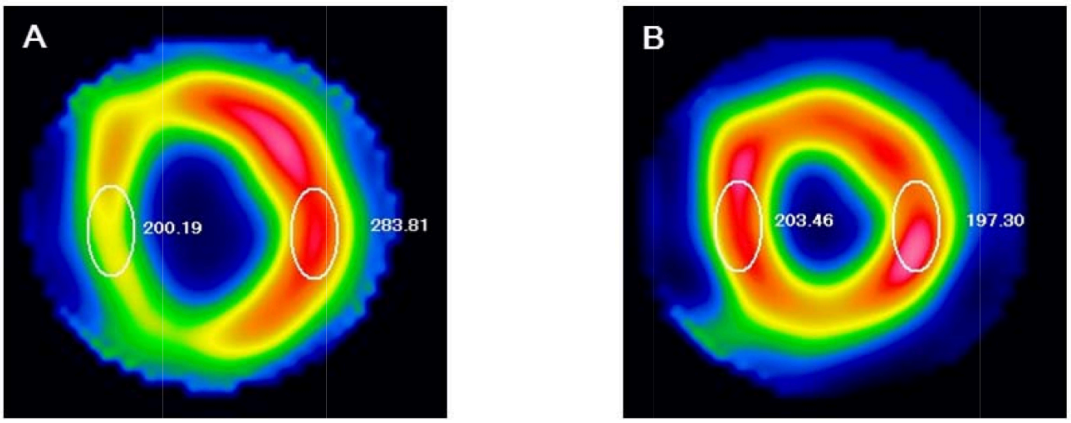

1.1.3.2 Effect of CRT on coronary flow and myocardial perfusion

CRT achieves "resynchronisation" via atrial coordinated synchronised pacing of the right and left ventricles. The LV lead is usually placed via the coronary sinus in either a lateral or posterolateral coronary vein.

Studies using PET to assess myocardial perfusion suggest that CRT does not increase global resting myocardial blood flow. [49-52] It may however result in regional changes in myocardial perfusion and oxygen demand. [41,53,54] These changes manifest as a reduction in myocardial oxygen demand and perfusion to the lateral wall with an equivalent increase in these indices in the septum with CRT. However, such regional changes in perfusion in response to CRT have not been shown consistently.[48] Further to this, it is unclear whether the homogenisation of blood flow to the septum and away from the lateral wall represents the correction of pathophysiological changes in coronary flow or simply a physiological response to the fact that the septum works harder and the lateral wall less hard once CRT is applied. The difficulty in comparing the many studies referenced above is a result of the small number of patients studied in each protocol and the different experimental designs (see Table 2).

Table 2- Summary of studies assessing the effect of CRT on coronary bloodflow, myocardial perfusion and metabolism

CRT	N=	ICM/ NCM	Method	Change in global oxidative metab.	Change in global MBF	Change in regional MBF	Change in regional oxidative metab.	Change in MBF with stress (MBFR)	CFV/ CFVR	Change in FDG uptake	Comments
Sundell[16] (2004)	10	0/10	PET	No change	No change	N/A	N/A	No change	N/A	N/A	8 months post implant
Neri[17] (2003)	8	0/8	PET	N/A	No change	No change	N/A	N/A	N/A	Homogenisation of FDG uptake	Pre and 3 weeks post implant
Nielsen[18] (2002)	14	7/14	PET	N/A	No change	No change	N/A	N/A	N/A	N/A	Comparison of acute pacing changes 13months after implant
Nowak[19 27] (2002 & 2004)	14	0/14	PET	No change	No change	No change	No change	N/A	N/A	Homogenisation of FDG uptake	PET pre CRT and 2 weeks later
Lindner[20] (2005)	42	11/42	PET	No change	No change	NICM: increase septum, reduce lateral wall. ICM: similar trend	NICM: increase septum, reduce lateral wall ICM: similar trend	N/a	N/A	N/A	All acute responders. PET performed at pre and 4 months post implant
Fang[23] (2012)	29	0/29	Echo	N/A	N/A	N/A	N/A	N/A	⇧ CFV	N/A	Responders post implant (mean 28 months)
Knaapen[21] (2004)	14	0/14	PET	N/A	No change	Homogenises Lateral wall to septum	N/A	Increased	N/A	N/A	Pre and 3 months post CRT insertion
Kyriacou[25] (2012)	10	3/10	Inv	N/A	N/A	N/A	N/A	N/A	⇧ CFV	N/A	Associated with increase in backward decompression (suction) wave
Defteros[24] (2010)	20	20/20	Inv	N/A	N/A	N/A	N/A	N/A	⇧ CFV	N/A	Increase noted in responders
Ukkonen[26] (2003)	8	6/8	PET	No change	N/A	N/A	Increased in septum	N/A	N/A	N/A	Acute study following Chronic implant
Ogano[9] (2014)	26	0/26	SPECT	N/A	N/A	Septal perfusion defect reversed	N/A	N/A	N/A	N/A	SPECT pre implant and at 6 Months

CFR- coronary flow reserve, CFV- coronary flow velocity, CMR- cardiac magnetic resonance

imaging, ICM- ischaemic cardiomyopathy, Inv,- Invasive study, MBF- myocardial blood flow, MBFR- myocardial blood flow reserve, NCM- non-ischaemic cardiomyopathy

Studies using transthoracic Doppler echocardiography demonstrated an increase in LAD flow during resynchronisation pacing and were replicated by Fang et al who demonstrated increased regional LAD flow in responders to CRT when paced biventricularly compared with RV pacing or their intrinsic rhythm. [54,55]Fang also replicated Skalidis' finding of attenuation of the LAD diastolic flow during dyssynchrony and further showed that the LAD flow was corrected during acute resynchronisation.

The effect of CRT, on the microvascular circulation measured by myocardial flow reserve or coronary flow reserve (in the absence of epicardial artery stenoses) is unclear. Using PET, Knaapen et al. demonstrated a significant increase in the myocardial flow reserve with CRT however Sundell et al demonstrated no change in the flow reserve. [53,56] This divergence may be partly explained by the different patient population in the studies. In Knaapen's study, 7 out 16 patients had ischaemic cardiomyopathy whereas the study of Sundell included a majority of patients with non-ischaemic dilated cardiomyopathy. Also, Sundell studied acute changes in blood flow in different pacing regimens in chronically implanted CRT patients as opposed to Knaapen who compared changes in blood flow before and after 3 months of CRT.

There is limited invasive data available assessing the acute effect of CRT on coronary flow. Nelson et al detected a non-significant reduction in coronary flow despite improved systolic function with CRT although this measure was not controlled for different heart rates. [33] Nelson observed that an improvement in systolic function occurred with a reduction in myocardial oxygen consumption. Conversely, during

administration of dobutamine to improve left ventricular contractility to the same extent as CRT, a significant increase in myocardial oxygen demand and extraction was seen. These findings provided a biologically plausible explanation to both the success of CRT as a treatment and the failure of positively inotropic agents to improve outcomes in heart failure patients.

The findings of this study have recently been refined by Kyriacou et al who compared the LV pressure generated in intrinsic LBBB with biventricular pacing at various atrio-ventricular timings.[34] The authors found that biventricular pacing actually increased myocardial oxygen consumption but that the concomitant increase in cardiac work was proportionately 80% greater; thus there was greater myocardial efficiency. Of note, Kyriacou's study had a mix of patients with an ischaemic and non-ischaemic substrate whereas Nelson's subjects were all non-ischaemic. Furthermore, Nelson allowed patients' heart rate to vary and then corrected for the variation between intrinsic rhythm and biventricular pacing. This has the advantage of being more physiological than atrial pacing above the sinus rate as biventricular pacing effects sympathetic activity and thus heart rate. In contrast Kyriacou paced patients at 100bpm avoiding the need for post hoc correction of the data, thus allowing "per beat" assessment of myocardial oxygen consumption.

The finding that CRT may increase myocardial oxygen consumption has important mechanistic and clinical ramifications implying that response to CRT relies, at least in part, on there being a means by which oxygen delivery can be increased or more efficiently extracted. This accords with recent work in a canine model in which biventricular pacing was unable to acutely increase LV contractility at lower coronary perfusion rates suggesting there is a minimum perfusion rate required to obtain an increase in contractility. [35]This threshold was within the pathophysiological range

found in vivo. The improvement in LV contractility above the threshold was however independent of any increases in regional coronary flow observed with biventricular pacing.

Deftereos et al. found that in patients with ischaemic cardiomyopathy, CRT is associated with higher CFRs when compared with RV pacing alone. [57]Interestingly, this improvement in CFR was almost exclusively observed in responders to CRT. This result coupled with previously noted observations by Skalidis implicates the microvascular circulation in the deleterious effect of LV dyssynchrony and supports the hypothesis that CRT may be able to reverse this.

It is therefore unclear whether the well-described changes in blood flow in response to CRT relate to changes in perfusion per se or merely represent the mechanical sequelae of restoration of a more physiological activation pattern. Wave intensity analysis of simultaneously acquired coronary flow and pressure may provide further insights into the effects of CRT on coronary blood flow and the relationship between coronary blood flow and the haemodynamic effects of CRT.

1.1.4 Wave intensity analysis

1.1.4.1 Background

Wave intensity analysis is an area of physics that first developed in the field of gas dynamics and jet engines after the Second World War. It has subsequently been successfully applied to the cardiovascular system to describe the energies that determine blood flow in the human body.[58,59]

1.1.4.2 Breaking down waves into constituent components

For the purpose of wave intensity calculations, arteries are treated as 1 dimensional long thin tubes. Wave intensity assumes laminar flow across the entire cross-section of the artery and is ill-suited for assessment of sections of the artery with unequal or pathological wall stress such as arterial bifurcations or areas of stenosis or occlusion.

Generally, waves have been by described by use of a Fourier decomposition which treats the measured waveform as the summation of many different waves at different frequencies and amplitudes. This is excellently demonstrated in Figure 6 by Parker et al taken from the website. (www.bg.ic.ac.uk/research/k.parker/wave_intensity_web)[60]

Figure 6- Fourier decomposition of aortic pressure waveform

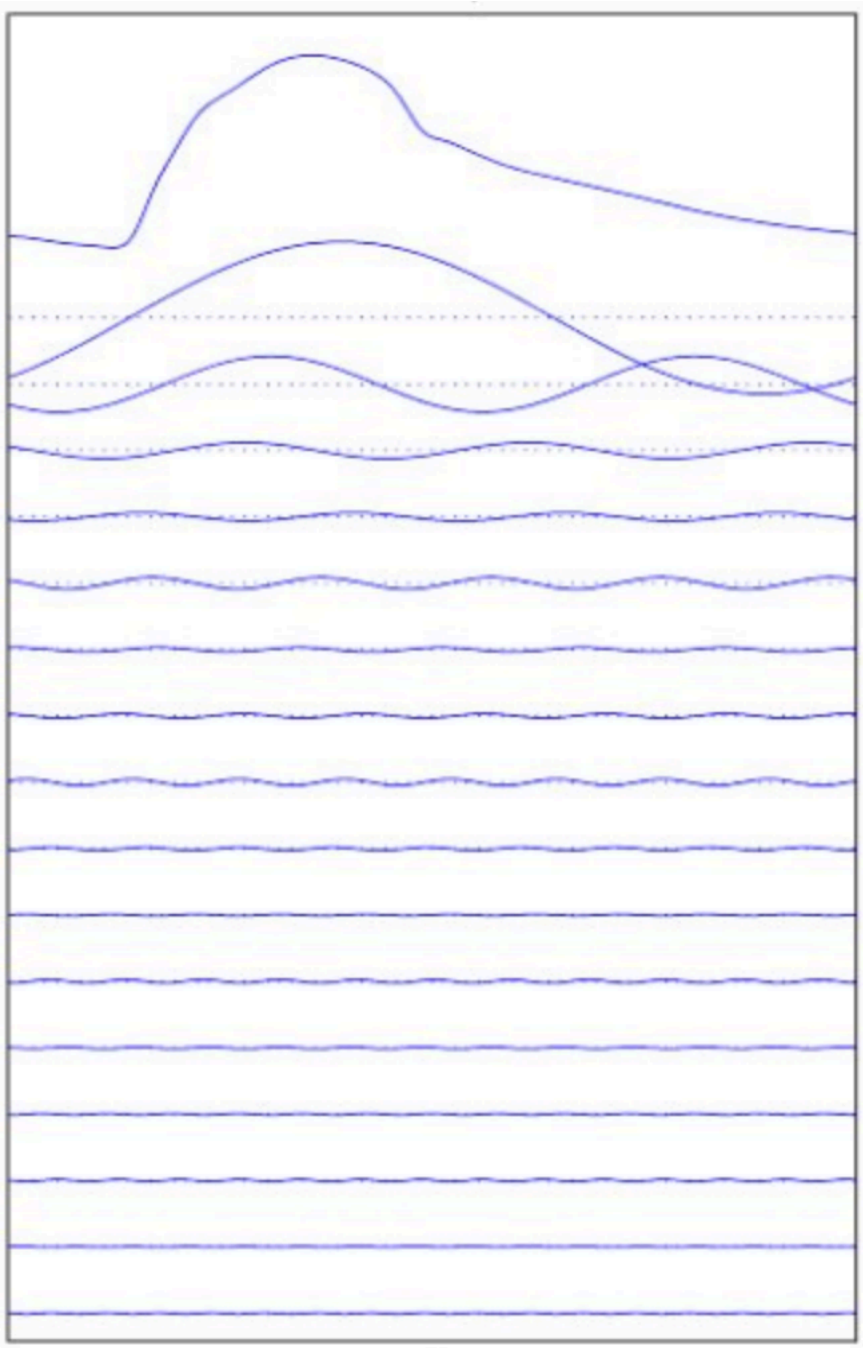

The top blue waveform is the aortic pressure waveform. The subsequent blue lines represent the different amplitude and frequency that superimpose to describe the aortic waveform. Note this is only one of infinite ways to describe a waveform using the Fourier decomposition.

As can be clearly appreciated, the sinusoidal waveforms gives very little in the way of time sensitive information which is critical to the analysis of events occurring during a single heartbeat. As a result of this, wave intensity analysis calculations are described as successive wavefronts rather than as the sum of different repetitive sinusoidal wavefronts. This allows clearer timing of events that summate to form the measured waveform and is limited only by one's ability to measure changes in the wave form in the time domain ie the temporal resolution (see Figure 7).

Wave intensity is defined as

$$dI = dP.\, dU$$

where dP is the change in pressure across a wavefront and dU is the change in velocity across a wavefront.. The unit of wave intensity is thus W/m^2

As a result of this, if waves are forward travelling they will have a positive sign whereas backward travelling will have a negative sign. This makes it simple to determine both the direction of travel of a wave and also easy to determine the dominant wave at any given time point.

Figure 7- Successive wavefront decomposition of aortic pressure waveform

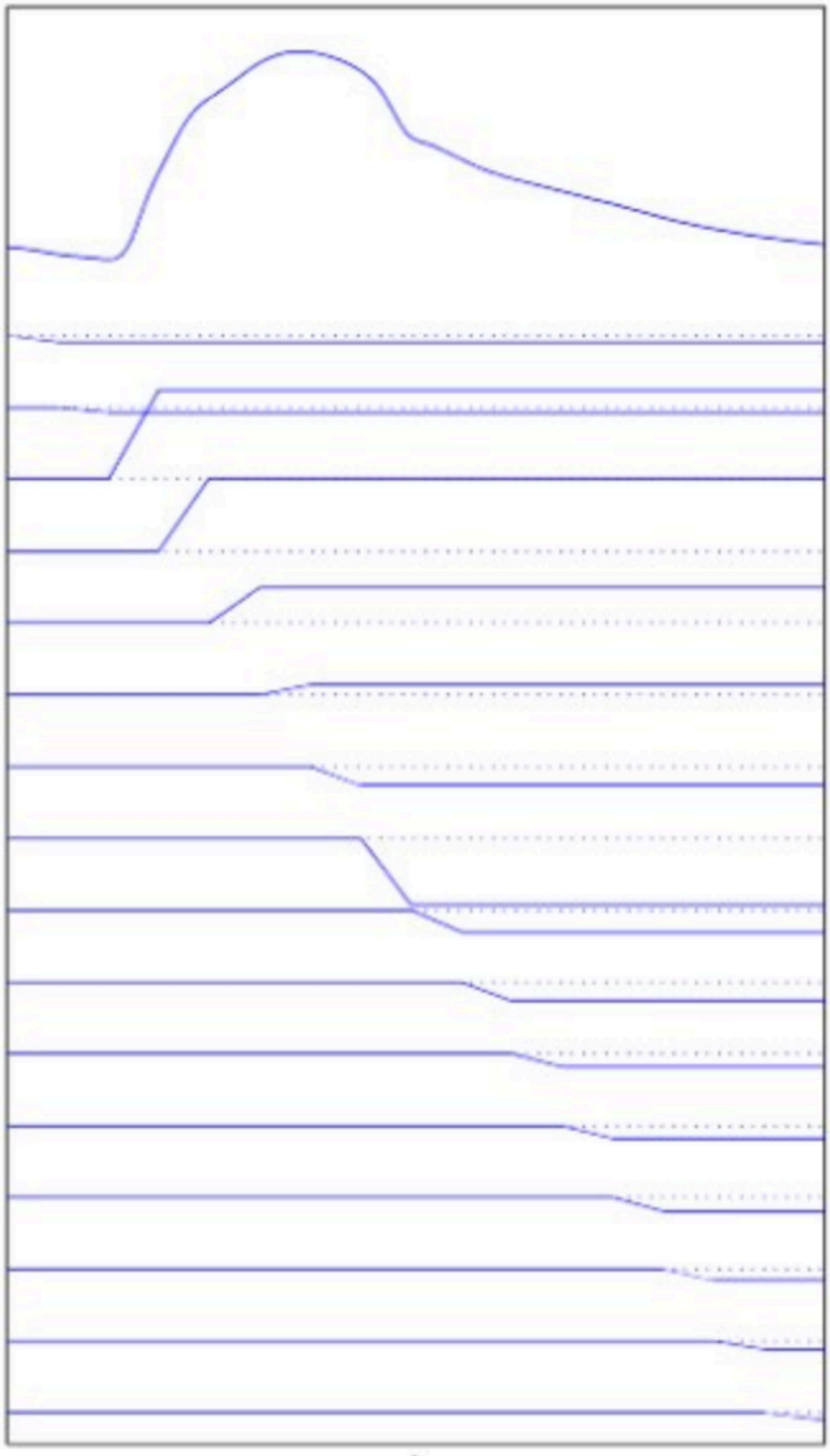

1.1.4.3 The relationship between dP and dU

Changes in pressure and velocity are not independent of each other and this needs to be incorporated into wave intensity calculations in the cardiovascular system. Thus by using the water hammer equations, incorporating a measure of blood density and estimating wave speed, forward waves can be calculated using the equation:

$$WI_{+} = \frac{1}{4\rho c}\left(\frac{dP}{dt} + \rho c\frac{dU}{dt}\right)^{2}$$

and backward waves can be calculated using a similar equation:

$$WI_{-} = -\frac{1}{4\rho c}\left(\frac{dP}{dt} + \rho c\frac{dU}{dt}\right)^{2}$$

where ρ is the density of blood and c is the wave speed. A full description of the mathematical underpinning of these equations to express wave energies in the human body can be found at www.bg.ic.ac.uk/research/k.parker/wave_intensity_web

1.1.4.4 The sum of squares method to calculate wave speed

Wave speed is calculated using the measured pressure and velocity waveforms. The main assumption for wave intensity calculation and derived waves is the single point measure of local wave speed. This is calculated using the sum of squares method.[61] This method of determining wave speed springs from the observation that using the incorrect speed results can result in wave intensities that either cancel each other out or that results in an overestimation of wave intensity (both backwards and forwards).[60,61]

It is therefore necessary to find the value of **c** that results in the least wave intensity across a cardiac cycle.

The sum of squares equation used to calculate the single point estimate for wave speed (c):

$$c = \frac{1}{\rho}\sqrt{\frac{\sum dP^2}{\sum dU^2}}$$

1.1.4.5 Wave intensity analysis in the coronary arteries

Cardiac catheters have been developed which allow simultaneous acquisition of both pressure and flow data. Using the equations above, it has therefore been possible to perform wave intensity analysis on coronary artery data using the sum of squares method to estimate the wave speed.

Wave intensity analysis of coronary flow and pressure has shown coronary blood flow to be dependent upon up to 6 waves within the cardiac cycle (see Figure 8). Typically however, four waves are identified: Forward Compression Wave (FCW), Backward Expansion Wave (BEW), Forward expansion wave (FEW) and Backward Compression Wave (BCW). The FCW and BEW are the largest and most reproducible.[62] The FCW and BCW both occur in systole. The FCW is supposedly derived from LV contraction with the FCW pushing blood down the coronary artery via the aorta. The genesis of the BCW is controversial but an intramyocardial increase in pressure compressing the microvasculature during systole is often cited as the

origin. [63-65] With regard to diastole, the BEW is generated by relaxation of the ventricle resulting in suction of blood down the coronary arteries towards the microvasculature whereas the small FEW is generated at the aortic end of the artery. It has a decelerating effect on blood flow but this deceleration effect is minimal when compared with the suction effect of the BEW hence the significant increase in coronary flow seen in diastole (see Figure 8).

Figure 8- Wave intensity of the coronary artery with coronary flow and pressure across a single heartbeat[66]

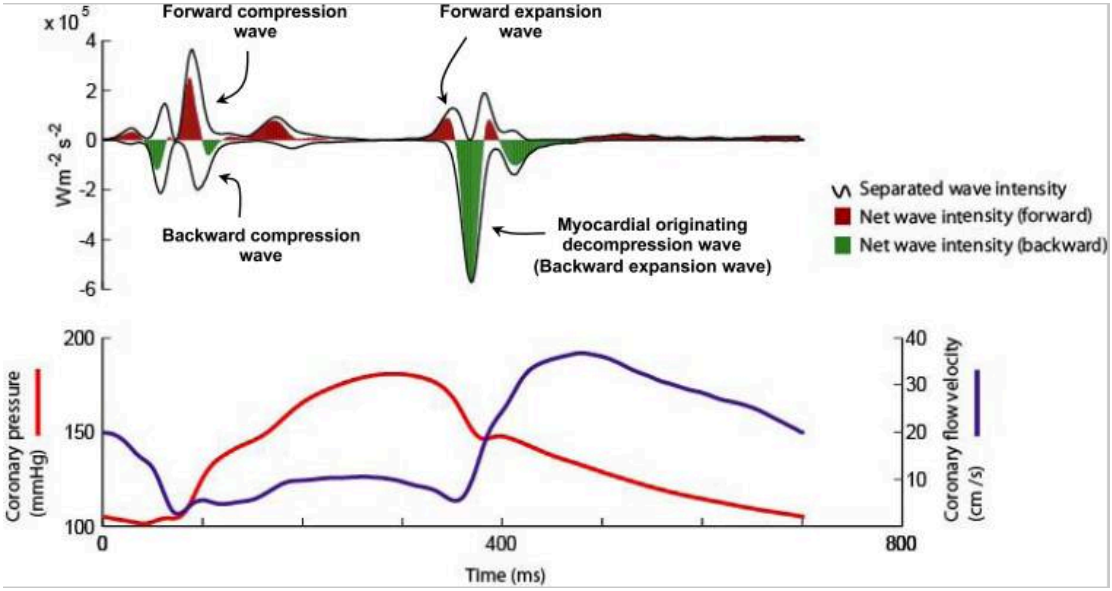

Wave intensity analysis has been successfully used to investigate various disease states and had provided significant insight into the pathophysiology of conditions and the effect of treatments. [67-70]

Specifically, wave intensity analysis has been used to further characterise changes in coronary flow in the Left Main coronary artery (LMCA) with CRT.[71] In this study, Kyriacou et al demonstrated an acute increase in LV contractility with biventricular pacing which was mirrored by an increase in coronary flow velocity, predominantly

due to an increase in the BEW, suggesting that improved relaxation of the ventricle resulted in improved coronary flow. [72] Following on from the previous discussion, in the absence of significant epicardial arterial disease or alteration to existing coronary disease, it can be presumed that this increase in coronary flow is either due to physiological auto-regulation mediated by changes in LV contraction and relaxation or due to a reduction in microvascular resistance secondary to these changes.

If we are able to alter both coronary flow and contractility, wave intensity analysis should enable clarification as to whether coronary flow changes drive changes in contractility in CRT patients or vice versa.

1.2 Cardiac MRI overview

Cardiac MRI has evolved over the last 20 years to provide the gold standard in dynamic cardiac imaging. This evolution has been driven not only by the quality of images derived which allow excellent reproducibility of measures but also the fact that unlike SPECT/ PET it does not rely on radioactive isotopes, unlike computed tomography it does not expose patients to ionising radiation and finally unlike echocardiography it does not rely on patients having adequate acoustic windows.

Patients are placed in a magnetic field causing all the hydrogen ions (present in water and thus blood and tissue) to align in the direction of the magnetic field. A further magnetic radiofrequency pulse (RF) is then delivered to excite and perturb the hydrogen ions. This perturbation moves the hydrogen ions beyond the original magnetic field axis (z axis) with magnetisation directed in the x and y axes away from the original magnetic field. When the RF pulse ends the hydrogen ions realign

themselves resulting in a measurable electric voltage which via a conductive field coil is processed into a greyscale magnetic resonance image. Application of a further magnetic field provides gradient in the x and y axes and allows 3 dimensional reconstruction of images.

1.2.1 Left ventricular Functional Assessment

CMR allows highly accurate assessment of ventricular size and function. This can be very helpful in the case of patients with poor acoustic window on echocardiography when attempting to determine suitability for CRT implantation.

1.2.2 Late gadolinium enhancement (LGE)

Beyond simply assessing ventricular function, CMR is unique amongst imaging modalities in its ability to characterise myocardial tissue. Gadolinium contrast has been used successfully in conjunction with CMR to identify areas of myocardial scar and also perfusion abnormalities.

It was only in 1999 that this technique was histologically validated in the canine model but it now forms part of the standard clinical protocol in CMR centres worldwide. The presence or absence of myocardial scar is potentially of importance when selecting patients for CRT.[73,74] A detailed explanation of how LGE images are acquired in the studies presented here appears in the Methods section.

By means of an overview however, gadolinium contrast tends to collect in the extracellular space rather than intracellularly and takes much longer (typically 15-30 minutes) to wash out of the extracellular space than the healthy myocyte. The

extracellular space is larger in areas of fibrosis and scar than in normal healthy tissue so gadolinium preferentially accumulates in this region. These properties combine to provide a window of opportunity approximately 15 minutes after contrast injection when gadolinium will be located specifically in areas of fibrosis and scar.

Specific CMR sequences are then used to take advantage of this window. Inversion recovery sequences invert magnetisation with a 180 degree pulse and a subsequent 90 degree RF pulse is then applied pushing any residual magnetisation into the transverse plane where it can be detected by the RF coil. After the pulse ceases, the hydrogen ions begin to return to their normal state; this is termed "inversion recovery". At a given inversion recovery time (TI) during this return, imaging acquisition can be performed to generate an image of the myocardium. In fact in clinical protocols, this acquisition is performed at many different TIs. This is called the Look-Locker sequence. By acquiring data at different TI, a sequence of images is rapidly acquired which due to the pharmacokinetics of gadolinium and its varying concentrations in normal and abnormal myocardial tissue will provide differing degrees of contrast between the two (see Figure 9). The TI with the best visible contrast between tissue types can then be selected and images of the entire myocardium acquired at that specific TI.

Figure 9- Differing TI relaxation properties of normal and infarcted myocardium.

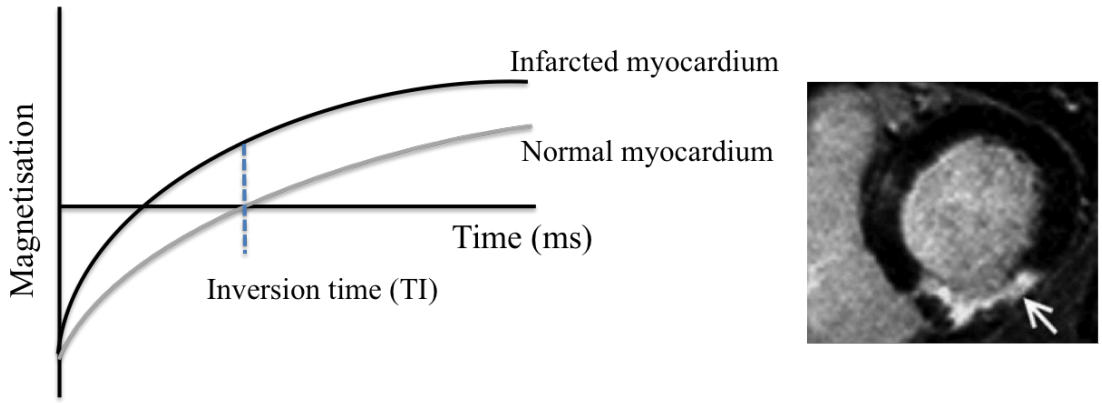

The blue line shows the optimum TI where the contrast between healthy myocardium (black) and scarred myocardium (white) is most apparent. This TI can now be used to collect short axis images of the entire myocardium

1.2.3 CRT outcomes and LGE imaging

One factor influencing the outcome of patients from CRT is the underlying cause of their heart failure with patients with an ischaemic aetiology faring far worse than those with a non-ischemic aetiology.[75] CMR LGE imaging characterises scar such that it is usually possible to determine the aetiology of a patient's cardiomyopathy based on the scar distribution and pattern. Ischemic scar is subendocardial extending towards the epicardium as infarct size increases whereas non-ischemic scar tends to be more diffuse with a tendency to appear in the midwall of the septum. Thus CMR can help to not only determine the aetiology of heart failure but also to help predict potential response to CRT.

The presence of LGE on CMR has been shown to negatively effect outcome following CRT in both ischaemic and non-ischaemic patients. In particular, the presence of LGE in the lateral wall of the LV (adjacent to where an LV lead would be positioned) has been shown to result in very poor outcomes from CRT and there is data to suggest that avoidance of scar when placing the LV lead is associated with improved CRT outcomes . [31,76-79]

1.2.4 T1 relaxation time, T1 mapping and CRT

Myocardial T1 mapping is a relatively newly developed technique where the longitudinal proton relaxation time is measured after inversion. Images are acquired at different TI for each voxel allowing a per voxel inversion recovery curve to be calculated based around the signal intensity at each TI (see Figure 10). The T1 relaxation time measures the time taken for the 63% of protons to realign themselves with the base magnetic field following termination of the RF pulse in the longitudinal axis.

T1 mapping is a measure of the water content of tissue and has been histologically validated as a marker of diffuse myocardial fibrosis. [80-82] The technique enables true quantitative signal intensity analysis without the need for a subjective determination of the optimal inversion time, which potentially undermines the objectivity of LGE imaging. In theory, it therefore provides intrinsic unbiased tissue characterisation.

Figure 10 - Acquisition of T1 map using data recorded at eleven different TI to fit an inversion recovery curve. The data are then merged to create a per voxel T1 map

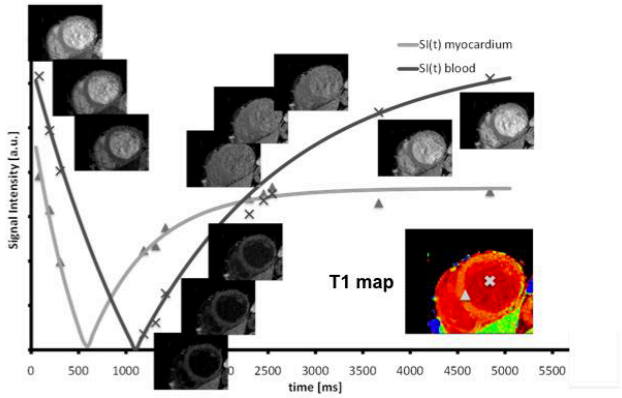

Modified Look-Locker Inversion Recovery Sequence (MOLLI) to calculate T1

This technique uses a Modified Look-Locker Inversion Recovery Sequence (MOLLI) as depicted in

Figure 10 with data from 11 different inversion recovery times from 3 different acquisitions merged into one dataset. The three acquisitions are taken over typically 17 heartbeats. The MOLLI sequence has a tendency to underestimate T1 values, particularly at higher heart rates so a correction is required.(7-9)

These data can be collected prior to the injection of gadolinium contrast ($T1_{native}$) and at a predefined time after injection ($T1_{post}$). $T1_{post}$ has the same potential issues as LGE imaging in that it depends upon the pharmacokinetics of gadolinium in a patient

at any given moment, the dose given and the time delay between injection and data acquisition. Other factors effecting the $T1_{post}$ measure because gadolinium is used include haematocrit leveland the renal clearance rate. This limits intra and inter patient reproducibility of $T1_{post}$.

Extracellular volume (ECV) Quantification

Quantification of the ECV has bee proposed as an alternative method to measure myocardial fibrosis. This in theory should overcome issues relating to haematocrit in the $T1_{post}$ sequence by incorporating it with the following equation. Thus,

$$ECV = (1 - \text{haematocrit}) \times \left((1/T1_{post}(\text{myocardium}) - 1/T1_{native}(\text{myocardium})) / (1/T1_{post}(\text{blood}) - 1/T1_{native}(\text{blood})) \right)$$

This equation calculates the ECV based upon the relative concentration of gadolinium in the myocardium relative to the blood and has been histologically validated in patients with both hypertrophic cardiomyopathy aortic stenosis.{Flett:2010eh} However, it requires a low dose infusion of gadolinium post intravenous bolus to achieve a dynamic steady state ie maintain a measurable gradient between myocardium and blood making the scan themselves challenging.

1.2.5 T1 mapping and CRT

Unlike LGE, T1 mapping has not been shown to be predictive of CRT response in a mixed cohort of ischaemic and non-ischaemic patients although there are only limited data examining this question.[76] The relationship between CMR imaging and advanced electrocardiography measures such as fragmented QRS and vectorcardiography has not been the subject of previous enquiry.

1.3 Vectorcardiography

Modern vectorcardiography (VCG) was developed in the 1950s by Dr E Frank.[83] The VCG was designed to provide 3 dimensional electrocardiographic information using 3 orthogonal planes (X, right to left axis; Y, head to feet axis; Z, antero-posterior axis). The VCG is acquired using 7 "Frank leads" (see Figure 11).

Figure 11- Figure from Frank's original paper showing electrode position and the 3 planes of the VCG

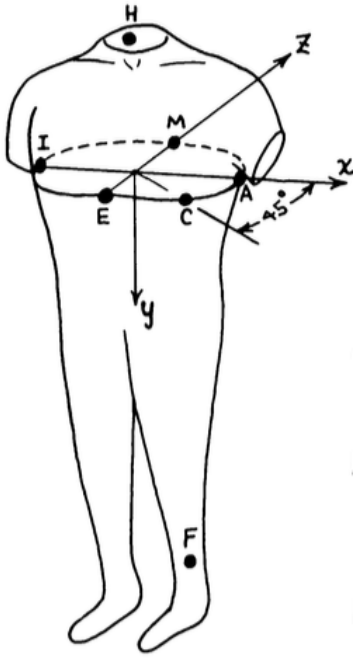

Performing a VCG using these leads is impractical as systems require electrodes to be placed on the back and as such the VCG has never entered mainstream clinical use. However, whereas the ECG only provides voltage data requiring intellectual supposition of vector direction, the VCG provides a visual depiction of the direction

of the dominant vector throughout the cardiac cycle. The VCG also provides data of both QRS area and duration and T wave area and duration. Using a mathematical transformation, the VCG can now be accurately synthesised using standard 12 lead ECG data.[84]

Nonetheless whilst the 12 lead ECG remains an integral to patient selection for CRT, a potential role for the VCG is only now beginning to be explored.

With regard to CRT, it has been suggested that both QRS area and T wave area might provide additive information that can be used to identify patients most likely to benefit from CRT implantation.[85] However, the relationship between structural changes in the ventricle and changes in VCG are unclear as is their relative contribution to identifying patients who may benefit from CRT implantation. It is suggested that the interaction between VCG and CMR is a relevant area of enquiry given that they both may help to improve patient selection for CRT.

1.4 Heart failure and implantable cardioverter defibrillators

1.4.1 The evidence base for ICDs

ICDs were first conceived in the 1980s but over the last 40 years the evidence base to support their use to protect against VA and sudden death has expanded significantly. Initial randomised studies investigated patients who had a secondary prevention indication (ie survivors of cardiac arrest or those with documented VA and found a survival benefit or reduction in sudden death in patients implanted with an ICD when compared with those randomised to taking amiodarone. This benefit was significant in in the Anti-arrhythmic versus Implantable Defibrillators Study (AVID) but did not reach significance in the Canadian Implantable Defibrillators Study (CIDS). [86,87]

Attention then turned to identifying patients who had not had an arrhythmic event but who might be at high risk of such events. Post myocardial infarction patients with an EF< 35% have been shown to benefit from prophylactic ICD implantation.[88] These finding were extended in SCD-HeFT trial which include patients with both an ischemic and non-ischemic cardiomyopathy.[89] However, the role of primary prevention ICDs in non-ischemic patients is not entirely clear. The DEFINITE study in 2004 found that ICDs reduced the risk of sudden death in NCM patients but not the risk of death by any cause.[90] Furthermore the mean follow up time of DEFINITE was 29 months. The recent DANISH study has found that ICDs provide no survival benefit in the NCM population at 7 years although there was a reduction in arrhythmic death and some benefit noted in younger patients.[91]

Interpretation of the findings of these studies is controversial. What is apparent is that our ability to select appropriate patients for primary prevention ICDs is still poor. The highest event rate (appropriate shock) was 16.4% in MADIT 2, compared with 5.4% in SCD HEFT and 4.4% in DANISH suggesting that large numbers of patients are being implanted with defibrillators "unnecessarily" and that the vast majority will never go on to receive an appropriate therapy. This would suggest that there is a need for improved risk stratification which goes beyond ejection fraction and the clinicians assessment that the patient is at risk of sudden death.[92]

1.4.2 Cardiac Magnetic Resonance Imaging to predict VA: LGE, Grayzone and T1 mapping

LGE

As noted above, CMR can potentially identify both myocardial scar (LGE) as well as diffuse myocardial fibrosis (T1 mapping). The majority of studies assessing the predictive power of these CMR protocols have been small.[93,94] However, a recent meta-analysis of >1100 patients with both NCM and ICM patients showed that the presence and extent of LGE was predictive of VA.[95]

Grayzone

Myocardial scar is not homogenous. At time of infarction, whilst there is cell necrosis resulting eventually in scar formation, other areas of myocardium often on the penumbra of infarcted areas form an admixture of viable and nonviable myocardium.[96] These areas can form bridging channels around and through scarred tissue that can form substrate for re-entrant arrhythmia and exhibit altered pro-arrhythmic automaticity.[97]

Similarly, post-infarction scars on CMR vary in signal intensity (SI) and can be divided into the scar core (High SI) and the peri-infarct region or grayzone (Abnormal SI but not as high). Different definitions have been used to define this area of moderate SI (see Methods section). The size of the grayzone has been shown to be a powerful predictor of mortality and predictor of both spontaneous VA and VA on programmed electrical stimulation. [98-100]

T1 mapping

T1 mapping has been shown to predict VA in a mixed cohort of NCM and ICM patients and has been shown to prognosticate in a perceived low risk cohort of patients with NCM.[101,102] Furthermore, it is biologically attractive that such a measure of diffuse fibrosis should predict VA in NCM patients.[103] It is unclear however, in a perceived high risk group of NCM patients with ICDs whether T1 mapping can specifically predict VA and appropriate therapy.

1.4.3 Fragmented QRS to predict ventricular arrhythmia

One of the potential clinical biomarkers that might be used to improve patient selection for both CRT and ICDs is the presence of fragmentation on the 12 lead ECG. Breadth of QRS is already a key determinant of suitability for CRT and for primary prevention ICD implantation but work over the last 10 years has sought to use the ECG in a much more sophisticated manner by looking for QRS fragmentation. [88,104].

The concept of fragmented intracardiac electrograms and the signal averaged ECG as potential markers of arrhythmic risk significantly predates the assessment of fragmentation on the 12 lead ECG.[105] It wasn't until 2008 that, Pietrasik et al first published data in a large number of patients supporting the use of fragmented QRS on the 12 lead electrogram as a mechanism to risk-stratify patients with cardiovascular disease.[106] Pietrasik found that fQRS predicted the risk of recurrent events in a post-MI population who has transiently had q waves post infarction. This work was rapidly followed up by studies from Das et al. who published several studies demonstrating

the independent prognostic risk of fQRS in patients with coronary artery disease. [107,108] This concept of risk was further refined to include the risk of ventricular arrhythmia in a mixed cohort of ischaemic and non-ischaemic cardiomyopathy.[109]In this study fQRS was found to be a stronger predictor of ventricular arrhythmia than wide QRS (defined as QRS>120ms). Subsequent studies on similar cohorts have had mixed results with some confirming fQRS as an independent predictor of sudden death and others failing to find such an association[110-112].

A recent large meta-analysis of >5000 patients which included the above described studies found that fQRS is associated with increased relative risk of all-cause mortality in ICM and NCM patients (RR 1.71 (CI 1.02-2.85)) - and of sudden cardiac death (RR 2.20 (CI 1.05-4.62)).[113] Subgroup analysis confirmed this risk separately in both aetiologies (NCM and ICM). Interestingly there was no increased risk in mortality in patients with ICDs and the authors propose that this may be the result of ICD therapies preventing this outcome. Furthermore, fQRS had no independent predictive value in patients with an ejection fraction <35% suggesting that fQRS failed to add any discriminatory value to patients who are already high risk for both VA and death. Importantly this cohort makes up the majority of those who qualify for a primary prevention device.

Thus, these findings are potentially important in assessing fQRS in a cohort of ICD patients with low ejection fraction as the fQRS may fail to add any further predictive value beyond current criteria.

FQRS and scar

Nonetheless it remains unclear quite what fragmentation on the QRS represents. Again the literature is not entirely consistent. Das et al demonstrated that fQRS has greater sensitivity than Q waves in detecting myocardial scar (85.6% vs 36.3%).[108] This large increase in sensitivity was offset by a slightly reduced specificity (99.2% vs 89%). Conversely, Wang et al found that fQRS had an exceptionally poor sensitivity in detecting myocardial scar when compared with q waves (1.7% vs 31.7%) and had a higher false positive rate in patients with normal perfusion scans (15.8% vs 1.4%).

The above studies have used nuclear scanning to determine scar but CMR is better able to characterise scar and perfusion abnormalities than nuclear imaging and as such would be a preferable modality with which to understand fQRS fully.[114]

A study of 86 patients found no relationship between LGE scar and fQRS in patients with NCM. Indeed, the presence of scar was not significantly different (50.9% in patients with fQRS vs 45.5% in patients without fQRS; p=0.62)[115] The same authors also found in a cohort of 186 patients who had a history of myocardial infarction that fQRS had poor accuracy compared with q waves for the detection of LGE on CMR.[116] In the study LGE was only qualitatively identified as present or absent and, if present, subendocardial or transmural. No study has sought to determine whether the volume of scar may be a factor in the presence or absence of fQRS. It may be that fQRS represents myocardial fibrosis or the peri-infarct region rather than scar but there are currently no data looking at fQRS and T1 mapping.

1.5 Cost effectiveness in the National Health Service- rationing healthcare provision

The National Health Service (NHS) provides the overwhelming majority of healthcare to the population of the United Kingdom. 98% of the funding it receives is from taxation and National Insurance contributions. The cost of the service is enormous and spiralling with an increasingly elderly population with more complex medical problems. In 2015-2016, health spending made up 29.7% of the public spending budget with the NHS annual budget calculated at £116.4 billion.(www.nhs.uk) The Department of Health is seeking to make £22 billion of efficiencies by 2020-2021.[117]

Meanwhile, the National Institute for Health and Care Excellence (NICE) continues to produce clinical guidelines incorporating clinical evidence and cost effectiveness to ensure patients are prescribed the most effective treatments to maximise potential outcomes given the inevitable financial restrictions that exist nowadays. Similar models of assessing treatments are beginning to be explored by other healthcare systems. Most notably, the American College of Cardiology and American Heart Association have stated that cost effectiveness should be referred to when new guidelines are drafted.[118]

Chapter 7 of the NICE guidelines manual, 2012 relates specifically to how cost-effective measures should be assessed. A gold standard methodology is described as the process by which decisions should be made as to which questions should be addressed. The guideline manual then states

"It is acknowledged that "NICE" has limited resources and time to construct new economic analyses. Therefore, the complexity and number of new analyses will vary depending on what are considered priority areas and what information is required for robust decision making."

With this in mind, it is necessary for health researchers to research the cost – effectiveness of their treatments wherever possible to try to maximise overall NHS budgets. This should be done using the methodology that NICE prescribes wherever possible and using appropriate quality adjusted life year and incremental cost effectiveness ratio cut-offs as adjudicated by NICE to inform decision as to likely cost-effectiveness.

Chapter 2 METHODS

2.1 SIMULTANEOUS INVASIVE ASSESSMENT OF CORONARY FLOW AND PRESSURE AND LV PRESSURE

The experiments detailed in Chapter 3 required the invasive measurement of several haemodynamic indices simultaneously. It was necessary to adapt tools generally available for clinical practice to enable these measures to be taken.

2.1.1 Ascending aorta/ aortic root pressure

As in clinical practice, aortic pressure was measured using a fluid-filled hollow multi-purpose catheter with pressure being transduced externally via the catheter. The pressure transducer was fixed to the catheter laboratory table to avoid error related to changes in position and initially zeroed at the level of the right atrium whilst the patient was lying on the catheter laboratory table. This allowed beat to beat measurement of aortic blood pressure

2.1.2 Coronary artery flow and pressure

Coronary artery flow and pressure from both the LAD and Left Circumflex artery measured using the 9500 Combowire (Volcano corporation, US). This is a 0.036mm diameter, 185cm guidewire which measures both flow velocity and pressure simultaneously (see

Figure 12).

Figure 12- Details of the Combowire design

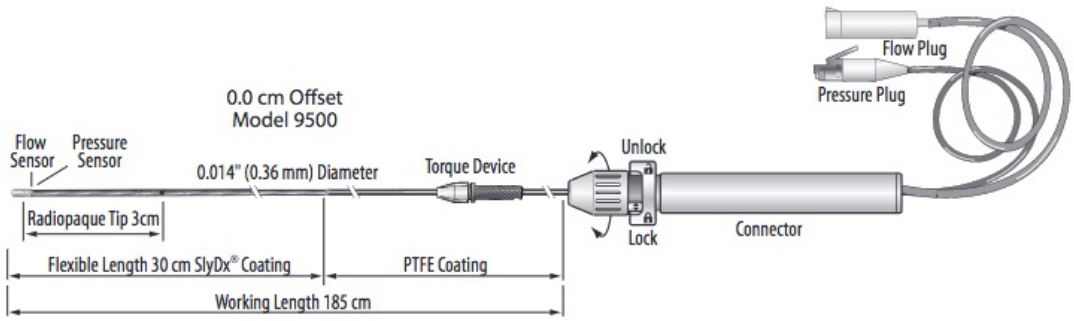

Coronary Flow Velocity measurement using the Combiwire

The coronary flow velocity is measured by pulsed ultrasound. A piezo-electric crystal on the tip of the wire acts as both transmitter and receiver of the ultrasound. A proportion of the pulsed ultrasound waves emitted from the crystal are reflected back by blood cells within the sample volume in the vessel to the crystal. The pulsed ultrasound allows the crystal to act as receiver in between ultrasound pulses. The returning waves have a lower frequency than the emitted wavefront as the blood cells are moving away from the crystal. This creates a Doppler shift which is proportional to the blood velocity. Changes in this shift can be transformed into velocity (cm/s) assuming a constant speed of sound in blood and consistent frequency in transmission of the ultrasound signal. The instantaneous peak velocity is the maximum velocity sampled and the average of these peaks can be used to obtain the Average Peak Velocity (APV) which is the index of flow generally used to describe coronary flow velocity data.

Ultrasound measurement requires the ultrasound beam to be parallel to the direction of flow to minimise underestimation of flow and thus in all experiments great care was taken to align the Combowire appropriately within the lumen of the vessel to optimise the Doppler signal.

Coronary Pressure measurement using the Combowire

The Combowire has a pressure sensor that uses the MEMS (Micro Electric Mechanical Systems) technology. The sensor has a thin silicon diaphragm over a reference pressure chamber in which tiny resistors are embedded. As pressure changes, flexing the diaphragm, so the resistance in the resistors alters. These changes in resistance can be converted in real time into a pressure reading.

"Simultaneous" measurement of pressure and flow

Theoretically, wave intensity analysis requires both pressure and flow to be acquired at the exact same point but the sensors are in fact 5mm apart which is the minimum electronically feasible distance that has currently been achieved. Davies et al. have shown that given the sampling frequencies used for both Doppler and pressure readings that any time delay is negligible (0.25-1ms) and thus this was not corrected for in the studies presented here. Furthermore the magnitude of delay is variable on wave speed making any correction for such a small delay very complex.[61]

2.1.3 Left ventricular pressure

Left ventricular pressure was measured using a Primewire (Volcano, Inc). This wire also uses MEMS technology and was placed in the LV cavity. The first derivative of pressure was used to assess LV contractility and lusitropy.

2.1.4 ComboMap system

The ComboMap console (see
Figure 13) receives inputs from the pressure transducer (aortic pressure), the Combowire (coronary flow and pressure) and the Prime wire (LV pressure) and displays data live (see Figure 14). It allows live assessment of data quality. Data can then be stored on a CD drive and analysed later.

Figure 13- ComboMap system (model 6800)

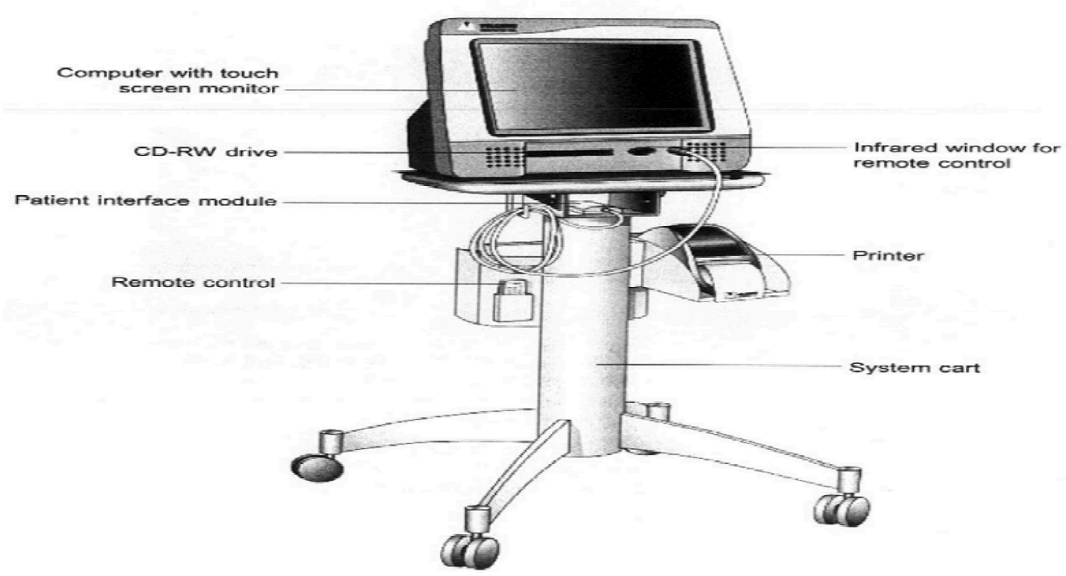

Figure 14- ComboMap console data screen (ECG, Pressure signals in red and yellow, Doppler envelope with blue line for max)

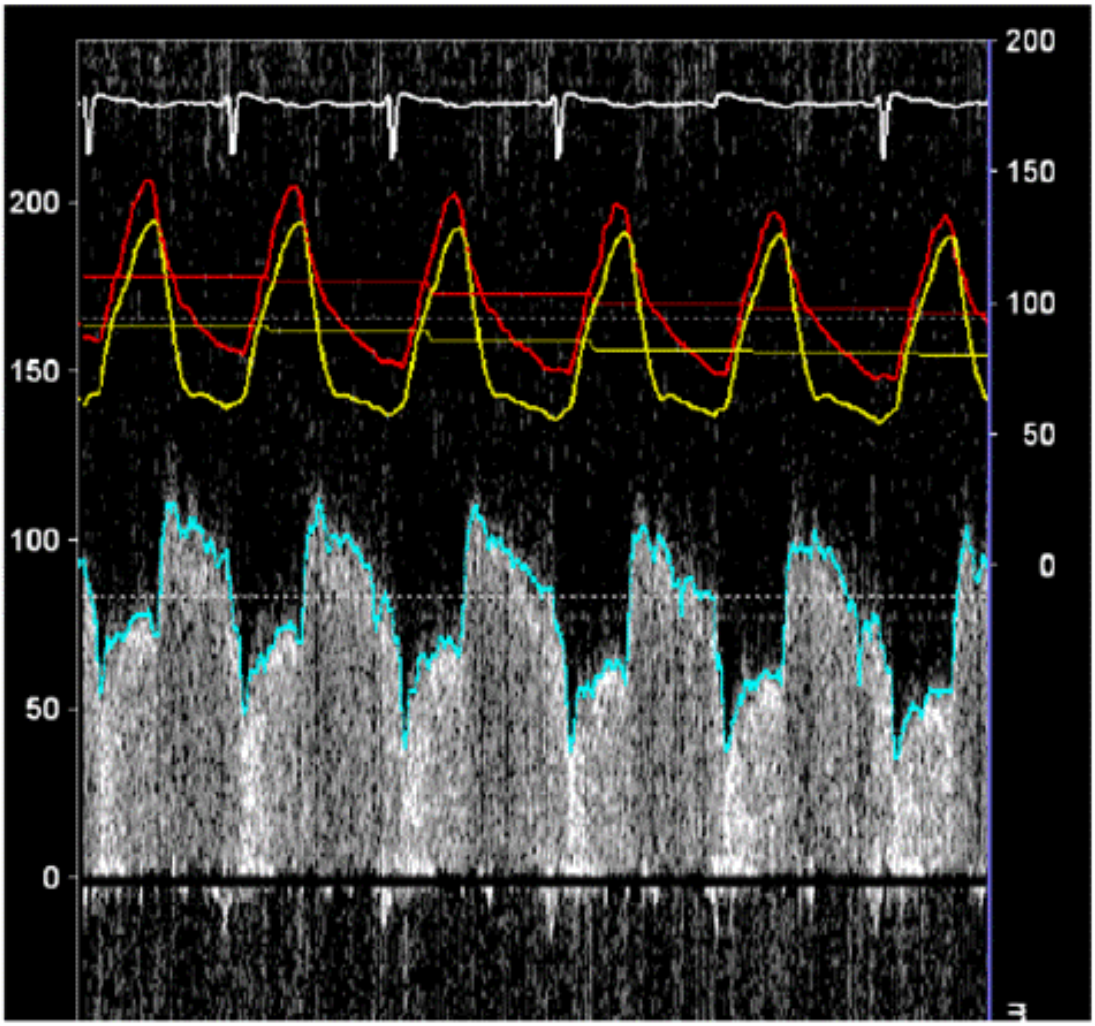

Calibration

The pressure signals for the Combowire, Prime wire and fluid filled catheter were compared at catheter laboratory table height and zeroed. The Doppler signal was optimised for each patient in each vessel. Both the wall filter and the instantaneous peak velocity (blue line in Figure 14) were adjusted to optimise the signal.

2.1.5 Post processing of data

Data was subsequently exported for analysis from the ComboMap and initially analysed using custom made software (Studymanager, AMC, Amsterdam). This programme

allowed visualisation of data so that noisy or incomplete data could be omitted from analysis.

For example, the programme automatically determines and annotates the R wave from which subsequent calculations are made. Our investigations resulted in changing QRS morphology and importantly changing amplitude in a pre QRS pacing spike. The programme allowed us to correct for failings in the automatic analysis. The raw data was not altered or alterable using the programme.

Following optimisation of the data, this could then be extracted and imported to a second custom made piece of software (Cardiac Waves, KCL, London). This software enabled wave intensity analysis to be applied to the coronary data and also provided the LV haemodynamic data of contractility and relaxation (positive dp/dt max and negative dp/dt max).

2.2 ACHIEVING ENDOCARDIAL PACING AND SYNCHRONIZING VENTRICULAR ACTIVATION WITH PRE-EXISTING DEVICE

The invasive studies used a population of patients with a CRT already in situ. To investigate the haemodynamic effects of endocardial LV pacing it was necessary to insert a roving mapping catheter (Biosense Webster) via the right femoral artery and a temporary pacing wire in the right atrium via the right femoral vein. Atrial capture was confirmed with standard threshold testing. The CRT devices and the mapping catheter were then programmed to sense the atrial pacing spike at a set atrioventricular delay.

Endocardial ventricular capture was confirmed by looking for changes in QRS morphology. If there was any doubt then the pacing output on the CRT device was dropped to below thresholds to ensure ventricular capture.

2.3 CARDIAC MAGENTIC RESONANCE IMAGING PROTOCOLS: LATE GADOLINIUM ENHANCEMENT, GRAYZONE AND T1 MAPPING

2.3.1 CMR Protocol

CMR imaging was performed as per King's College London/ Guy's and St Thomas' Foundation Trust, standard clinical protocols. All scans were acquired on a 1.5 Tesla MRI scanner with a 32 channel coil (Philips Healthcare, Netherlands). An initial survey scan was performed to ensure registration and thoracic localisation. A stack of 12 to 14 short– axis balanced steady state free precession slices covering the LV were acquired initially which allowed measurement of mass, volume and ejection fraction. Gadobutrol contrast (0.2mmol/kg) was then injected intravenously and 10-15 minutes post injection, a Look-Locker sequence was acquired to determine the optimum TI contrasting the myocardium to blood pool. Subsequently, a further stack of short axis slices of the LV was acquired using an inversion-recovery gradient echo sequence with a repetition time/echo time of 3.4 and 2.0ms respectively, a flip angle of 25 degrees and a voxel size of 1.8x1.8x8mm. Images were triggered via the ECG for collection at end-diastole. These images were used for assessment of scar and grayzone.

T1 mapping images were obtained pre and post the administration of gadolinium contrast. A single mid ventricular slice was acquired using a modified Look- Locker sequence with 11 phases over 3 cardiac cycles (3+3+5, repetition time/ echo time =

3.3/1.5ms, flip angle = 50 degrees, voxel size 1.8x1.8x 8mm with heart rate adapted triggered delay and a adiabatic prepulse to ensure complete inversion.

A region of interest was then sampled post data acquisition remote from LGE enhancement in the septum to obtain $T1_{native}$ and $T1_{post}$ results.

2.3.2 CMR Image analysis

All images were analysed using CVI 42 (Circle Cardiovascular Imaging Inc., Canada). Volume, mass and function were measured and derived by visual assessment of the endocardial and epicardial borders in end diastole and end systole with subsequent automated calculation using the software.

The quantitative assessment of scar with LGE was performed using the "X" standard deviation method and the full width half maximum method. The "X" standard deviation method defines scar as the region with signal intensity "X many" standard deviations above a remote reference region of interest in the myocardium deemed to be normal. The full width half maximum calculation defines scar as the region within the myocardium that has a signal intensity of at least 50% of the maximum signal intensity measured.

The quantitative assessment of grayzone was also calculated using two methods. The first assessment subtracted the area of LGE identified using scar at 3 standard deviations from that at 2 standard deviations to describe the peri-infarct region. The second calculated the percentage of myocardium between scar using full width half maximum technique and scar using the 2 standard deviation technique.

All scar and grayzone measures were then expressed as a percentage of LV mass to normalise for ventricular size across patients.

2.3.3 T1 mapping quantification

The T1 maps were analysed using customised software with motion correction. (Osirix, Pixmeo, Geneva and Insight Toolkit). As previously described, we performed linear regression analysis of the measured native T1 values on heart rate and then applied heart rate correction using a function of the mean heart rate of the study population to the native T1 values. [81,101]

2.4 ASSESSING FRAGMENTATION ON THE 12 LEAD ECG

The method by which the presence of fragmentation on the 12 lead ECG is determined varies depending upon QRS duration. This is due to the presence of notching in both LBBB and RBBB which would always fulfil the criteria set out for fragmentation in narrow QRS ECGs (<120ms). For my study I used the well-validated criteria used by Das et al for both narrow and wide qrs.[108,119]

Narrow QRS (<120ms)

One of three criteria are required to confirm QRS fragmentation in patients with a narrow QRS. These are

1) an additional R' wave making an RSR' pattern
2) notching in the nadir of the S wave
3) >1R' (fragmentation)

in 2 contiguous leads

Several different morphologies of QRS fulfil these criteria which appear in Figure 15 taken from Das et al.[108]

Figure 15- Morphologies of fQRS in narrow QRS

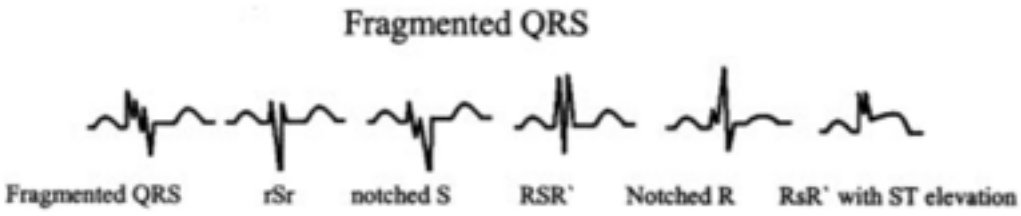

Wide QRS (>120ms)

Fragmented LBBB/RBBB

RBBB and LBBB were defined by the standard ECG criteria (QRS duration ≥ 120 fragmented BBB was defined as various RSR patterns with or without a Q wave, with >2 R waves (R') or >2 notches in the R wave, or >2 notches in the downstroke upstroke of the S wave, in 2 contiguous leads corresponding to a major coronary territory (see Figure 16 and

Figure 17).

Fragmented paced QRS

Paced QRS (pQRS) was defined as a wide QRS complex (duration >120 ms and without any evidence of QRS fusion) initiated by a paced spike in patients with a pacemaker or ICD. Fragmented paced QRS was defined by the presence of >2 R' or >2 notches in the S waves in 2 contiguous leads.

Figure 16- Two ECGs demonstrating fragmented wide QRS taken from Das et al.[119]

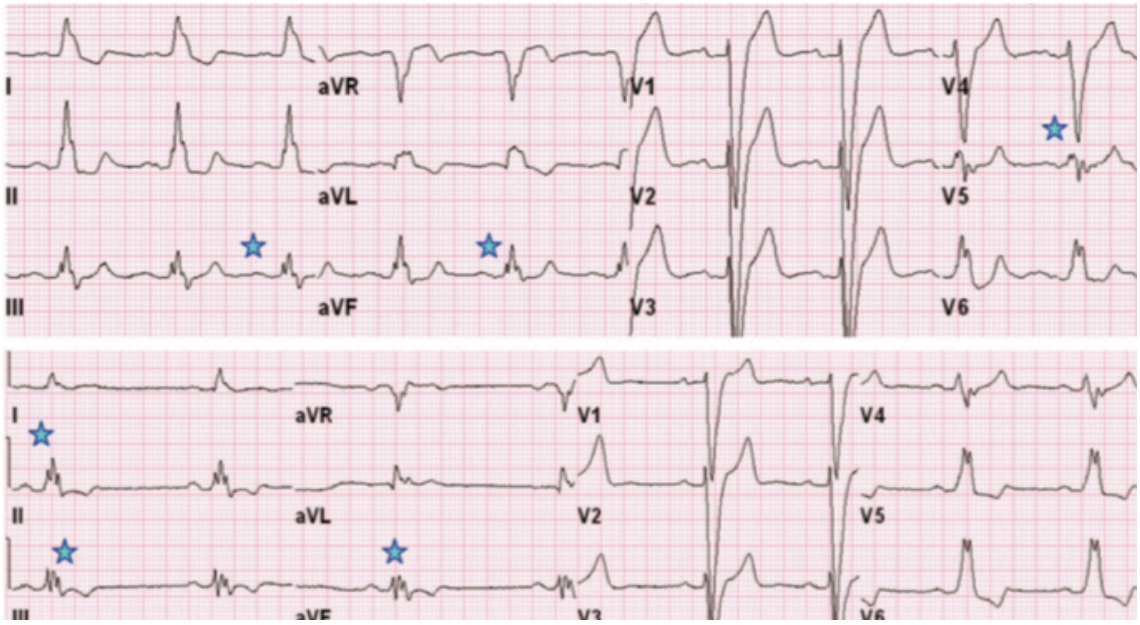

Blue stars denoted fragmented QRS

Figure 17- An ECG of non-fragmented wide QRS taken from Das et al.[119]

Ensuring assessor competence in the assessment of fragmentation and settling disagreement

For the study in which I looked at fragmentation, I enlisted the help of two colleagues, both cardiologists to review the ECGs. They were both blinded to the CMR and outcome data. I created a training set of 20 ECGs which they reviewed and then we discussed difficult cases as a group. For the study ECGs. Both colleagues analysed the ECGs separately and I reviewed the results. There was 94% concordance between the two cardiologists and the remaining ECGs were adjudicated unanimously.

2.5 VECTORCARDIOGRAPHY

Standard digitised 12 lead ECGs were acquired prior to CRT implantation. (MAC 5500HD, GE Healthcare, Chicago, US). The digital PDF files with vector graphics were used to extract the original digital ECG-signal. VCGs were semi-automatically

synthesized from these digital ECG signals using a custom-made software programmed in MATLAB 2016 (Mathworks, Natick, NA).[85] The Kors transformation matrix was used to transform the 12-lead ECG to reconstructed VCGs.[120] The onset and end of the QRS-complex and end of the T-wave were manually set on the three overlaid orthogonal leads (X, Y, and Z)of the VCG. QRS duration (QRSd) was defined as the onset to end of the QRS complex on the VCG orthogonal leads (see Figure 18). QRS_{area}, T_{area} and $QRST_{area}$ were defined as the 3D areas of respectively the QRS complex, T wave and QRST loop from the VCG between the loop and baseline in X, Y, and Z direction calculated as $QRS_{area} = (QRS^2_{area,x} + QRS^2_{area,X} + QRS^2_{area,X})^{1/2}$, $T_{area} = (T_{area}{}^2{}_{,x} + T_{area}{}^2{}_{,X} + T_{area}{}^2{}_{,X})^{1/2}$ and $QRST_{area} = (QRST_{area}{}^2{}_{,x} + QRST_{area}{}^2{}_{,X} + QRST_{area}{}^2{}_{,X})^{1/2}$.[85]

Figure 18 - An example of a synthesised VCG in a study patient with LBBB

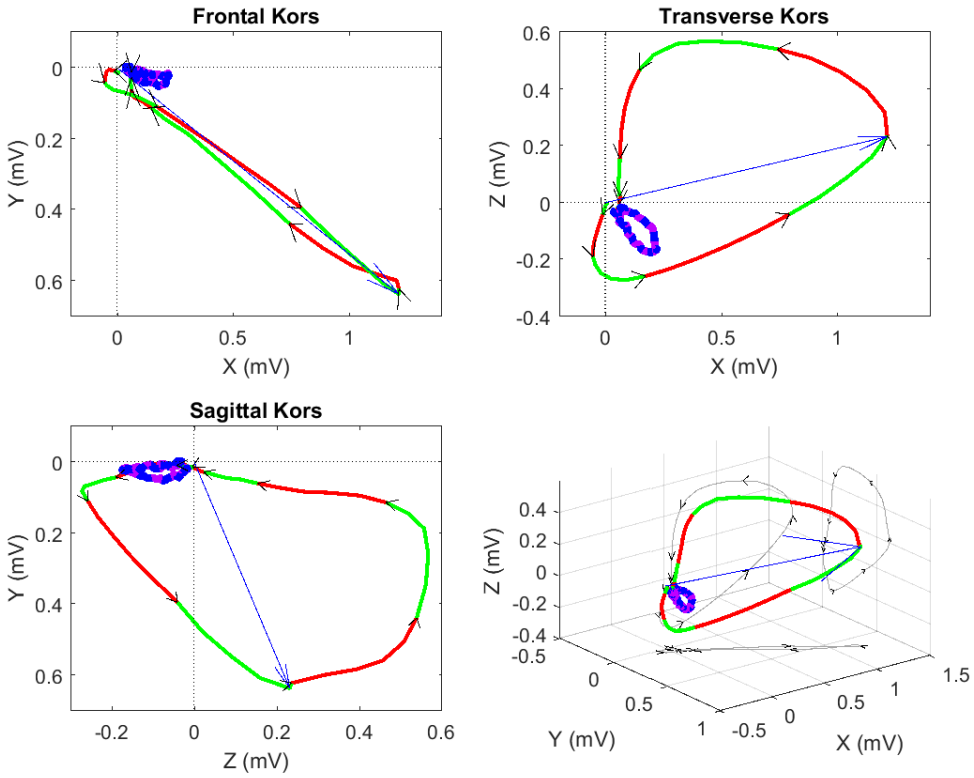

2.6 ASSESSING CRT RESPONSE BY ECHOCARDIOGRAPHY

Left ventricular reverse remodelling was defined as a reduction in the LV ESV of >15% at 6 months post CRT implant as measured on transthoracic echocardiography using Simpson's method of LV functional assessment using the 2 chamber and 4 chamber views.

Chapter 3 INVESTIGATIONS INTO THE HAEMODYNAMIC EFFECTS OF CARDIAC RESYNCHRONISATION THERAPY

3.1 EFFECTS OF ENDOCARDIAL PACING AND EPICARDIAL PACING ON CORONARY FLOW

3.1.1 Abstract

Background:

The increase in global coronary flow seen with conventional biventricular pacing is mediated by an increase in the dominant backward expansion wave (BEW). Little is known about the determinants of flow in the left-sided epicardial coronary arteries beyond this or the effect of endocardial pacing stimulation on coronary physiology.

Methods and Results:

11 patients with a chronically implanted biventricular pacemaker underwent an acute haemodynamic and electrophysiological study. 5/11 patients also took part in a left ventricular endocardial pacing protocol at the same time. Conventional biventricular pacing (BIVCS) resulted in a 9% increase in flow (average peak velocity) in the left LAD mediated by a 13% increase in the BEW(p=0.004). Endocardial pacing (BIVEN) resulted in a 27% increase in flow mediated by a 112% increase in the forward compression wave (FCW) and 43% increase in the BEW (p=0.048 & 0.036 respectively). There were no significant changes in circumflex (Cx) parameters. BIVCS resulted in homogenization in timing of coronary flow compared with baseline (mean difference in time to peak in LAD vs. Cx of the FCW 39ms (baseline) vs 3ms (BIVCS)(p=0.008); BEW 47ms (baseline) vs 8ms (BIVCS)(p=0.004.))

Conclusions:

Epicardial and endocardial pacing result in increased coronary flow in the LAD and homogenization of the timings of waves that determine flow in the LAD and Cx. The

increase in both the FCW and BEW with endocardial pacing may be the result of a more physiological activation pattern than epicardial pacing which resulted only in an increase in the BEW.

3.1.2 Background

Cardiac resynchronisation therapy (CRT) is an effective treatment for patients with systolic heart failure and electrical dyssynchrony, resulting in improvements in both symptoms and mortality.[10] Depending upon the endpoint assessed, between 30% and 40% of patients fail to improve with CRT.[24] Metrics created to improve patient selection and predict response have often appeared encouraging in small single centre studies but have lacked reproducibility when extrapolated to multi-centre trials.[18] As a result, there has been increasing interest in both the pathophysiology of dyssynchronous heart failure in an attempt to understand the mechanical sequelae of electrical dyssynchrony and new methods of ventricular stimulation such as endocardial and multipoint pacing to improve CRT response. [28,32,121-123] One area of research is the effect of impaired electrical activation and CRT on coronary haemodynamics and physiology, as recent data from animal models have indicated the importance of blood flow in CRT response.[35]

The coronary vasculature is unique in the human body in that the majority of flow occurs during diastole. Using advanced invasive techniques, it has been possible to demonstrate that flow is mediated principally by the forward propulsion of blood through the coronary tree in systole (a dominant forward travelling compression wave (FCW)) and by a relatively larger backward travelling expansion (suction) wave (BEW) generated by relaxation of the ventricle in diastole.[62] There is now evidence that the amplitude and wavelength of these waves are effected by CRT when measured in the

left main coronary artery (LMCA).[71] However, relative workload and myocardial stress is not homogenous in the dyssynchronous left ventricle. Ventricular activation with left bundle branch block (LBBB) results initially in septal contraction with delayed activation and contraction of the lateral wall. This early contraction occurs prior to development of tension in the lateral wall resulting in reduced septal work compared with normal contraction. Conversely the lateral wall contracts against a pressure-loaded ventricle causing an increase in lateral wall work compared with synchronous activation. [37,124]

Conventional biventricular pacing delivered epicardially from the coronary sinus (BIVCS) can increase left anterior descending (LAD) coronary flow and acute changes in LAD flow may predict response to CRT but little is known about the effects of BIVCS on the wave energy that determines coronary flow in the left-sided coronary system. [55,125]Similarly, whilst there is increasing data about the beneficial acute effects of LV endocardial pacing (BIVEN) on cardiac work and acute contractility, there are no data describing the effects of LV endocardial pacing on coronary blood flow. [32,126]Given the heterogeneity of regional work in the dyssynchronous ventricle a more detailed examination of the individual epicardial arteries may give insights into the regional effects of myocardial contraction on the different constituents of coronary blood flow during both epicardial and endocardial LV pacing.

We sought to describe the effects of both standard CRT via LV epicardial pacing from the coronary sinus and BIVEN on coronary flow. By applying wave intensity analysis to simultaneously obtained coronary pressure-Doppler flow data we sought to describe the effect of pacing from different sites (epicardial and endocardial) on coronary physiology in both left sided epicardial arteries.

3.1.3 Methods

The study received approval from the Local Research Ethics Committee and was conducted in accordance with the Declaration of Helsinki. All participants provided written and informed consent. We obtained simultaneous electrophysiological and haemodynamic measurements in 11 patients with a previously implanted standard CRT device with an epicardial LV lead in the lateral/postero-lateral wall. Arterial access was gained in both the femoral and radial arteries. A 0.014″ Doppler wire (ComboWire™ model 9500, Volcano Corporation) was advanced to the proximal LAD and was advanced to a central location within the proximal LAD where a high signal-to-noise ratio was obtained. A Primewire (Volcano Corporation) was placed in the LV cavity to allow measurement of acute contractility by dp/dt max.[33]

To study the effects of LV endocardial pacing on coronary flow, 5 of the 11 patients agreed to undergo a more comprehensive study in which a roving endocardial pacing catheter was placed in the LV to perform LV endocardial pacing. Several endocardial positions (mean 4 (2 for each artery)) were tested in the 5 patients and the site with the highest APV in each artery selected for analysis. Patients underwent an acute pacing protocol with assessment of different pacing configurations. The study was then repeated with the Combowire moved from the LAD to the circumflex artery (Cx). In 5 cases the Cx was assessed before the LAD. Intracoronary adenosine was given as a bolus dose of 36mcgs to induce hyperaemia to further investigate the effect of pacing from different sites on coronary haemodynamics.

Baseline measurements were taken for patients in sinus rhythm in AAI mode. For patients in atrial fibrillation or with complete heart block, the baseline comparator rhythm was right ventricular pacing with atrial synchronous pacing in the latter group.

When comparisons were made between baseline and right ventricular pacing those whose baseline required RV pacing were omitted from analysis. All studies were performed with pacing 10 beats above the intrinsic rate or at 70 bpm in the case of patients with underlying AV block to control for the Bowditch effect.[127] Atrio-ventricular (AV) and ventriculo-ventricular (VV) delays were set as per previous standard clinical echo optimisation using the doppler mitral inflow and left ventricular outflow tract velocity time integral metrics respectively. Baseline measures were reassessed between different pacing configurations to control for possible drift.

Patients received dual antiplatelet therapy prior to the procedure in case of the need for emergency percutaneous intervention and received boluses of heparin to keep an activated clotting time (ACT)>300s.

The first three to five beats recorded after a change in pacing protocol were selected for analysis according to the following criteria which are similar to those employed by other groups:[71]

1) Elapse of an initial 10 seconds to stabilise the new pacing parameter
2) Exclusion of the beat preceding an ectopic and the three beats following an ectopic
3) When a physician who was blinded to the study hypotheses deemed the signals to be of sufficient quality for analysis

Data analysis involved a two stage process. The raw data was analysed using the Studymanager programme (Volcanocorps, Philips, Netherlands). Wave intensity analysis was then applied to the coronary data using a custom-made programme, Cardiac Waves (KCL, London). Data were sampled at 250 Hz. Details of the

methodology used to perform wave intensity analysis for data analysis have been previously described. Briefly, a Savitzky–Golay convolution method was adopted, using a polynomial filter to refine the derivates of the aortic pressure and velocity signals.[58,128] The selected three to five consecutive cardiac cycles were gated to the ECG R wave peak, with ensemble averaging of aortic pressure, P_d, APV, and heart rate. Net coronary wave intensity (dI) was calculated from the time derivatives (dt) of ensemble-averaged coronary pressure and flow velocity (U) as follows: $dI=dP_d/dt \times dU/dt$. [58,62] Coincident (microcirculation- derived) backward and (aorta-derived) forward propagating waves were separated assuming blood density to be 1050 kg/m^3 and estimating coronary wave speed using the sum of squares method. [58,61]The area beneath the 2 most prominent wave energies identified were analyzed and included in this article. These were the positive, forward-directed (aorta-derived) compression wave (FCW), occurring at the onset of systole and the backward expansion waves (BEW), the first negative wave occurring at the onset of ventricular relaxation, identified by the onset of diastole. An example of the data following analysis is demonstrated in graphic form in Figure 19.

Figure 19- Example of WI and LV contractility data from a single heart beat

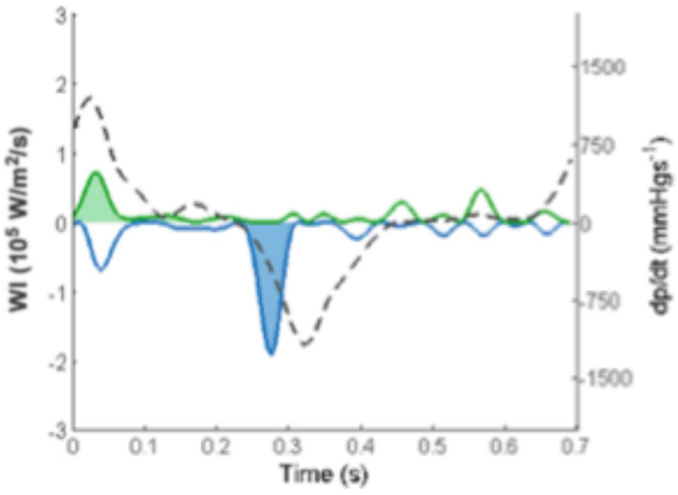

Acute contractility data measured by dP/dt (black dashed line) and the constituent waveforms (forward-travelling waves are shown in dark green, and backward-travelling waves are shown in blue). The large shaded green area is the forward compression wave; the larger blue area is the backward expansion wave. dP/dt, rate of rise of LV pressure; WI, wave intensity.

3.1.4 Statistical Analysis

Statistical analysis was performed using IBM SPSS version 22.0. Rather than assume normality, coronary flow data was analysed as a non-parametric variable using the Friedman's test (the non-parametric equivalent of the ANOVA test for repeated measures.)[71] Where the Friedman test was significant comparisons between pairs of states were made by using the Wilcoxon signed rank test, with probability values calculated comparison-wise. For normally distributed data, paired two-sided student t-tests were used to compare means. Demographic data is presented as means with standard deviations. Data regarding the AV and VV delays is presented as medians and ranges to provide clinically interpretable data.

3.1.5 Results

12 patients consented to take part in the study. In 1 patient it was not possible to complete the protocol due to problems in getting a stable signal from the Combowire and this patient was excluded from further analysis. Patient demographics for the remaining 11 patients are shown in Table 3. There were no complications as a result of the acute procedure. The median AV delay was 125ms (range 100-140ms) and the median VV delay was LV ahead by 30ms (range 0ms - LV ahead by 40ms).

Table 3- Demographic data of patients

	Mean (S.D)
Age (years)	59.9 (9.38)
Gender	9 male, 2 female
Aetiology (ICM- defined as previous infarct of flow limiting coronary disease at angiography)	8 NCM/ 3 ICM
QRS morphology	8 LBBB 2 NSIVCD 1 RBBB
QRS duration (ms)	156.6 (20.1)
EF pre implant (%)	24 (10.5)
Sinus Rhythm	8/11
Time since implant (days)	1027 (967)
ACE inhibitors	11/11
Betablockers	11/11
Aldosterone Antagonists	9/11

3.1.5.1 Effect on coronary flow with different pacing states

There was no change in LAD flow when intrinsic conduction was compared with RV pacing (-4.5%, p=0.123). Conventional biventricular pacing (BIVCS) from the chronically implanted epicardial LV lead increased LAD flow significantly from baseline (+8.7%; p=0.033) and was further increased with the optimal endocardial pacing site (BIVEN) (+27.0%; p=0.021) (see).

Figure 20). BIVEN pacing resulted in an increase in LAD flow from BIVCS but this was not significant (+6.6%; (mean increase from baseline in 5 pts BIVCS +20.2% vs BIVEN +27.0%; p=0.748). APV from the Cx showed no significant variation between baseline, BIVCS, RV and BIVEN p=0.615 (see).

Figure 20).

Figure 20- Percentage changes from baseline of coronary flow (APV) in the LAD and the Cx with different forms of pacing.

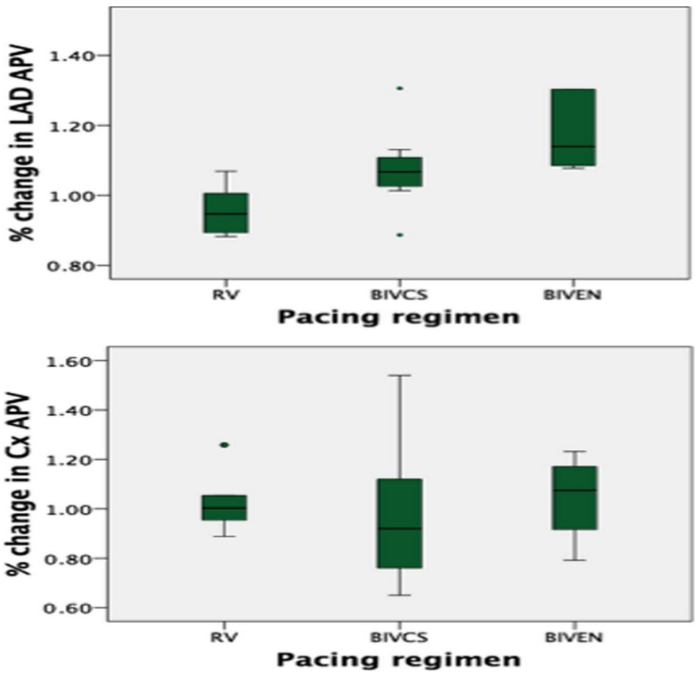

APV, average peak velocity; BIVCS, conventional biventricular pacing; BIVEN, biventricular endocardial pacing; Cx, circumflex artery; LAD, left anterior descending artery; RV, right ventricle.

Analysis of the 8 patients with LBBB demonstrated a significant increase in LAD flow with BIVCS from baseline (+10.2%, p=0.034) with no significant change in Cx flow (p=0.917). Analysis of the 8 patients in sinus rhythm demonstrated a significant

increase in LAD flow with BIVCS from baseline (+10.1%, p=0.005) with no significant change in Cx flow (p=0.6)

3.1.5.2 Effect of pacing on wave intensity analysis energy profile

There was a significant increase in the magnitude of the BEW in the LAD with BIVCS when compared with baseline (mean area 6422.8 $W/m^2/s$ at baseline increased to 7281.9 $W/m^2/s$ with BIVCS; (13% mean increase) p=0.004). BIVEN facilitated a significant increase in the area above the wave to a mean of 8200.3 $W/m^2/s$ vs 5744.1 $W/m^2/s$; p=0.036. The difference between BIVEN LAD BEW and BIVCS LAD BEW was 1594.0 $W/m^2/s$ but this was not significant; p=0.139 (see .

Figure 21).

Figure 21- Percentage change from baseline of the area above the BEW and below the FCW in the LAD with different pacing regimens

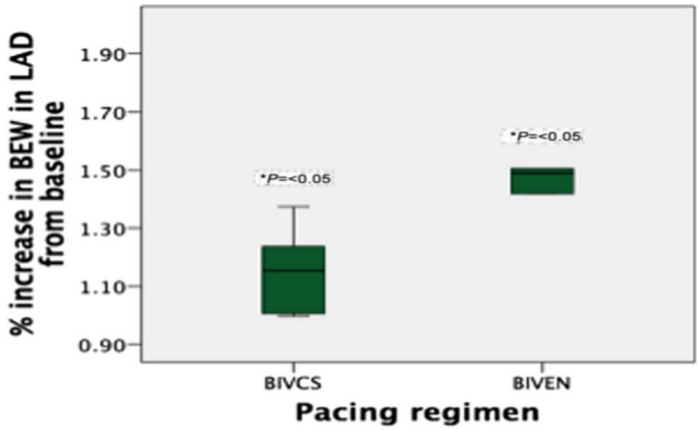

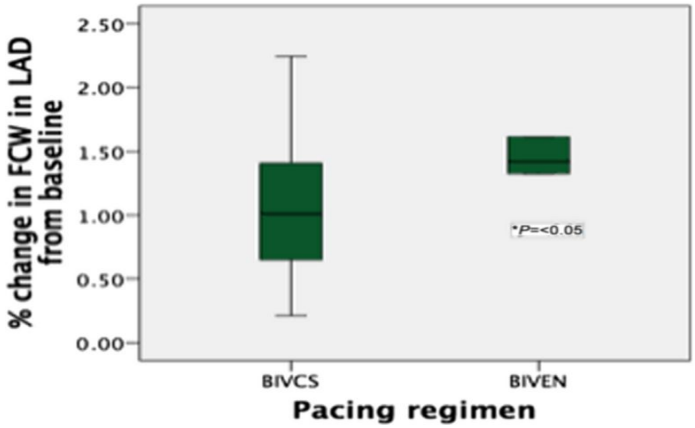

Percentage change from baseline of the area above the BEW and below the FCW in the LAD with different pacing regimens. BEW indicates backward expansion wave; BIVCS, conventional biventricular pacing; BIVEN, biventricular endocardial pacing; FCW, forward compression wave; LAD, left anterior descending artery.

There was no difference in the area under the FCW in the LAD with a mean increase from 2668.5W/m^2/s at baseline to 3027.0 in BIVCS (p=NS). However, the optimal BIVEN position also resulted in a significant increase in the energy of the FCW (mean area 1984.1 8 W/m^2/s to 4220.4 W/m^2/s; (112% mean increase) p=0.048) (see).

Figure 21 and Figure 22).

Figure 22- An example of wave intensity analysis in the left anterior descending artery of 1 patient: (A) baseline, (B) BIVCS, (C) BIVEN. Note the increase in the BEW in BIVCS and the increase in both the BEW and forward compression wave with BIVEN

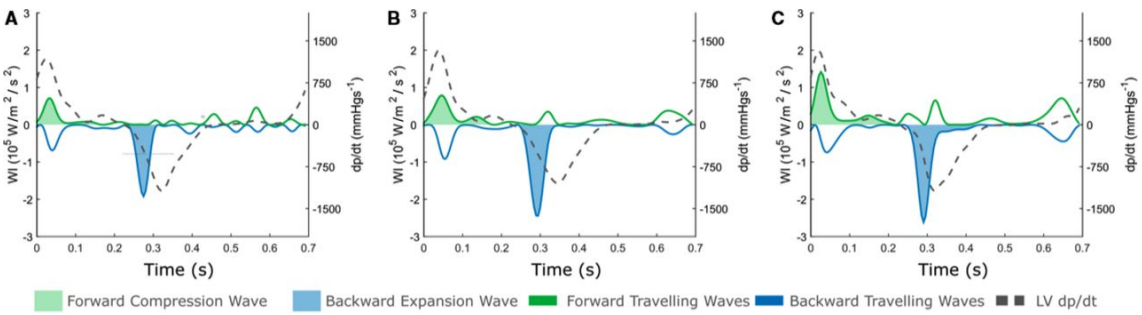

BEW indicates backward expansion wave; BIVCS, conventional biventricular pacing; BIVEN, biventricular endocardial pacing; WI, wave intensity.

There was no difference in the magnitude of the BEW in the Cx with BIVCS when compared with baseline (mean 11047.2 W/m^2/s at baseline reduced to 8666.6 W/m^2/s) (p=0.237). There was a non-significant reduction in the size of the BEW for the patients who underwent the endocardial procedure (mean area under the BEW at baseline 13704.6 8 W/m^2/s vs largest endocardial 5825.5 W/m^2/s; p=0.053). With regard to the area under dominant FCW, there was no change in the energy from baseline with BIVCS (baseline 4501.64 8 W/m^2/s vs BIVCS 3229.2 W/m^2/s; p=0.123) and best BIVEN (baseline 4548.4 8 W/m^2/s vs endocardial 1910.3 W/m^2/s p=0.176)(see Figure 23).

Figure 23- Percentage change from baseline of area above the BEW and below the FCW in the Cx with different pacing regimens

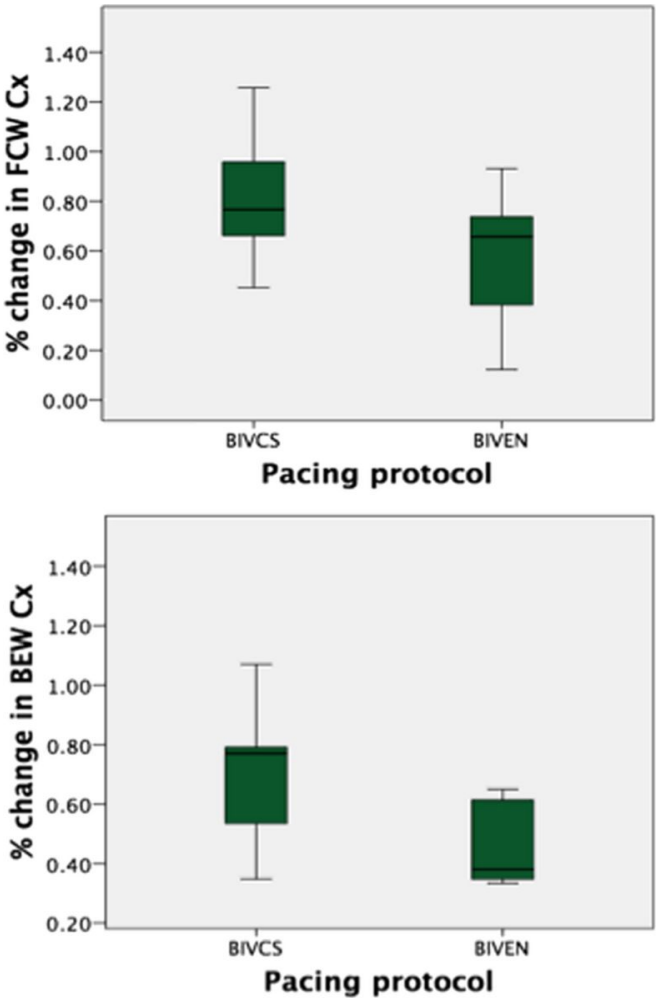

BEW indicates backward expansion wave; BIVCS, conventional biventricular pacing; BIVEN, biventricular endocardial pacing; Cx, circumflex artery; FCW, forward compression wave.

3.1.5.3 Change in timings of coronary waves with application of biventricular pacing: coronary resynchronization

The time to the peak of the dominant BEW was significantly delayed between the LAD and Cx at baseline in patients with a non-ischaemic aetiology (284ms in the LAD compared with 331ms in the Cx (p=0.01)(see Figure 24). This was corrected by BIVCS (mean LAD 289ms vs mean Cx 297ms (p=0.566)) The reduction of the difference

between the time to peak of the BEW in LAD vs Cx by BIVCS was significant (mean 47ms at baseline vs 8ms;p=0.004)(see Figure 24).

When assessing the FCW in a similar manner, the time to peak of the FCW at baseline was significantly different between the LAD and Cx (30ms vs 69ms; p=0.03) with a reduction in the difference of these timings with BIVCS (56ms (LAD) vs 53ms (Cx); p=0.715ms). The reduction of the difference to peak of the FCW was also significant 39 ms vs 3ms; (p=0.008)(see Figure 24).

Figure 24- Coronary resynchronization: Delay between the time from R wave to peak of the FCW and BEW in the LAD artery and circumflex artery corrected by biventricular pacing

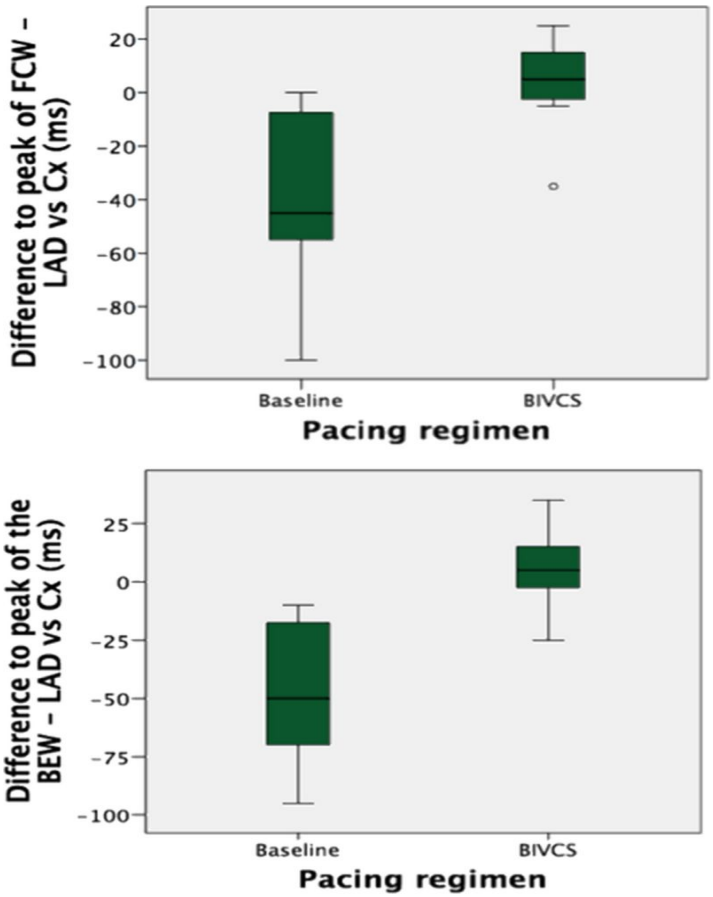

BEW indicates backward expansion wave; BIVCS, conventional biventricular pacing; Cx, circumflex artery; FCW, forward compression wave; LAD, left anterior descending artery.

3.1.5.4 Coronary Flow Velocity Reserve (CFVR) in the LAD and Cx

Hyperaemia was induced at baseline and with BIVCS pacing. There was a significant difference between the baseline LAD CFVR ((mean 2.35) and with BIVCS (mean 2.05);p=0.02). Conversely, there was a non-significant increase in the CFVR in Cx artery from 2.1 to 2.46 with BIVCS pacing; (p=0.349)(see Figure 25).

Figure 25- The effect of withdrawal of CRT on CFVR in chronically implanted CRT patients. BIVCS indicates conventional biventricular pacing

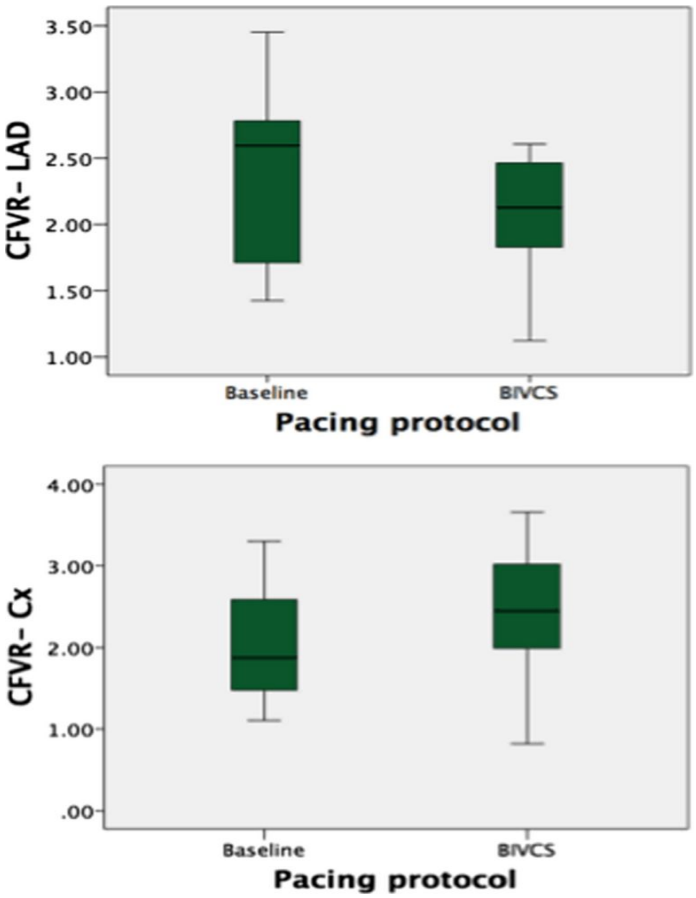

CFVR, coronary flow velocity reserve; CRT, cardiac resynchronization therapy; Cx, circumflex artery; LAD, left anterior descending artery.

3.1.6 Discussion

To our knowledge, this study is the first to comprehensively analyse the effect of epicardial and endocardial pacing on the constituent waveforms of coronary flow in the LAD and Cx coronary arteries.

The principal findings were as follows:

(i) increased flow in the LAD with BIVCS and BIVEN was the result of increase in the BEW.
(ii) In addition to an increase in the BEW, BIVEN pacing increased coronary flow with a significant increase in the FCW in the LAD.
(iii) The time to the peak of the FCW and BEW is homogenized between the LAD and Cx following CRT.
(iv) Cx flow and the constituent determinants of flow did not alter with BIVCS or BIVEN

The effect of biventricular pacing on coronary flow and physiology has been an area of inquiry for many years with discussion as to whether changes noted are merely the result of restoration of synchronous mechanical activation or related to changes in underlying myocardial oxygen supply and demand.[38,46] There has been a gradual refinement of our understanding of how coronary physiology is affected by the dyssynchronous ventricle in recent years.[71,129] However, there remains significant disagreement within the literature as to the effect pacing has on coronary flow.[33,71,130] Our findings provide new insight on the effect of epicardial and LV endocardial pacing on coronary physiology.

3.1.6.1 Coronary flow: comparison with previous studies

The significant increase in flow in the LAD with BIVCS pacing accords with recent studies. [55,129]However, the neutral effect on coronary flow in the Cx artery differs with Itoh et al who found that biventricular pacing increased both LAD and Cx flow but this was in the *acute* setting soon after device implant. Our data may offer some explanation with regard to the differing results of studies looking at regional and global myocardial blood flow non-invasively: these demonstrate either no change in regional myocardial blood flow or correction of a septal perfusion defect with CRT. [41,48,50,52]Our findings of minimal changes in the Cx combined with an increase in the LAD with BIVCS and BIVEN may explain these apparent divergent findings. If we accept that CRT increases global (LMCA) flow velocity, as per Kyriacou et al., our findings suggest that this increase in flow preferentially affects the LAD i.e there is an increase in flow to the LAD with unchanged Cx flow rather than a redistribution of an unchanged global blood flow towards the LAD. This may explain why imaging modalities do not report a redistribution in flow (as there is none) but why CRT has been noted to reverse septal perfusion abnormalities (through increase LAD flow secondary to increased global flow).

Equally, the noted significant reduction in CFVR in the LAD with BIVCS and non-significant increase in CFVR in the Cx contrasts with other studies showing increased CFVR in the LAD with CRT. [129,130]Our findings may appear counterintuitive as one might expect more physiological electrical activation to have a positive effect on parameters such as CFVR. However, our reported reduction in CFVR with BIVCS may

reflect the multi-faceted aetiology of the impaired septal flow at baseline and during hyperaemia in this cohort of patients with *chronically* implanted biventricular devices.

CFVR levels in the LAD and Cx were below those seen in health suggesting a generalised blunted hyperaemic response reflecting microvascular dysfunction which cannot be overcome by CRT. Components of microvascular dysfunction which CRT is likely unable to overcome include the anatomical disruption of the microvasculature by fibrosis and extracellular matrix, decreased myocardial capillary density and impaired capillary vasodilation. [131-134]Indeed the only component of microvascular resistance that seems likely to be altered by CRT is the effect of compressive forces related to high end diastolic pressures.[46]

It is important to interpret our findings within the context of our studied population i.e patients who had chronically received CRT and thus potentially undergone ventricular remodelling. It is suggested that the sudden withdrawal of BIVCS pacing results in new onset mechanical dyssynchrony and thus acts as potential sudden mechanical obstruction to LAD flow with attendant increase in diastolic pressures.[135] When BIVCS pacing is reintroduced this obstruction is relieved resulting in an increase in flow. Conversely this mechanical obstruction can be overcome during hyperaemia both at baseline and with BIVCS pacing as a result of the chronic remodelling process resulting in similar hyperaemic flows. The net effect of this is a reduction in CFVR when BIVCS is compared with baseline. Conversely the flow in the Cx artery is relatively unaffected by the cessation of BIVCS pacing (with a trend to a reduction in flow). In the presence of a fixed hyperaemic flow this will manifest as the non-significant trend towards an increase in the CFVR with BIVCS pacing.

The potential explanation for the increase in LAD flow may be a result of increased contractility. This would be biologically attractive and accord with Kyriacou's work on the effect of CRT on myocardial oxygen demand.[34] The increase in flow in the LAD from baseline to BIVCS could represent a physiological increase in blood flow to help meet the increased myocardial oxygen consumption required as a result of the increased contractility and septal work. However, our findings do not preclude a second possibility that the increase in LAD APV when pacing BIVCS is the result of changes in microvascular resistance secondary to correction of mechanical dyssynchrony and the wave intensity data are consistent with the hypothesis that these local factors may play an important role.

3.1.6.2 Wave intensity analysis of the left sided coronary circulation:

The increase in LAD flow with BIVCS was significantly related to an increase in flow mediated by the BEW suggesting increased suction by improved *regional* relaxation of the microvasculature. The increase in LAD flow during BIVEN was related to an increase in both the FCW and BEW. Whilst the reason for the increase in BEW with BIVEN is likely similar to that proposed for BIVCS, it is suggested that the increase in the FCW in the LAD is likely related to both global effects of forward propulsion but also importantly changes in the septal microvasculature as there was no increase noted in the FCW in Cx. This change in microvasculature might be the result of the more physiological activation pattern that LV endocardial pacing is thought to be able to achieve by early activation of the specialised Purkinje network.[136]

With regard to the Cx artery, we found a non-significant trend to reduction in both the FCW and BEW. With regard to the BEW this would conform with the hypothesis that

BIVCS pacing reduces work in the lateral wall and that therefore the local intramyocardial pressure generated to create the suction for the BEW is reduced. This combined assessment of the changes in the FCW and BEW with different pacing regimens demonstrates that both *regional* and *global* mechanisms are involved in determining coronary flow to different parts of the myocardium. This duality is further developed when considering the synchronisation of timings of the FCW and BEW in the LAD and Cx following CRT.

3.1.6.3 "Coronary Resynchronisation"

By measuring the time to the peak of the FCW and BEW in both the LAD and CX at baseline and with BIVCS pacing we are able to demonstrate for the first time in humans that there is a difference between the timings of flow in the LAD and Cx arteries in dyssynchronous heart failure. Furthermore, we have shown that this is corrected significantly with regard to the time to peak of both the FCW and BEW. The implications of this are twofold. Firstly, such homogenisation is suggestive of generalised cardiac resynchronisation. Secondly however, it has previously been recognised that the waves measured in coronary flow are, in patients with normal coronary arteries, generated by the global effects of cardiac contraction and relaxation causing propulsion of blood forward (FCW) and suction of blood backwards (BEW) respectively. Changes in the size of waves have been correlated to wall thickness in concentric hypertrophy suggesting that waves are dependent on the myocardium and microvasculature per se and are not just generated by the intracavity pressure gradients.[71]

Our findings relating to dyssynchronous heart failure and the effect of BIVCS pacing are the first to demonstrate the effect of both regional and global forces on the coronary waves. It is proposed that the ability of CRT to homogenize these timings suggests that dyssynchrony causes regional changes in the microvascular energetics which are correctable with biventricular pacing. With regard to the FCW the timings are homogenized to a timepoint between the time to peak of the LAD and the Cx at baseline. This accords with the concept that the FCW is generated by the forward propulsion of blood down the coronary arteries as a result of LV systolic contraction. Conversely, the homogenization of the larger BEW is largely achieved by a reduction in the time to peak of the BEW in the Cx artery rather than significant change in the LAD timings. This is biologically attractive as any negative pressure generated in the LV cavity in diastole relies on the microvasculature as a conduit to create the suction for the BEW. Thus delayed lateral wall relaxation before resynchronisation of this conduit will result in a delayed time to peak in the BEW in the Cx artery and the reduction of the time to peak of the BEW that we observed following CRT.

From the clinical perspective, our study offers potentially new explanations as to how conventional CRT may exert its benefit. It is suggested that changes in coronary blood flow and wave energy need to be studied in prospective studies at the time of implant to determine if they may offer a role in patient selection. As noted above, both electrical resynchronisation and correction of mechanical dyssynchrony have not been found to be accurate predictors of response to CRT.[137] Whilst changes in coronary haemodynamics are also unlikely to be a single predictor of response, it may be that they have a role in a more integrated patient selection pathway in difficult cases or be used as a target for "optimisation" in non-responders using emerging non-invasive techniques.[138] Further dedicated studies are required to assess these potential clinical applications.

There is evidence that BIVEN has an acute effect on LV function beyond conventional CRT but further research is necessary to determine the mechanisms by which this occurs. It is again suggested that this be performed at the time of device implant with attention paid to coronary wave energetics as a component in such studies. [32,139]It is highly desirable that we have an understanding of the mechanistic effects of such systems before their use in the clinical environment becomes routine.

3.1.6.4 Study Limitations

The patients studied were not selected for any particular clinical characteristics and reflect a real world CRT population. However our sample size is small and it is important that we remain guarded with regard to the generalizability of our results to the whole CRT population. However, the number of patients studied is similar to other similar invasive studies.[57] The invasive procedural burden for patients is very high and not suitable for routine clinical practice. However, emerging non-invasive techniques[71] to measure wave intensity are increasingly being described and these may allow larger studies to be performed.[138] All patients studied were chronically implanted with CRT devices. This makes extrapolation of our findings to pre-implant patients difficult; however many of the findings could, if anything, be amplified in the pre-implant population. Nonetheless the prolonged time between implantation of the device and study participation means that any association between blood flow changes, wave energetics and "response" to CRT cannot be clearly made. As noted above, further studies at the time of implant are required. By fixing the heart rate we controlled for the effect that changes in chronotropy can cause to inotropy (the Bowditch effect). However, this does prevent reflex heart rate regulation to changes in inotropy.

3.1.7 Conclusions

The data presented develop our understanding of coronary physiology in dyssynchronous heart failure with biventricular pacing beyond the left main coronary artery and give new insight into the effect of regional and global mechanics as well as coronary wave energies on coronary flow. BIVCS and BIVEN increase the microcirculatory derived BEW in the LAD with no change in the Cx artery. The time to peak of the BEW is homogenized in the LAD and Cx following CRT. Together these findings suggest that the coronary BEW is susceptible to changes in local forces rather than being solely dependent on increased global LV systolic and diastolic function as had previously been reported. The demonstrated increase in LAD coronary flow with an increase in the LAD FCW with endocardial rather than epicardial pacing offers offers an exciting mechanism to further increase coronary flow, which may be mediated by a more favourable and physiological activation pattern of the left ventricle.

3.2 CHANGES IN CONTRACTILITY DRIVE CHANGES IN CORONARY FLOW NOT VICE VERSA: INSIGHTS INTO CARDIAC-CORONARY COUPLING

3.2.1 Abstract

Background

Biventricular pacing has been shown to increase both cardiac contractility and coronary flow acutely but the causal relationship is unclear. We hypothesised that changes in coronary flow are secondary to changes in cardiac contractility. We sought to examine this relationship by modulating coronary flow and cardiac contractility.

Methods

Contractility and lusitropy were altered by varying the location of pacing in 8 patients. Coronary autoregulation was transiently disabled with intracoronary adenosine. Simultaneous coronary flow velocity, coronary pressure and left ventricular pressure data were measured in the different pacing settings with and without hyperaemia and wave intensity analysis performed.

Results

Multisite pacing was effective at altering left ventricular contractility and lusitropy (pos. dp/dt_{max} -13% to +10% and neg. dp/dtmax -15% to +17% compared to baseline). Intracoronary adenosine decreased microvascular resistance (362.5 mmHg/s/m to 156.7 mmHg/s/m,$p<0.001$) and increased LAD flow velocity (22cm/s vs 45cm/s,$p<0.001$) but did not acutely change contractility or lusitropy. The magnitude of the dominant accelerating wave, the Backward Expansion Wave, was proportional to the degree of

contractility as well as lusitropy (r=0.47, p<0.01 and r=-0.50,p<0.01). Perfusion efficiency (the proportion of accelerating waves) increased at hyperaemia (76% rest vs 81% hyperaemia, p=0.04). Perfusion efficiency correlated with contractility and lusitropy at rest (r=0.43 & -0.50 respectively,p=0.01) and hyperaemia (r=0.59 & -0.6,p<0.01).

Conclusions

Acutely increasing coronary flow with adenosine in patients with systolic heart failure does not increase contractility. Changes in coronary flow with biventricular pacing are likely to be a consequence of enhanced cardiac contractility from resynchronization and not vice versa.

3.2.2 Introduction

Cross-talk between the coronary vasculature and cardiac muscle has been proposed as a theory to understand the simultaneous effects of coronary blood flow on cardiac contractility and vice versa.[140]

Reduced coronary flow in the Left Anterior Descending (LAD) Artery and corresponding perfusion defects have been noted in patients with dyssynchronous left ventricular activation.[41,52,53] Furthermore, Cardiac Resynchronization Therapy (CRT) has been shown to increase LAD flow and correct these perfusion defects.[57] It is unclear whether the observed increases in LAD flow are a bystander effect of electrical resynchronization or whether the increase in coronary flow is mechanistically important in mediating some of the physiological effects of CRT, resulting in the recruitment of hibernating myocardium.[35]

Coronary wave intensity can be calculated from simultaneously acquired coronary flow and pressure measurements. It provides temporal information on the nature and origin of forces that drive and impede myocardial perfusion.[65] This makes it an ideal tool to investigate cardiac-coronary coupling, specifically the relationship between changes in LAD flow, acute left ventricular (LV) contractility and electrical activation. Typically, as many as six waves have been described with the vast majority of flow being driven by a dominant backward travelling expansion wave (BEW) that 'sucks' blood through the coronary artery and a dominant forward compression wave (FCW) which derives from the ejection of blood from the left ventricle into the aorta and down the coronary arteries.[62,64] The effect of changes in both contractility and microvascular resistance on coronary wave energy have previously been studied in a canine model and used to identify the causes of the systolic impediment to coronary flow velocity.[141] Kyriacou et al. demonstrated in a group of patients with CRT that an acute increase in contractility was associated with an increase in the BEW in the left main coronary artery.[71] This is the only clinical study to date where coronary wave energy and coronary flow have been correlated with changes in acute LV contractility. Contractility and microvascular resistance have not previously been *simultaneously* modulated in humans and hence their relative impact on wave energy remains unclear.

We hypothesised that increased LAD coronary flow with hypaeremia would not effect LV contractility. We also sought to characterise the relationship between changes in acute LV contractility and lusitropy with the dominant wave energies driving coronary flow velocity in patients with dyssynchronous heart failure.

3.2.3 Methods

We investigated a group of patients with a CRT device as a clinical model that allowed manipulation of both coronary blood flow and contractility. Patients who had been implanted with a CRT device and were known to have unobstructed coronary arteries at invasive angiography were invited to take part.

Cardiac contractility and lusitropy were altered by pacing from different points in the left and right ventricles. The first derivative of LV pressure was used to assess contractility and relaxation (pos. dp/dt_{max} and neg. dp/dt_{max} respectively). Microvascular resistance was altered by inducing hypaeremia with intracoronary adenosine.

The study received approval from the Local Research Ethics and was conducted in accordance with the Declaration of Helsinki. All patients gave written informed consent prior to taking part in the study.

Patients received dual antiplatelet therapy prior to the procedure and received unfractionated heparin to keep an activated clotting time >250s. Arterial access was gained via femoral and radial arteries. A 0.014″ Doppler wire (ComboWire^{TM} model 9500, Volcano Corporation) was advanced to the proximal LAD to make simultaneous measurements of intracoronary pressure and Doppler flow velocity. A Primewire (Volcano Corporation) was placed in the LV cavity to measure pos. dp/dt_{max} and neg. dp/dt_{max}.

Acute contractility was modulated by pacing the ventricle from different points using the in situ CRT device. The site of ventricular stimulation was altered allowing atrio-

ventricular synchronous pacing from the right ventricle alone, the left ventricle alone and biventricularly via the epicardial pacing lead. In 5 of the 8 patients, we also used a roving endocardial pacing catheter to perform LV endocardial pacing, which additionally allowed atrial synchronous biventricular endocardial pacing (with both a septal and lateral position used for the endocardial component) and simultaneous right ventricular endo, LV endo and LV epicardial pacing. All studies were performed with pacing at 10 beats above the intrinsic atrial rate to control for the Bowditch effect.[127] An atrially paced, ventricular sensed rhythm was used as the baseline in patients with in tact AV nodes. An atrially paced, right ventricular paced rhythm was used as the baseline in patients with AV block.

Intracoronary adenosine was given as a bolus dose of 36 microgrammes to induce hyperaemia, at each pacing protocol.

2.3 Data selection and beat analysis

The first three to five beats recorded after a change in pacing protocol were selected for analysis according to our previously published protocol. A period of at least 10 seconds was allowed for stabilisation with each new pacing parameter.

Signals were sampled at 200 Hz and the raw data was exported to a custom-made study manager programme (Academic Medical Center, Amsterdam, Netherlands) for data extraction of selected beats at each different condition. Wave intensity analysis was then applied to the coronary data using custom-made software, "Cardiac Waves" (King's College London, London, United Kingdom). Details of the methodology used to perform wave intensity analysis have been previously described.[69] Briefly, a Savitzky–Golay convolution method was adopted using a polynomial filter to refine the derivatives of the intracoronary pressure and velocity signals. The selected three to five

consecutive cardiac cycles were gated to the ECG R wave peak, with ensemble averaging of aortic pressure, distal coronary pressure (P_d), Average Peak velocity (APV) and heart rate. Net coronary wave intensity (dI) was calculated from the time derivatives (dt) of ensemble-averaged coronary pressure and flow velocity (U) as follows: $dI=dP_d/dt \times dU/dt$. Net wave intensity was then separated into forward and backward components.

The area beneath the 4 most prominent wave intensity peaks identified were analysed and included in this article. These are 1) the positive, aorta-derived FCW, occurring at the onset of systole, 2) the negative backward compression wave (BCW) also occurring at the onset of systole, 3) the negative BEW, the first backward wave occurring after the onset of ventricular relaxation, identified by the onset of diastole and 4) the positive Forward Expansion Wave (FEW)(see Figure 19).

Coronary Flow Velocity Reserve was calculated as the ratio between APV at rest and hyperaemia. Microvascular resistance (MR) was calculated as the ratio of the P_d and APV.

We also calculated coronary perfusion efficiency (P.E). This is a metric which quantifies accelerating wave energy as a proportion of total coronary wave energy generated by the FCW and BEW which are the waves that theoretically drive rather than impede coronary flow velocity.[68] PE is calculated using the magnitude of the areas under the curve (AUCs) of the component waves i.e.

$$(FCW+BEW))/(FCW+FEW+BEW+BCW).$$

Statistical analysis was performed using IBM SPSS 21.0. Baseline demographics are presented as either mean & standard deviations or as proportions. Baseline clinical haemodynamic data are presented as median with interquartile ranges. Normally

distributed data are compared using paired and independent student t-tests and non-normally distributed data using the non-parametric equivalents. Similarly, Pearson and Spearman correlation co-efficients are quoted to express associations between variables for normal and non-normally distributed data respectively.

3.2.4 Results

Acute contractility and coronary data were obtained in 39 different pacing settings in the LAD from 8 patients (see Table 4). There were no complications arising from the study protocol.

Table 4- Demographic data

Characteristics	Mean (+/- S.D) or Percentage
Age (y)	56.9 (10.6)
Male	7/8
QRS duration pre CRT (ms)	150.8 (23.4)
Ejection Fraction (%)	23 (10.8)
NYHA Class	2.7 (0.49)
Ace Inhibitors / Angiotensin Blockers	8/8
Betablockers	8/8
Aldosterone Receptor Antagonists	6/8

Baseline pos. dp/dt max was 1110 mmHg/s (IQR 711 to 1177 mmHg/s) and baseline neg. dp/dt_{max} was -912 mmHg/s (IQR -861 to -1214 mmHg/s). Baseline APV was 17.4cm/s (IQR 13.7 to 24.7cm/s) and CFVR was 2.3 (IQR 1.5 to 2.7).

Pacing via different modes led to significant variation in contractility and lusitropy. The percentage change from baseline in pos. dp/dt_{max} varied between -13% (IQR -7% to -14%) and +10% (7.5% to 14.5%) and in neg. dp/dt_{max} between -15% (IQR -13% to -22%) and +17% (IQR 9% to 33.8%). The effect of hyperaemia on different coronary wave energies is shown in Table 5.

Table 5-The effect of hyperaemia on the different coronary wave energies

	Rest median (IQR)	Hyperaemia median (IQR)
FCW LAD	2774 (1501 to 3614) p<0.01 vs hyperaemia	5622 (3753 to 9756)
BCW LAD	2370 (1815 to 3784) p<0.01 vs hyperaemia	3703 (2178 to 5137)
BEW LAD	7118 (4713 to 9098) p<0.01 vs hyperaemia	12068 (8880 to 18103)
FEW LAD	176 (35 to 493) p<0.01 vs hyperaemia	393 (201 to 1017)

3.2 Variation in coronary flow and LV contractility

Across the range of pacing settings, there was a slight reduction in LV contractility (pos. dp/dt_{max}) with hyperaemia vs rest (1037 +/- 336 mmHg to 1056 +/- 330 mmHg, p=0.05) and no significant change in lusitropy (neg. dp/dt_{max}, -908 +/- 263 mmHg versus -905 +/- 261 mmHg, p=0.25). Coronary flow velocity in the LAD increased significantly with hyperaemia (22.2cm/s +/- 8.6 to 45.3 cm/s +/-18.1; p<0.001) due to a fall in microvascular resistance from 362.5 (sd 125.5) mmHg/s/m to 156.7 (sd 50.2) mmHg/s/m. Resting microvascular resistance correlated with neg. dp/dt_{max} (r=-0.46, p<0.01) but not pos. dp/dt_{max} r=0.25,p=0.13. There was no correlation between minimal microvascular resistance and contractility indices. The comparison of coronary wave energies at rest and hyperaemia are shown in Table 5.

3.3 Relationship between coronary wave indices and LV haemodynamics

BEW magnitude correlated with the degree of contractility and lusitropy (r=0.47, p<0.01 and r=0.50, p<0.01 respectively) at rest. In contrast, there was no relationship between the magnitude of the FCW and LV indices. The magnitude of both BEW and FCW at hyperaemia correlated with the degree of contractility (FCW, r==0.37,p=0.02;BEW, r=-0.65,p<0.01) (see

Figure 26) and lusitropy (FCW,r=-0.67,p<0.01, BEW,r=0.72,p<0.01 for each) (see

Figure 27).

Figure 26- The correlations between the Forward Compression Wave and Backward Expansion Wave with pos. dp/dtmax at hyperaemia

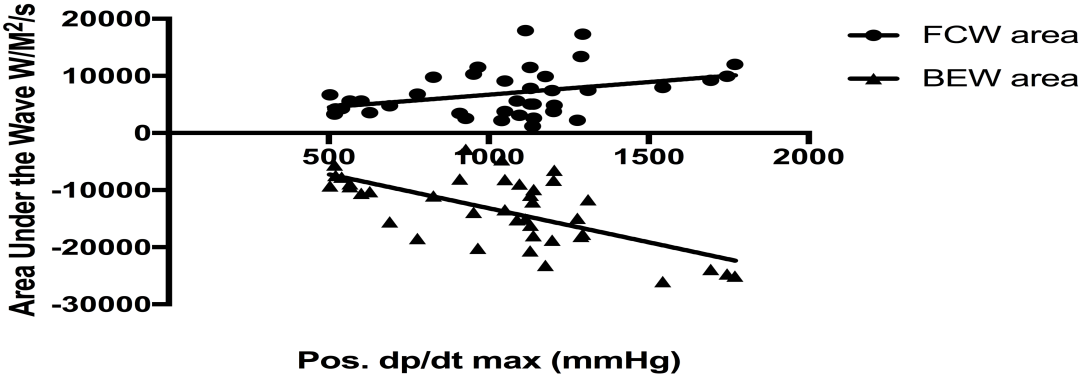

BEW- Backward Expansion Wave; FCW- Forward Compression Wave

Figure 27- The correlations between the Forward Compression Wave and the Backward Expansion with neg dp/dt max at hyperaemia

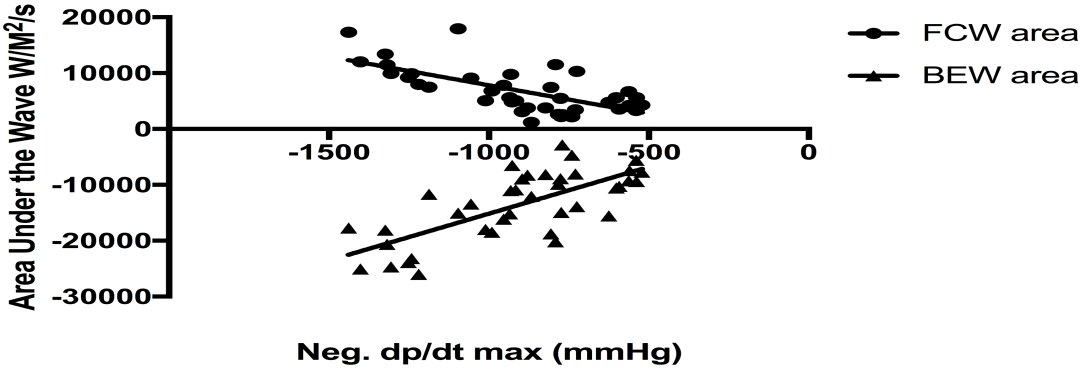

BEW- Backward Expansion Wave; FCW- Forward Compression Wave

Perfusion efficiency (proportion of accelerating wave energy) was 76.2% +/- 7.0% at rest and 80.8% +/- 9.8% at hyperaemia (p= 0.04). Perfusion efficiency correlated with contractility and lusitropy at rest (r=0.43,p<0.01 and r=-0.50,p=0.01) and more so during hyperaemia (r=0.59, p<0.01 and r=-0.6, p<0.01) (see Figure 28).

Figure 28- Increased perfusion efficiency in the LAD correlates with increased contractility and lusitropy at hyperaemia

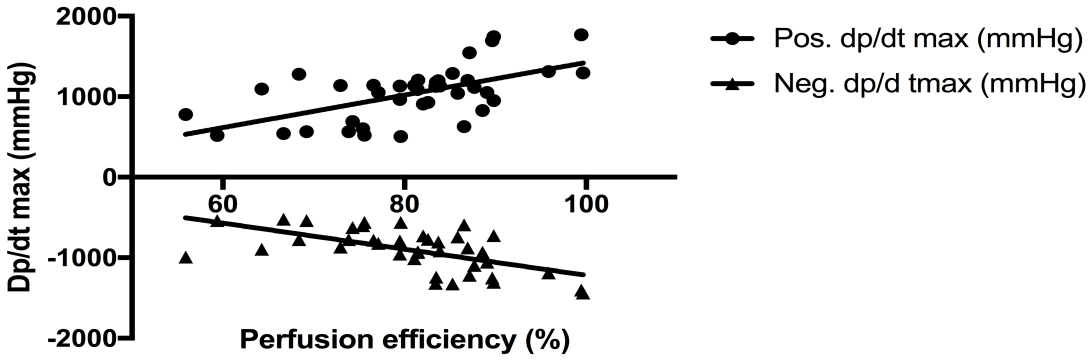

3.4 Summary of Main Findings:

The main findings of this study are

1) Ventricular stimulation from different sites is an effective means of modulating contractility and lusitropy in patients who have impaired left ventricular function and can be used in an experimental model to examine coronary-cardiac coupling.

2) The magnitude of the dominant accelerating wave, the BEW, and total accelerating wave energy correlate with the degree of left ventricular lusitropy and contractility.
3) Increasing coronary flow by pharmacological hyperaemia has no acute effect on LV contractility indices.

4.0 Discussion:

We believe this is the first description of a clinical model based on the simultaneous use of multisite pacing and adenosine induced hyperaemia to assess the effects of cardiac contractility and microvascular resistance on coronary wave energy. The large changes in coronary flow created by directly reducing microvascular resistance have no effect on indices of acute contractility, although the latter have been shown to have a significant effect on the coronary wave intensity profile. In the previous experiment I demonstrated that acutely increased LAD flow velocity correlates with increased pos. dp/dt_{max} in CRT patients compared to right ventricular pacing, although the mechanistic relationship between LV contractility and coronary flow was unclear at that stage. The current study provides clarity on the causal relationship and suggests that the previously observed changes in LAD flow are a consequence of resynchronization rather than being a determinant of the acute response in LV contractility following CRT.[142] It has previously been shown in an animal model that there is a minimum perfusion requirement, within the pathophysiological limits seen in vivo, to allow a positive acute response to CRT.[35] Our data suggest that where this perfusion threshold is met, a further increase in coronary blood flow velocity will not result in increased contractility.

It is possibile that adenosine induced increase in flow velocity represents a distinct entity to the autoregulatory changes that may occur at the time of a pacing-mediated increase in contractility. For instance, the hyperaemic response will result in a matched increase in myocardial venous emptying and thus any changes in contractility as a result of the Gregg effect through stretch induced calcium release and increased calcium sensitivity may not occur. However our model is unlikely to be affected by either the Anrep and Gregg effect as each pacing protocol lasted for no more than 30s and both the Anrep and Gregg effects take longer to exert their influence on cardiac contractility.[143]

Conventional interpretation of the dominant wave energy profiles in the coronary arteries links them to left ventricular contractility and lusitropy. This relationship has previously been confirmed in vivo, in the LMCA, although most studies reporting changes in coronary wave energy have investigated more distal epicardial arteries.[69] The most dominant wave is the BEW, an accelerating wave in early diastole that coincides with the rapid fall in ventricular pressure. We have demonstrated that the magnitude of the BEW is proportional to the degree of lusitropy as quantified by the neg. dp/dt_{max} in the left ventricle at rest. The fact that the BEW magnitude also correlates well with pos. dp/dt_{max} suggests that contractility and lusitropy are coupled in this population.

The other important accelerating wave is the FCW, which corresponds temporally to peak aortic pressure and systolic coronary blood flow. While left ventricular contractility is a determinant of peak aortic pressure, at rest we did not find a correlation between pos. dp/dt_{max} and the FCW magnitude, suggesting that this relationship may be more complex as has been suggested in previous animal studies.[71] Indeed, these studies have failed to show a strong correlation between LV contractility in the LAD and our

findings are in keeping with this. An increase in the FCW has been noted in the aorta alongside a presumed increase in LV contractility with dobutamine but this has not been demonstrated in the coronary circulation and ours is the first in human experiment to provide a detailed examination of these relationships when contractility is being measured.[144]

It may be that the lack of correlation between the FCW and contractility is due to the CRT model itself, in that LBBB ventricular conduction is asynchronous and as such this may disrupt the correlation between contractility and the FCW via the LAD.[46,145] From the clinical perspective, it is clear that the changes in LV contractility are not the result of changes in coronary flow and it appears that the noted changes in WIA are a passive phenomenon related to changes in LV haemodynamics.

At hyperaemia both the FCW and BEW correlated with both pos. dp/dt_{max} and neg. dp/dt_{max}. Both the FCW and BEW are thought to be generated by changes in intracavity LV pressure. If one removes the insulator effects of the microvasculature with adenosine then the waves should better correlate with acute measures of contractility and lusitropy. This would be particularly the case with the BEW which "sucks" blood during diastole towards the LV cavity via the microvasculature from the epciardial arteries. If the resistance in the microvasculature is removed with adenosine then an impediment to this relationship is removed. Indeed, this may account for the stronger correlations being seen with the BEW than the FCW as well as the improved correlations noted at hyperaemia.

A further explanation for the better correlation of the BEW than the FCW to LV haemodynamics may simply relate to the differing order of magnitude of the two waves,

with the area under the curve of the BEW being typically 3 times larger than the FCW making it less prone to noise and sampling error within the experiment. This might account for less pronounced and clear correlations in the data.

Further research is therefore required to elucidate the FCW and pos. dp/dt_{max} relationship.

The ratio of accelerating to decelerating wave energy can be regarded as a measure of myocardial perfusion efficiency and this metric has previously been applied to understanding altered coronary wave profiles in symptomatic aortic stenosis and in hypertrophic obstructive cardiomyopathy.[67,68] Our data show that enhanced contractility and lusitropy at rest are associated with greater perfusion efficiency and that these correlations are stronger at hyperaemia. These findings are consistent with previous work that has shown biventricular pacing to be highly efficient when it increases cardiac contractility with favourable changes in cardiac work at minimal cost with regard to oxygen demand.[33,34,135] It should be noted that our data show improved perfusion efficiency rather than coronary flow per se.

Study limitations

Due to the complexity of the procedure, the number of patients investigated was small which limits the statistical power of the study and may affect the generalizability of our conclusions. This limitation applies to similar complex invasive clinical studies.[72] The use of pos. dp/dt_{max} and neg. dp/dt_{max} to assess the acute haemodynamic response of CRT is well validated in CRT research.[146] Whilst other measures of contractility can be used, the use of a conductance catheter for example would have increased the procedural burden to an unacceptably high level. Furthermore, whilst peak measures

may vary to some extent, the variability would not be sufficient to negate our chief clinical finding that a significant increase in coronary flow does not result in a significant increase in LV haemodynamics. Nonetheless it is important that future studies consider experimental methodologies that might allow other measures of contractility and relaxation to be assessed. Finally, we have looked at the relationship between coronary haemodynamics and acute changes in contractility and lusitropy. Whether these conclusions can be applied to interpreting the chronic remodelling and long-term changes in myocardial perfusion in patients undergoing CRT needs further exploration.

We calculated wave speed using the sum of squares method; however, during hyperaemia, the wave speed estimated using this method might differ from the true wave speed.[147]

3.2.5 Clinical and Research Implications

- Changes in coronary wave energy and flow velocity seen with different types of pacing do not cause changes in acute cardiac contractility but conversely, the changes in coronary blood flow and wave intensity are the result of changing contractile force. Thus whilst there may be a minimal perfusion required for CRT to exert its benefits, it is unlikely that treatments aimed at increasing coronary flow will improve ventricular function per se in patients with unobstructed coronary arteries.[35]

- Varying the site and mode of pacing, using a multisite model, successfully alters acute left ventricular contractility and lusitropy in patients with contractile

dyssynchrony. This model could be used to elucidate the mechanism and evaluate the efficacy of potential therapies in future.

3.2.6 Conclusions:

We report the successful implementation of a novel model in heart failure patients that allows the acute manipulation of the two main determinants of coronary flow (LV contractility and microvascular resistance).

Increasing coronary flow did not result in increased contractility in this cohort of patients with normal coronary arteries and systolic heart failure, whereas altering LV pacing site did. We can conclude that any observed changes in coronary haemodynamics with biventricular pacing are likely a consequence of improved cardiac contractility from resynchronization-related cardiac output changes, rather than the cause of enhanced cardiac contractility.

Chapter 4 ADVANCED IMAGING AND ELECTROGRAM INTERPRETATION TO PREDICT RESPONSE TO CARDIAC RESYNCHRONISATION THERAPY AND PREDICT RISK OF VENTRICULAR ARRHYTHMIA

4.1 SUBSTRATE DEPENDENT RISK STRATIFICATION FOR IMPLANTABLE CARDIOVERTER DEFIBRILLATOR THERAPIES USING CARDIAC MAGNETIC RESONANCE IMAGING: THE IMPORTANCE OF T1 MAPPING

4.1.1 Abstract

Introduction:

The role of implantable cardioverter defibrillators in non-ischemic cardiomyopathy is unclear and better risk-stratification is required. We sought to determine if T1 mapping predicts appropriate defibrillator therapy in patients with non-ischemic cardiomyopathy. We studied a mixed cohort of ischemic and non-ischemic patients to determine whether different CMR applications (T1 mapping, late gadolinium enhancement and Grayzone) were selectively predictive of therapies for the different arrhythmic substrates.

Methods:

We undertook a prospective longitudinal study of consecutive patients receiving defibrillators in a tertiary cardiac center. Participants underwent CMR myocardial tissue-characterization using T1 mapping and conventional CMR scar assessment before device implantation. QRS duration and fragmentation on the surface

electrocardiogram were also assessed. The primary endpoint was appropriate defibrillator therapy.

Results:

130 patients were followed up for a median of 31 months (IQR (+/-9 months). In non-ischemic patients $T1_{native}^{-}$ was the sole predictor of the primary endpoint (HR 1.12 per 10ms increment in value (95% C.I 1.04-1.21; $p \leq 0.01$). In ischemic patients, $Grayzone_{2SD\text{-}3SD}^{-}$ was the strongest predictor of appropriate therapy (HR 1.34 per 1% left ventricular increment in value (95% C.I 1.03-1.76;p=0.03). QRS fragmentation correlated well with myocardial scar core (ROC AUC 0.64; p=0.02) but poorly with $T1_{native}^{-}$ (ROC AUC 0.4) and did not predict appropriate therapy.

Conclusions:

In the medium-long term, $T1_{native}^{-}$ mapping was the only independent predictor of therapy in non-ischemic patients whereas Grayzone was a better predictor in ischemic patients. These findings suggest a potential role for $T1_{native}^{-}$ mapping in the selection of patients for ICDs in a non-ischemic population.

4.1.2 Introduction

Implantable cardioverter defibrillators (ICD) are an effective therapy for life-threatening ventricular arrhythmias (VA).[89] Arrhythmic risk stratification however is imperfect with a significant number of ICD recipients not receiving therapy. The recently published DANISH trial failed to demonstrate a long-term survival benefit in a non-ischemic, primary prevention population of patients implanted with ICDs compared with a matched cohort without an ICD.[91] However, the study demonstrated a significant reduction in sudden cardiac deaths in the ICD population leading the authors to suggest that there is a need for better risk stratification in the non-ischemic population who receive an ICD under current guidelines. [148]There is also growing evidence that ventricular tachycardia (VT) ablation may have a prophylactic role in ICD patients, delaying the time until VA. [149,150]This may be clinically beneficial as appropriate ICD therapies have been shown to be a bad prognostic indicator.[151] Improved risk stratification of VA in patients prior to ICD implantation is therefore desirable as it may enhance patient selection with regard to both device eligibility and suitability for prophylactic VT ablation.

Cardiac Magnetic Resonance Imaging (CMR) has the potential to improve this risk stratification; it can identify areas of myocardial scar which act as substrate for VA in both ischemic and non-ischemic cardiomyopathy (ICM & NCM).[95,103,152] Patients with ICM often have regional fibrosis while NCM patients may exhibit a more diffuse pattern of fibrosis.[153] Advanced tissue characterisation by CMR to assess the peri-infarct region or Grayzone has been shown to predict VA in ICM patients.[98] Diffuse myocardial fibrosis acts as potential VA substrate in NCM and can be quantified non-

invasively using CMR protocols such as T1 mapping. [80,81,154]Native T1 mapping ($T1^{-native}$) using CMR allows the quantitative assessment of myocardial tissue in vivo without the administration of contrast and is elevated in the presence of edema, diffuse fibrosis and myocardial scarring. The $T1^{-native}$ value is thus an inherent tissue- specific property and these values have been shown to be highly effective in differentiating healthy myocardium from diffusely diseased tissue.[155] We have previously demonstrated that T1 mapping predicts appropriate ICD therapy in a mixed cohort of ICM and NCM ICD patients at 15 month mean follow up.[101] It is not clear whether $T1^{-native}$ remains predictive of VA in the medium to long term in ICD patients and whether the different MRI protocols assessing focal and diffuse fibrosis have specific value for ICM and NCM respectively.

Given the pathophysiological mechanisms of VA, we hypothesized that Grayzone assessment would be the most powerful predictor of VA in the ICM population whereas T1 mapping would be the most powerful predictor of VA in NCM patients. We also hypothesized that non-invasive markers such as surface ECG fragmentation (fQRS) would correlate with CMR indices of scar and fibrosis and predict VA.

4.1.3 Methods

Consecutive patients undergoing ICD implantation for primary and secondary prevention between May 2011 and January 2013 in our hospital were invited to participate in this prospective study. All patients were on optimal medical therapy including anti-arrhythmic therapy as per their attending cardiologist. The study protocol was approved by the South London Research Ethics Committee and conducted in accordance with the Declaration of Helsinki. All study participants underwent CMR

assessment and coronary angiography before device implant. Ischemic etiology was defined by standard criteria (presence of any epicardial coronary artery stenosis >75%, prior history of myocardial infarction or coronary revascularization with a scar pattern consistent with myocardial infarction on CMR imaging) and NCM by the absence of the above criteria

4.1.3.1 CMR imaging protocol and analysis:

The details of the CMR protocol are described in the Methods section. In brief, CMR imaging was performed using a 1.5-T scanner with a 32-channel coil (Philips Healthcare, Best, The Netherlands). Contrast injection (gadobutrol 0.2mmol/kg body weight) was used for CMR scar assessment from which scar indices were calculated using both the 2-standard deviation (SD) method ($Scar_{-2SD}$), (defined as the region with signal intensity (SI) 2 SD above the remote reference myocardium) and the full-width half-maximum (FWHM) method ($Scar_{-FWHM}$), defined as the region with SI above the 50% of the maximal SI of the enhanced area. To determine the extent of scar distribution we also extended the 2-standard deviation method up to 6 standard deviations (see Figure 29). The extent of the Grayzone was quantified as previously described.[156] Both the Grayzone and scar indices were indexed as a percentage of LV mass for analysis.

Figure 29- Acquisition of Grayzone and native T1 data.

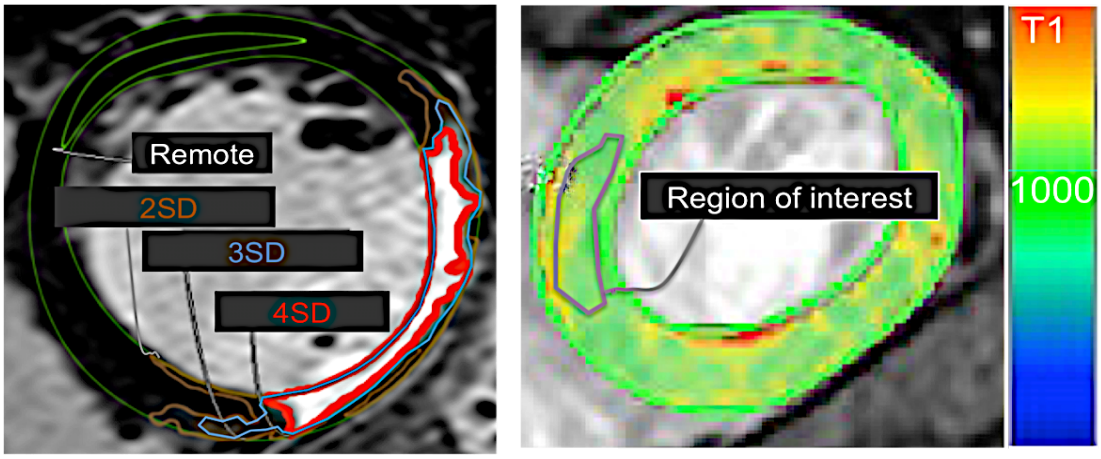

Left panel: A late gadolinium mid-ventricular slice CMR demonstrating the acquisition of scar data using the Standard Deviation (SD) technique. Note the remote reference point and diminishing size of scar as SD increases. Right panel: A T1 map of a mid-ventricular CMR slice with a mid-septal region of interest used for analysis.

A single mid ventricular short-axis slice (in the same geometry as the mid-ventricular CMR slice) was acquired for T1 mapping both before and after the administration of contrast using a modified Look-Locker inversion-recovery sequence with 11 phases (3+3+5) (repetition time/echo time = 3.3/1.5ms; flip angle =50°; voxel size = 1.8 x 1.8 x 8mm; with heart rate adapted trigger delay and adiabatic prepulse to achieve a complete inversion) (see Figure 29). Two independent CMR experts blinded to the study endpoint evaluated the CMR images separately. Discrepancies were adjudicated by joint discussion.

4.1.3.2 ECG Protocol- Assessment of fragmentation

The details of ECG assessment are described in the Methods section. Briefly, standard 12-lead ECGs recorded at the standard sweep speed of 25 mm/s were collected prior to

device implant. These were analysed by two cardiologists blinded to patient characteristics and endpoints to assess for fQRS. In case of discrepancy, the data were jointly reviewed with a third expert to reach a consensus. The assessment of fQRS was performed according to previously published criteria with QRS duration >120ms differentiating wide from narrow for the purposes of fQRS analysis.[108,109] This allowed assessment of fQRS as a categorical variable for all QRS durations.

4.1.3.3 Follow up Endpoints

All patients underwent ICD or Cardiac Resynchronization Therapy-Defibrillator implantation. A standardized program for VA detection and therapy was used.[101] (VA >170 beats/min with detection count >16 intervals received Anti-Tachycardia Pacing (ATP) and then shock therapy if ATP failed. VA> 210 beats/min, detection count: 24/30 intervals were treated with shock therapy. Standard supraventricular tachycardia detection discriminators were enabled according to the recommendations of device manufacturers (St Jude Medical Inc, St Paul, MN and Medtronic, Minneapolis, MN; onset: 81% for Medtronic devices and 18% for St Jude Medical devices; stability: 40ms for both types of device; morphology: passive.) Patients were followed up at 3-month intervals and at each follow-up an experienced device physiologist reviewed any recorded events with an electrophysiologist with both investigators blinded to the CMR data. Remote monitoring was applied where available and patients were encouraged to perform downloads if they felt symptomatic or thought they had received a therapy. Downloads were reviewed in the same manner as the standard follow ups and patients were asked to attend pacing clinic urgently where therapy had been applied. Death was ascertained by review of hospital medical records and if there was concern about loss of follow up, the family physician was contacted for clarification.

The primary endpoint was the delivery of appropriate ICD therapy for VT or ventricular fibrillation. A composite secondary endpoint of appropriate therapy or death was also assessed.

4.1.4 Statistical Analysis

Continuous demographic variables are shown as the mean ± SD; time to events are shown as median ± Inter quartile range (IQR) and categorical variables are shown as percentages. The unpaired Student's t-test was used to compare normally distributed continuous variables; otherwise the Mann-Whitney U or Wilcoxon test was used. Categorical variables were compared using the $\chi 2$ test. The 95% confidence interval (CI) was determined on the basis of the normal distribution of variables. The first episode of appropriate therapy or death was considered as the event of interest for quantifying various associations depending upon the endpoint being assessed. Cox proportional hazard regression analyses were performed to assess the univariable and multivariable adjusted association between pre-specified variables and the primary endpoints. For multivariable-adjusted analyses, a forward selection process using only variables significantly associated with the outcome of interest in univariable analyses (at $p<0.05$) was used to further determine any independent predictors of the primary endpoint. All reported associations in this study are hazard ratios (HRs) with their corresponding 95% confidence intervals. Only patients who had complete information on CMR–derived indices and T1 mapping–derived indices were included in multivariable adjusted analysis.

The multivariable adjusted analysis studied each of the CMR indices that rely on late gadolinium enhancement (scar, Grayzone and midwall-fibrosis (NCM only)) separately to avoid confounders and limit the number of variables in each model. $T1_{native}$ and $T1_{post}$ were analysed as continuous variables with HRs reported for every 10ms increment increase in T1 value. Both the Grayzone and scar indices were indexed as a percentage of LV mass and analysed as continuous variables and HRs calculated for every 1% increase.

Receiver operating characteristics (ROC) curves using $T1_{native}$ and $Grayzone_{2SD\text{-}3SD}$ were plotted to identify variable cut-off points with 90% sensitivity to discriminate the primary endpoint. The estimated cut-off values were retrospectively used to reclassify and dichotomize the study subjects into high-and low-risk categories determined by whether subjects had met the primary endpoint. Kaplan-Meier survival curves were then plotted to study the cumulative event rates between groups of participants, with the log-rank test providing further evidence regarding any significant differences between them. All the above analyses were performed for the total population and for each etiology separately. All data analyses were performed using SPSS statistical software (version 23, IBM, NewYork, NY).

4.1.5 Results

A total of 130 patients were recruited, 72 with ICM (55.4%) and 58 with NCM (44.6%). Etiologies of the NCM cohort were 52/58 idiopathic dilated cardiomyopathy, 5/58 with hypertrophic cardiomyopathy and 1/58 with sarcoidosis). Of the entire cohort 93/130 ICD recipients (71.5%) were implanted with an ICD for a primary prevention indication. All patients' imaging was analyzed for Grayzone and scar core. One hundred

study participants underwent T1 mapping and, of this subset, 95 paired native and post contrast T1 mapping images were suitable for analysis. Due to a number of clinical considerations such as claustrophobia, lack of contemporaneous haematocrit and poor breath-holding technique the remaining 30 patients did not have T1 mapping in additional to conventional late gadolinium enhanced scar images.

Demographic data is presented by etiology (ICM and NCM) and is shown in Table 6. Patients with NCM were younger ($p<0.05$) and were less likely to have QRS fragmentation than ICM patients ($p<0.01$). The ICM population had significantly increased markers of regional fibrosis (Grayzone and scar core burden) compared with the NCM cohort (Grayzone$_{-FWHM}$ 10.07±4.83 vs 6.51±6.02, Scar$_{-2SD}$ 24.95±8.98 vs 14.98±13.28 , all $p=<0.001$) In contrast there was no statistical difference in the T1$_{-native}$ values between ICM and NCM patients (1054±7.15 vs 1073±7.55.$p=0.18$).

Table 6- Demographic data by aetiology

Variable	ICM	NCM	P value
Age (years)	72 ±10.28	58.5 ±15.91	**< 0.05**
Male	58 (80.6%)	46 (79.3%)	0.86
COPD *	10 (13.9%)	10 (17.2%)	0.59
Diabetes	14 (19.4%)	7 (12.1%)	0.25
Hypertension	25 (34.7%)	20 (34.5%)	0.97
Atrial fibrillation	14 (19.4%)	19 (32.8%)	0.08
eGFR> 60 ml/min †	47 (65.3%)	44 (75.9%)	0.19
Secondary prevention	23 (31.9%)	14 (24.1%)	0.32
CRT‡	32 (52.8%)	33 (56.9%)	0.63
QRS>120ms	29 (46%)	29 (55.8%)	0.29
Fragmented QRS	36 (57.1%)	16 (30.8%)	**<0.001**
EF MRI < 35%§	57 (79.2 %)	35 (60.3%)	**0.02**
$T1_{-Native}$	1054±7.15	1073±7.55	0.18
$T1_{-post}$	41.86±5.25	40.32±12.02	0.2
$Grayzone_{-2SD-3SD}$	6.01±2.25	5.25±4.69	0.25
$Grayzone_{-FWHM}$	10.07±4.83	6.51±6.02	**<0.001**
$Scar_{-2SD}$	24.95±8.98	14.98±13.28	**<0.001**
$Scar_{-3SD}$	18.97±7.61	9.73±9.0	**<0.001**
$Scar_{-4SD}$	14.28±6.46	6.03±5.81	**<0.001**
$Scar_{-5SD}$	10.30±5.41	3.67±3.62	**<0.001**
$Scar_{-6SD}$	7.16±4.58	2.10±2.35	**<0.001**
$Scar_{-FWHM}$	14.92±6.47	8.45±8.56	**0.03**
ECV‖	28.98±7.94	30.21±5.83	0.32
Midwall Fibrosis	N/A	27 (52%)	N/A

4.1.5.1 Primary Endpoint

During a median follow-up period of 938 days (IQR 672 to 1192 days), 36 patients (27.7 %) experienced the primary endpoint. The median time to first ICD therapy was 329 days (IQR 116 to 532 days). The proportion of those meeting the primary endpoint

was greater in the secondary prevention group (16 of 37 (43.2%)) than in the primary prevention group (20 of 93 (21.5 %);p =0.01). The cumulative event rate was similar between ICM and NCM patients (18 of 72 (25%) and 18 of 58 (31.0%); p=0.43). Of the 18 ICM patients meeting the primary endpoint 7/18 patients were treated for ventricular fibrillation and 11/18 for VT (mean heart rate 196bpm). Of the 18 NCM patients meeting the primary endpoint 8/18 patients were treated for ventricular fibrillation and 10/18 for VT (mean heart rate 199 bpm). The median time to first appropriate therapy was similar for both etiologies (NCM- 335 days (IQR 171 to 537 days), ICM- 287 days (IQR 67 to 481 days); p=0.44.) With regard to the secondary endpoint, 56 patients experienced either appropriate therapy or died (44% ICM, 35% NCM; p=NS).

4.1.5.2 Predictors of Primary and Secondary Endpoints in the combined ICM and NCM cohort

The results of univariable and multivariable adjusted analyses for the primary and secondary endpoints in the entire cohort are shown in Table 7. MRI indices of regional (scar and Grayzone) and diffuse fibrosis ($T1^{-native}$ mapping) were independently associated with ICD therapy. The same CMR indices were also independently associated with the secondary endpoint. Extra Cellular Volume (ECV) and fQRS did not predict either endpoint.

Table 7- Univariable and multivariable analysis for primary and secondary endpoint

A

Univariate analysis	Primary Endpoint		Secondary Endpoint	
Variable	Hazard Ratio 95% C.I.	P value	Hazard Ratio 95% C.I.	P value
Age	0.98 0.96-1.01	0.17	1 0.98-1.02	0.85
Gender (Male)	1.61 0.63-4.15	0.32	1.42 0.67-3.05	0.36
COPD§	1.59 0.73-3.51	0.24	1.54 0.79-3.01	0.21
Diabetes	1.67 0.76-3.68	0.2	2.13 1.11-4.09	**0.02**
Hypertension	0.17 0.87-3.25	0.12	1.5 0.86-2.64	0.16
Atrial fibrillation	0.56 0.28-1.11	0.1	1.64 0.90-2.96	0.11
Secondary prevention	2.47 1.28-4.80	**<0.01**	1.96 1.10-3.47	**0.02**
QRS>120ms	1.02 0.51-2.03	0.96	1.32 0.73 -2.40	0.36
Fragmented QRS	0.56 0.37-1.16	0.12	1.2 0.66-2.18	0.54
EF MRI >35%#	0.58 0.26-1.27	0.17	0.38 0.18-0.80	**0.01**
$T1_{native}$	1.09 1.04-1.14	**<0.01**	1.07 1.03-1.12	**0.001**
$T1_{post}$	1 0.97-1.04	0.83	1.01 0.98- 1.05	0.43
$Grayzone_{2SD-3SD}$	1.18 1.08-1.28	**<0.01**	1.15 1.06-1.24	**<0.001**
$Grayzone_{2SD-FWHM}$	1.09 1.03-1.15	**<0.01**	1.12 1.07-1.13	**<0.01**
$Scar_{2SD}$	1.04 1.02-1.08	**<0.01**	1.04 1.02-1.07	**<0.001**
$Scar_{3SD}$	1.05 1.01-1.08	**0.01**	1.05 1.01-1.08	**<0.01**
$Scar_{4SD}$	1.04 0.99-1.09	0.06	1.05 1.02-1.09	**<0.01**
$Scar_{5SD}$	1.04 0.98-1.09	0.21	1 0.95-1.05	0.94
$Scar_{6SD}$	1.01 0.97-1.04	0.82	1.43 0.78-2.59	0.24
$Scar_{FWHM}$	1.05 1.01-1.09	**0.02**	1.32 0.73-2.40	0.36
ECV**	1.1 0.95-1.07	0.75	1.2 0.66-2.18	0.54

B

Multivariate analysis	Primary Endpoint		Secondary Endpoint	
Variable	Hazard Ratio	P value		P value
Secondary prevention	2.15 1.10-5.31	0.28	1.66 0.82-3.33	0.16
$T1_{native}$	1.09 1.10-1.15	**<0.01**	1.08 1.04-1.12	**<0.001**
$Grayzone_{2SD-3SD}$	1.16 1.04-1.30	**0.01**	1.12 1.01-1.23	**0.03**
$Grayzone_{2SD-FWHM}$	1.07 1.01-1.14	0.24	1.06 1.01-1.12	**0.03**
$Scar_{2SD}$	1.04 1.00-1.07	**0.03**	1.04 1.01-1.07	**0.01**
$Scar_{3SD}$	1.04 0.99-1.08	0.07	1.04 1.01-1.08	**0.03**
$Scar_{FWHM}$	1.04 0.99-1.09	0.08	1.05 1.01-1.09	**0.02**
EF MRI>35%	NS at univariate analysis		0.34 0.13-0.89	**0.03**
Diabetes	NS at univariate analysis		1.96 0.92-4.17	0.79

*(appropriate therapy: shock and ATP * (ICM† and NCM‡ combined))*

4.1.5.3 Predictors of appropriate therapy according to aetiology

ICM: The results of univariable and multivariable adjusted analysis in ICM group for the primary endpoint are shown in Table 8 and Table 9 respectively. $T1_{-native}$, scar and Grayzone remained predictive of the primary endpoint in multivariable adjusted analysis. fQRS did not predict occurrence of the primary endpoint in multivariable adjusted analysis. With regard to the secondary endpoint, at multivariable adjusted analysis scar and Grayzone indices remained predictive however $T1_{-native}$ was not (See Table 8).

Table 8- Univariable analysis for primary endpoint ICM only

Variable	Hazard Ratio	(95% C.I.)	P value
Secondary Prevention	2.18	0.85-5.57	0.10
$Grayzone_{-2SD-3SD}$	**1.52**	**1.22-1.88**	**<0.001**
$Grayzone_{-FWHM}$	**1.13**	**1.05-1.21**	**<0.001**
$Scar_{-2SD}$	**1.10**	**1.04-1.16**	**<0.001**
$Scar_{-3SD}$	**1.09**	**1.02-1.16**	**<0.01**
$Scar_{-FWHM}$	**1.09**	**1.02-1.17**	**0.02**
Fragmented QRS	0.35	0.13-0.97	0.04
$T1_{-native}$	**1.08**	**1.08-1.16**	**0.03**

Table 9 - Multivariable adjusted analysis for primary endpoint split by aetiology (ICM and NCM)

Multivariate analysis	**Primary Endpoint**		**Secondary Endpoint**	
ICM	**Hazard Ratio 95% C.I**	**P value**	**Hazard Ratio 95% C.I**	**P value**
Grayzone$_{2SD-3SD}$	1.34 1.03-1.76	**0.03**	1.27 1.04-1.56	**0.01**
Grayzone$_{FWHM}$	1.1 1.02-1.20	**0.01**	1.1 1.02-1.18	**0.01**
Scar$_{2SD}$	1.07 1.01-1.14	**0.02**	1.06 1.01-1.11	**0.01**
Scar$_{3SD}$	1.07 1.01-1.14	**0.03**	1.06 1.01-1.11	**0.03**
Scar$_{FWHM}$	1.07 0.99-1.16	0.08	1.05 0.99-1.13	0.06
T1$_{native}$	1.08 1.00-1.16	**0.04**	1.06 1.01-1.12	0.33
Fragmented QRS	0.43 0.13-1.43	0.17	NS at univariate analysis	
NCM	**Hazard Ratio 95% C.I**	**P value**	**Hazard Ratio 95% C.I**	**P value**
Secondary Prevention	2 0.66-6.06	0.22	1.89 0.64-5.81	0.27
Grayzone$_{2SD-3SD}$	1.12 0.99-1.27	0.08	1.11 0.98-1.25	0.11
Grayzone$_{FWHM}$	1.07 0.99-1.16	0.11	NS at univariate analysis	
Scar$_{2SD}$	1.04 0.99-1.09	0.07	NS at univariate analysis	
Scar$_{3SD}$	1.06 0.99-1.13	0.07	NS at univariate analysis	
Midwall Fibrosis	2.92 0.77-10.99	0.11	NS at univariate analysis	
T1$_{native}$	1.12 1.04-1.21	**<0.01**	1.1 1.03-1.18	**<0.01**

NCM: The results of univariable and multivariable adjusted analysis in NCM group for the primary endpoint are shown in Table 9 and Table 10. Whilst univariable analysis revealed a significant association between the primary endpoint and secondary prevention, Grayzone$_{-2SD-3SD}$, Grayzone$_{-FWHM}$, Scar$_{-2SD}$, Scar$_{-3SD}$ and T1$_{-native}$, multivariable adjusted analysis revealed that only T1$_{-native}$ was independently associated with the primary endpoint. With regard to the secondary endpoint only T1$_{-native}$ remained predictive following multivariable adjusted analysis (See Table 9).

Table 10- Univariable analysis for primary endpoint: NCM only

Variable	Hazard Ratio	(95% C.I.)	P value
Secondary Prevention	**2.94**	**1.15-7.49**	**0.02**
Grayzone$_{-2SD-3SD}$	**1.11**	**1.01-1.22**	**0.03**
Grayzone$_{-FWHM}$	**1.07**	**1.00-1.13**	**0.05**
Scar$_{-2SD}$	**1.03**	**1.02-1.07**	**0.04**
Scar$_{-3SD}$	**1.05**	**1.00-1.09**	**0.05**
Scar$_{-FWHM}$	1.04	0.99-1.09	0.07
Fragmented QRS	0.94	0.33-2.71	0.91
Midwall Fibrosis	**3.76**	**1.21-11.63**	**0.01**
T1$_{-native}$	**1.10**	**1.03-1.18**	**<0.01**

4.1.5.4 Post hoc risk re-stratification according to aetiology

ROC analysis suggested the use of Grayzone$_{-2SD-3SD}$ >4.0% of left ventricular mass and T1$_{-native}$ >1003ms as potentially markers with 90% sensitivity to dichotomize risk of the primary endpoint.

Mixed Cohort:

When applied to the mixed cohort both the T1 and Grayzone cut-off significantly identified patients at increased risk of reaching the primary endpoint but both also failed to identify a significant minority of patients who went on to meet the primary endpoint despite being dichotomized into proposed low risk cohort. (see Kaplan-Meier curves in Figure 30)

Figure 30- Post hoc analysis using either Grayzone$_{-2SD\text{-}3SD}$ and a retrospectively applied cut-off of >4% of LV mass or T1$_{-Native}$ and a retrospectively applied cut-off of >1003ms to dichotomize the mixed NCM and ICM cohort patients into high and low risk

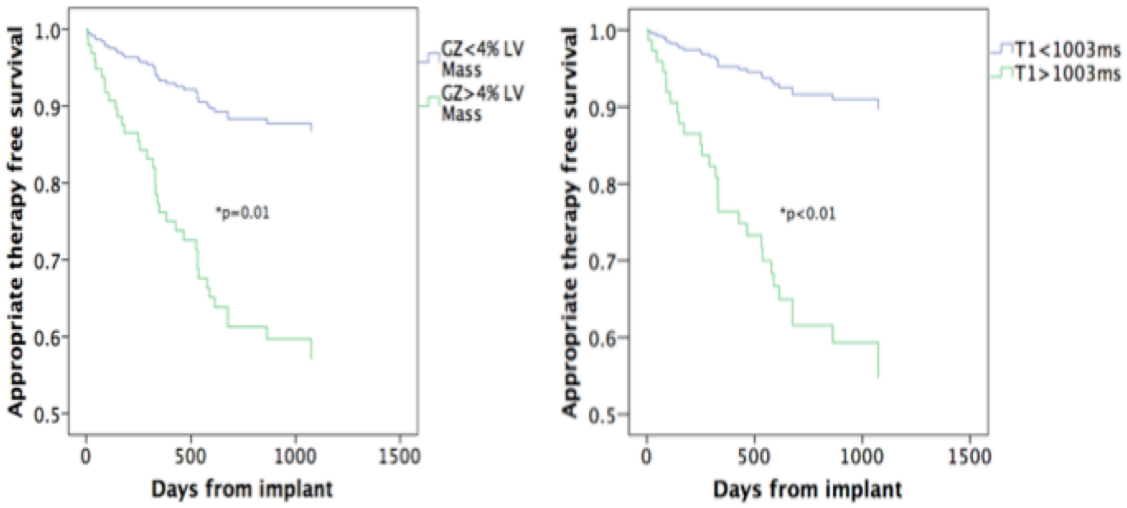

ICM:

16 of the 54 patients (29.6%) who did not experience the primary endpoint were reclassified into low risk based on a dichotomizing cut off of Grayzone$_{-2SD\text{-}3SD}$ >4.0% of left ventricular mass. All of the 18 patients who met the primary endpoint remained

classified as high risk using this cut-off (Log rank test 6.2; p=0.01, see Kaplan-Meier curve in Figure 31).

Figure 31- Post hoc analysis using Grayzone$_{-2SD-3SD}$ and a retrospectively applied cut-off of >4% of LV mass to dichotomize ICM patients into high and low risk (Log rank Chi-Square 6.2; p=0.01)

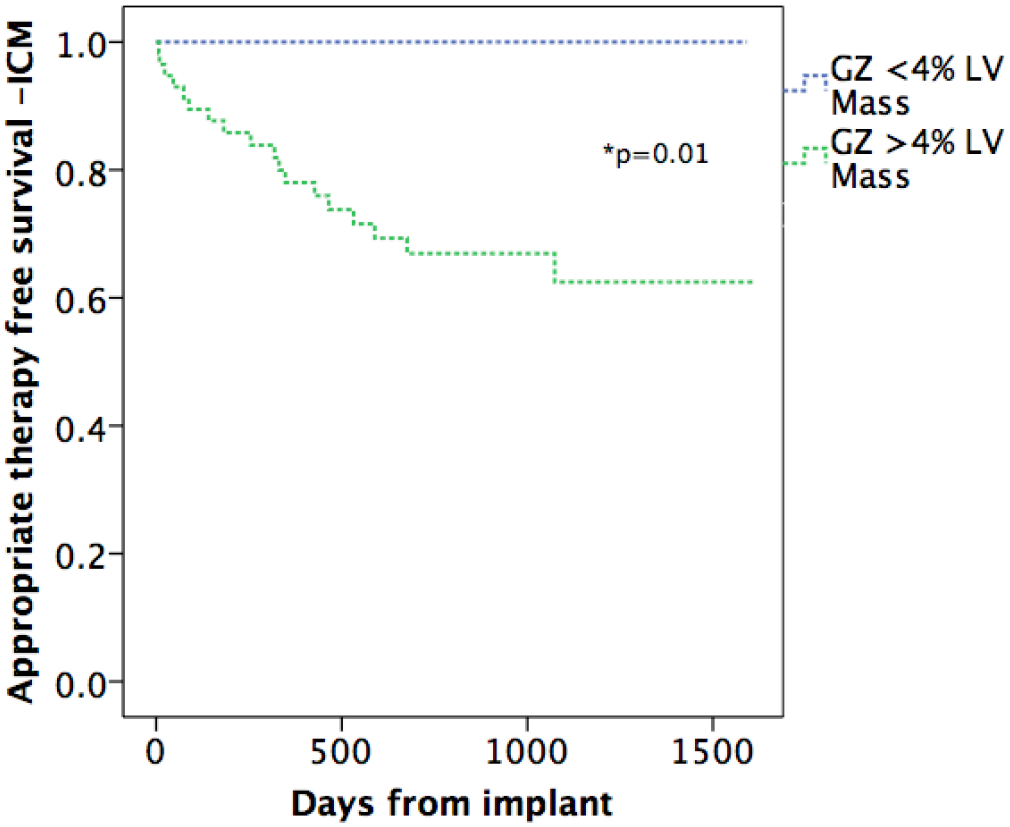

On the basis of T1$_{-native}$ using a cut-off of 1003ms, 16 of the 40 participants (40%) were correctly reclassified into the low-risk category as they had not met the primary endpoint. 3 out of 14 patients (21.4%) who had met the primary endpoint were reclassified into the low-risk group using the cut-off. (Log rank test 1.6; p=0.20)

NCM: In the NCM group, 8 of the 27 patients (29.6%) who did not meet the primary endpoint were reclassified into low risk based on retrospective application of $T1_{native}$ cut-off and all 14 patients experiencing a positive endpoint remained in the high risk cohort (Log rank Chi-Square 4.8; p=0.03, see Kaplan-Meier curve in Figure 32). Using the $Grayzone_{2SD\text{-}3SD}$ cut-off, 24 out of 40 patients (60%) who did not meet the primary endpoint were risk restratified as low risk. However the Grayzone cut-off also reclassified 6 out of 18 patients (33.3%) who met the primary endpoint as low risk. (Log rank Chi-Square 4.0; p=0.05)

Figure 32- Post hoc analysis using $T1_{Native}$ and a retrospectively applied cut-off of >1003ms to dichotomize NCM patients into high and low risk (Log rank Chi-Square 4.8; p=0.03)

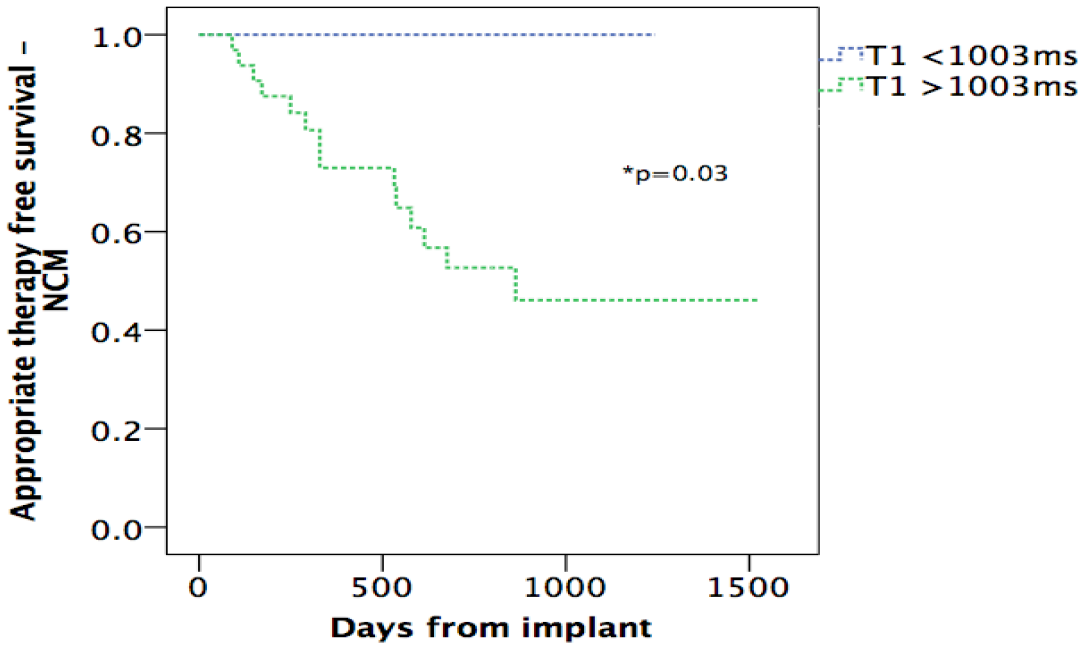

Using $T1^{-native}$ to risk stratify NCM patients and $Grayzone^{-2SD\text{-}3SD}$ to risk stratify ICM patients the net reclassification of high risk to low risk is 29.6% without reclassification of any patients incorrectly to low risk.

4.1.5.5 Risk re-stratification in primary prevention patients

In the primary prevention cohort 20 of the 93 participants (26.6%) with a primary prevention ICD who failed to meet the primary endpoint were correctly reclassified to the low-risk group on the basis of the Grayzone cut-off, while two patients with a positive endpoint were mistakenly reclassified into the low-risk group. 20 of the 51 patients (40%) who had an ICD implanted but did not experience the primary endpoint were correctly reclassified into the low-risk category on the basis of $T1^{-native}$ cut-off, while again two of the participants experiencing a positive end point were mistakenly reclassified into the low-risk group.

However, using the T1 cut-off only for the NCM primary prevention patients, 6/22 (27.3%) patients who did not reach the primary endpoint were correctly reclassified to low risk whilst the 8 patients who received appropriate therapy remained as high risk. There were no reclassifications of patients who met the primary endpoint to low risk.

Equally, using the Grayzone cut-off for primary prevention ICM patients 11 out of 39 (28.2%) patients were reclassified as low risk without any of the 10 patients who met the primary endpoint being reclassified as low risk.

4.1.5.6 Relationship of fQRS with regional and diffuse fibrosis

The Receiver Operator Curves (ROC) assessing the relationship between $T1_{-native}$, $Grayzone_{-3SD-2SD}$ and $Scar_{-2SD}$ with fQRS had Areas under the Curve (AUC) of 0.4, 0.56 and 0.59 respectively. The difference between the AUC for $T1_{-native}$ and $Scar_{-2SD}$ was significant (z score -2.34, p=0.02). Further post hoc analysis showed an increasing AUC and thus improved association with fQRS by increasing the $Scar_{-(X)SD}$ value up to $Scar_{-6SD}$ suggesting a correlation between fQRS with more homogeneous scar core than with heterogeneous Grayzone. However this correlation did not reach a significant level (see Figure 33, Z score 0.6, p=0.55).

Figure 33- The relationship between scar core and increasing AUC for relationship with fragmented QRS

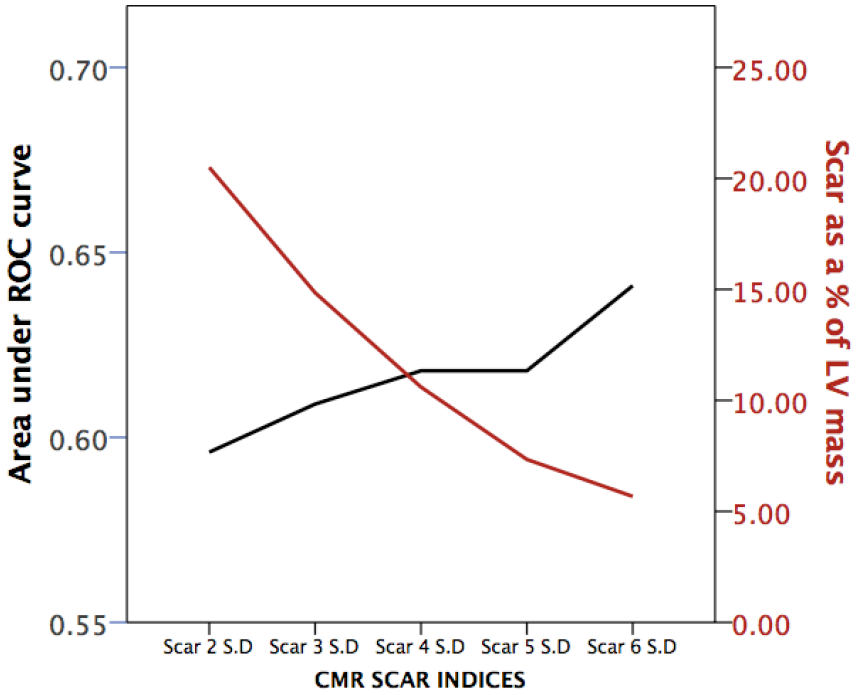

As the signal intensity of defined scar core increases (2 standard deviation method up to 6 standard deviation method) so the proportion of scar as a percentage of LV mass falls and the relationship with fragmented QRS as measured by ROC curves increases.

4.1.5.7 Reproducibility of T1 mapping

T1 measurements were repeated in a subgroup of randomly selected patients from the study cohort (10 with NCM and 10 with ICM). For $T1^{-native}$ measurement, the intraobserver average difference in values was 5 ± 3ms and the coefficient of variation was 0.3% ± 0.2%; the interobserver average difference in values was 6 ± 5 ms and the COV was 0.4% ± 0.3%.

4.1.6 Discussion

The present study extends our previous findings of the independent predictive value of $T1^{-native}$ for appropriate ICD therapy in patients with both ICM and NCM from the short to the medium- long term. More interestingly, by dichotomizing patient by etiology we show for the first time that $T1^{-native}$ is the only independent predictor of appropriate therapy in patients with NCM and demonstrate the powerful predictive value of Grayzone in ICM.

The study is the first to incorporate supposed clinical predictors of VA (fQRS) and advanced CMR techniques in the same patient cohort and clearly shows the superiority of the CMR indices over fragmentation. The study demonstrates that fQRS is not a correlate of diffuse fibrosis, but may be more related to scar core.

4.1.6.1 CMR indices and aetiology

The $T1^{-native}$ value was the only predictor at multivariable analysis of the primary endpoint and secondary endpoints in the NCM cohort. In contrast, in the ICM cohort, indices of scar and Grayzone as well as $T1^{-native}$ were predictive of the primary

endpoint. However, the $T1^{-native}$ value was not predictive of the secondary endpoints in the ICM cohort whereas indices of scar and Grayzone continued to remain significant.

Taken together these findings are consistent with the differing pathophysiological features of the two etiologies. VA in ICM is related to sub-endocardial scar following infarction with a peri-infarct Grayzone offering a potentially highly arrhythmogenic substrate.[98] It is therefore unsurprising that across all endpoints the measures of scar and Grayzone remain independent predictors of VA in ICM. Conversely, NCM is characterized by diffuse fibrosis and it is consistent therefore that $T1^{-native}$ should remain predictive of VA across all endpoints whereas scar and Grayzone are not. [80,157]

4.1.6.2 Fragmented QRS

We found no evidence that the presence of fQRS offers any predictive value for VA. Our findings are in keeping with previously published work in a similar ICD patient population which showed a trend towards increased arrhythmic risk in patients *without* fQRS.[110] Our CMR analysis allows us to further characterize what pathophysiological features fQRS may represent. Contrary to our hypothesis that fQRS represents areas of peri-infarct tissue or diffuse fibrosis, the ROC analysis seems to suggest that fragmentation relates to scar core (which accords with our analysis of scar core and arrhythmic risk).

4.1.6.3 Comparison with previous studies

The ability of T1 mapping to predict ICD therapy in NCM is in keeping with a recent publication from our institution demonstrating the ability of native T1 mapping to predict mortality in NCM.[102] Further to Puntmann et al's findings, our results

demonstrate the predictive role of native T1 mapping in a significantly higher risk group of NCM patients with a much higher event rate.

4.1.6.4 Clinical Implications of risk restratification

The risk re-stratification data has two potential clinical implications:

First, the Grayzone cut-off value used for ICM and the $T1_{native}$ cut-off value used for NCM create a cohort in whom VA is unlikely. This offers the possibility to further risk stratify patients who would currently receive an ICD into a lower risk cohort. This is particularly pertinent in the NCM group: The recently published DANISH study failed at 6-7 years to demonstrate a survival benefit with ICDs in a non-ischemic cohort despite a reduction in sudden cardiac death.[91] Importantly, the survival curves merged at the end of the study having previously suggested a trend towards benefit in those implanted with an ICD whereas the risk reduction for sudden death with an ICD began to emerge at 2 years and persisted throughout the study. Thus, there may be a medium-term survival benefit using ICD in NCM patients which may warrant ICD implantation, particularly if a cohort of patients at risk of sudden death and VA can be correctly identified. T1 mapping is potentially such a tool with a powerful predictive value for VA and a biologically plausible underpinning to substantiate its use. Identification of these patients would also highlight them as being at generally high risk of death from other causes in the medium to long term.

Secondly the risk re-stratification analysis may be used to identify which patients remain at high risk of VA. This is of particular interest in the ICM cohort where there is growing interest in prophylactic VT ablation. [150,158,159] Patient selection for VT ablation remains a controversial area with some centres advocating ablation in all patients

receiving an ICD with other centres choosing to ablate only in incessant drug refractory VT. The cut-offs used in our study could be used to select patients for prophylactic VT ablation particularly in the primary prevention cohort where both $T1_{native}$ and Grayzone reclassified a significant number of patients correctly to low risk with only a small number of patients (3 and 2 respectively) incorrectly classified to low risk.

In contrast to using the cut-offs as decision aids for ICD implantation, there is less clinical significance to the incorrect reclassification of patients to low risk when considering suitability for VT ablation as there is no denial of proven life-saving therapy.

4.1.7 Study Limitations

Whilst representing a relatively unselected cohort of patients (channelopathies were excluded) the sample size is not sufficiently large to draw firm conclusions and there is a need for further work to validate these results in larger, randomised studies. The absolute T1 values of interest can be influenced by a number of technical parameters including magnetic field strength and acquisition sequence as well as post- acquisition image processing including motion correction and image registration. T1 mapping was limited to just a single slice of myocardium and an assumption made that the tissue characterized in the region of interest was representative of the remote myocardium. This methodology has been previously shown to increase T1 mapping reproducibility and, as noted above, there was a high level of inter and intra-observer reproducibility. [154]Conducting a single-center study allows standardization of the imaging protocol; however, it may have introduced systematic bias making adoption of cut-off values in other centers potentially misleading. Nonetheless there is now evidence that T1

mapping protocols can be reproduced across multiple centers with low inter and intra-observer variability. A separate validation cohort is needed to verify the values derived from the AUC analysis of $T1^{native}$ and $Grayzone^{2SD-3SD}$ for prediction of the primary endpoint before these values should be used in clinical practice. However, work from our institution has previously shown at 1.5 Tesla in the healthy human heart a mean $T1^{native}$ of 950ms ± 21ms (Upper limit using 2 standard deviations- 992ms) which would suggest our T1 cut-off of 1004ms is plausible.

The device programming represents our institution's preferred therapies in 2011 when the study began. However the MADIT-RIT study demonstrated the benefits of less aggressive programming and this has resulted in changes to our current practice.[160] It may be that the effect size is thus overstated as some tachyarrhythmias may have self-terminated with less aggressive programming, however many patients had VF initially and others recurrent VT suggesting that our results remain valid.

95/130 patients had T1 images that were suitable for analysis. However, we do not believe it likely that failure to obtain these images in the 3 remaining patients resulted in any significant bias. It is likely as CMR continues to evolve that shorter acquisition times will allow greater patient tolerance of more complex protocols.

4.1.8 Conclusion

In the medium to long-term, T1 mapping appears to be a powerful predictor of VA in NCM whereas Grayzone is a stronger predictor in ICM. Both indices outperformed fQRS in the prediction of VA. Both T1 mapping and Grayzone have the potential to refine ICD implantation decisions and also to inform patient selection for VT ablation but the CMR index used in these assessments should be based on the underlying cardiomyopathic etiology.

4.2 THE RELATIONSHIP BETWEEN VECTORCARDIOGRAPHY AND MYOCARDIAL SCAR IN CARDIAC RESYNCHRONISATION THERAPY RESPONSE

4.2.1 Abstract

Background: Vectorcardiography (VCG) parameters and myocardial scar both affect cardiac resynchronization therapy (CRT) response. The purpose of this study was to investigate the relationship between VCG and myocardial scar, defined by cardiac magnetic resonance (CMR) imaging, and whether combining these metrics may improve CRT response prediction.

Methods: Consecutive patients referred for CRT who underwent pre-procedural CMR were included. VCGs were synthesized from electrocardiograms using the Kors transformation matrix. QRS duration (QRSd), QRS_{area} and T_{area} were derived from the VCG. CMR parameters reflecting regional focal scar core ($Scar_{2SD}$) and scar border zone ($Gray_{2SD}$), and diffuse fibrosis (pre-T1, extracellular volume [ECV]) were assessed. CRT response was defined as echocardiographic reduction in left ventricular end-systolic volume (ΔLVESV) of ≥15% after six months follow-up.

Results: Thirty-three patients were included, of whom 58% were CRT responders. $Scar_{2SD}$ and $Gray_{2SD}$ inversely correlated with VCG parameters, whereas pre-T1 and ECV did not show a significant correlation with VCG parameters. QRS_{area} showed the strongest association with $Scar_{2SD}$ (R=-0.58, p<0.001). Receiver operating characteristics curve (ROC) analyses showed that $Scar_{2SD}$, $Gray_{2SD}$ and QRS_{area} predicted CRT response with AUCs of 0.692 (CI: 0.503-0.881, p=0.063), 0.759 (CI:

0.586=0.933, *p*=0.012) and 0.737 (CI: 0.564-0.910, *p*=0.022) respectively. A combined ROC derived cut-off threshold for $Scar_{2SD}$ and QRS_{area} resulted in a CRT response percentage of 92% for patients with large QRS_{area} and small $Scar_{2SD}$ or $Gray_{2SD}$.

Conclusion: QRS_{area} on the VCG is inversely associated with focal scar burden, but not diffuse fibrosis, on CMR. The interaction between focal scar and VCG, combined CMR-VCG analysis provides incremental predictive value to CRT response.

4.2.2 Introduction

CRT is an effective treatment for patients with symptomatic heart failure (HF), reduced systolic left ventricular (LV) function, and wide QRS complex. Nevertheless, about one-third of patients eligible according to current guidelines fail to benefit from CRT. Suboptimal CRT response has been attributed to factors including QRS duration (QRSd) <150 ms, non-left bundle branch block (non-LBBB) morphology, ischemic cardiomyopathy, and suboptimal LV lead position. [27,104,161]

Objective parameters, derived from the three-dimensional (3D) vectorcardiogram (VCG), have been shown to more accurately predict CRT response than QRSd or morphology.[162] The VCG represents the electrical heart vector in three orthogonal directions (X, Y, and Z) and can be derived from a true VCG lead system or synthesized from the standard 12-lead ECG using a mathematical transformation matrix.[120] The 3D area of the VCG QRS- (QRS_{area}) and T-loop (T_{area}) are supposed to reflect unopposed electrical forces during ventricular depolarization and repolarization respectively. Both QRS_{area} and T_{area} have been shown to be strong predictors for LV reverse remodeling after CRT.[85,162] In a single small study it was observed that QRS_{area} was relatively

reduced in patients with ischemic cardiomyopathy, suggesting an association between QRS_{area} and myocardial scar. [163]

Ischemic cardiomyopathy, the presence and size of scar burden, and positioning the LV lead in scar are negatively associated with CRT outcome.[85,94,164] CMR is able to characterize different types of myocardial scar including focal scar with LGE and diffuse fibrosis with T1 mapping. Recent work demonstrated that focal scar, but not diffuse fibrosis, was associated with poor CRT response.[76]

Summarizing the above literature, it appears that an electrical substrate and low myocardial scar burden is favorable for response to CRT. The association between the electrical substrate as measured by VCG and myocardial scar as measured by CMR is however not known.

The purpose of this study was therefore to investigate 1) the association between VCG parameters and myocardial scar (both focal and diffuse) on CMR in HF patients with ventricular conduction disturbance, and 2) whether combining VCG with CMR scar parameters improves prediction to CRT response.

4.2.3 Methods

4.2.3.1 Study population

Consecutive patients referred for CRT device implantation who underwent CMR imaging as part of their clinical workup were prospectively enrolled at Guys and St

Thomas' NHS Trust hospital as previously described. The South-East London Research Ethics Committee approved the study protocol and all patients gave written consent.

4.2.3.2 Vectorcardiography analysis

Standard 12-lead ECG's were recorded prior to CRT implantation in supine position using the ECG machine MAC 5500 HD (GE Healthcare, Chicago, IL). The digital PDF ECG files with vector graphics were used to extract the original digital ECG-signal. VCGs were semi-automatically synthesized from these digital ECG signals using custom software programmed in MATLAB.[85] The Kors transformation matrix was used to transform the 12-lead ECG to VCG.[120] The onset and end of the QRS-complex and T-wave were manually set on the three overlaid orthogonal leads (X, Y, and Z) of the VCG by two electrophysiologists blinded to CRT outcome. QRS_{area} and T_{area} were defined as the 3D areas of respectively the QRS- and T-wave loop from the VCG between the loop and baseline in X, Y, and Z direction calculated as $QRS_{area} = (QRS_{area,x} + QRS_{area,y} + QRS_{area,z})^{1/2}$, $T_{area} = (T_{area,x} + T_{area,y} + T_{area,z})^{1/2}$.[85,163]

4.2.3.3 CMR analysis

CMR Imaging Patients underwent CMR prior to their CRT implantation using a 1.5T scanner with a 32–channel coil (Philips Healthcare, Best) as described above. Two independent CMR experts, blinded to CRT outcome, assessed the CMR images. In case of discrepancy, consensus between the reviewers was reached. LV mass was quantified using CVI 42 (Circle Cardiovascular Imaging Inc, Calgary) software and used to index the LGE quantification of focal scar. The extent of Scar core was quantified using the 2-standard deviation (2SD) method, defined as the region with signal intensity (SI) >2SD above reference myocardium ($Scar_{2SD}$). The extent of Gray zone was quantified by the

difference in SI between $Scar_{2SD}$ and $Scar_{3SD}$ ($Gray_{2SD}$). All LGE scar parameters were expressed as a percentage of LV mass (%LV). T1 relaxation maps were processed using a customized software plugin with Osirix (Pixmeo, Geneva), from which the diffuse fibrosis parameters pre-contrast T1 (pre T1) and extracellular volume index (ECV) was calculated.

4.2.3.4 CRT implantation and response

The LV lead was preferentially targeted to a postero-lateral, lateral or anterolateral coronary sinus tributary, with pacing sites preferentially chosen in a basal position remote from CMR scar. Trans-thoracic echocardiography was assessed pre- and six months post-CRT implantation using a GE Vivid 7 scanner (General Electric-Vingmed, Milwaukee, Wisconsin). Standard 2D images of LV dimensions and ejection fraction (LVEF) were acquired in standard apical 2- and 4-chamber views. LV end-diastole and end-systole volumes (LVEDV, LVESV) were used to estimate LVEF using the 2-dimensional modified biplane Simpson's method (EchoPac 6.0.1, General Electric Vingmed). CRT response was defined as an echocardiographic LVESV reduction of ≥15% of baseline afters six months follow-up. Echocardiography was performed by sonographers blinded to both VCG and CMR data.

4.2.4 Statistical analysis

Statistical analyses were performed using SPSS 24.0 (SPSS Inc., Chicago, Illinois) and MATLAB (Matlab 2016B, MathWorks, Natick, MA). Continuous variables are expressed as mean±SD or median and interquartile range (IQR) and dichotomous variables in frequencies and percentages. Spearman correlation analyses were carried

out between and within VCG and CMR parameters. Parameter differences between CRT responders vs. non-responders were compared using Mann Whitney U-tests. Receiver operating characteristics (ROC) curves were generated to evaluate the diagnostic accuracy of all parameters in identifying CRT response and to find optimal cut-off values. These cut-off values were used to dichotomize the population to groups ≤cut-off and >cut-off, and the number of CRT responders for every subgroup were compared using Chi-squared analyses. The most promising VCG and CMR scar parameters were combined in a cross-tab to evaluate its joint effect on CRT response prediction. Differences within the crosstabs were evaluated using Fisher's exact tests. Significance was defined as p-value <0.05 using two-tailed analysis.

4.2.5 Results

Thirty-three consecutive patients with either non-ischemic (n = 17) or ischemic (n = 16) cardiomyopathy were included. Patient characteristics are provided in Table 11, showing a typical CRT population.

Table 11- Baseline demographic data

Demographics	
Total patient no.	33
Age (years)	65±12
Male	27 (82%)
Ischemic cardiomyopathy	16 (49%)
NYHA (II/III/IV)	1 (3%) / 31 (94%) / 1 (3%)
CRT with ICD	31 (94%)
Posterolateral scar	22 (67%)
LVEF (%)	24±8
ECG QRS duration (ms)	150±22
ECG LBBB	12 (36%)
CRT response (LVESV ≥15)	19 (58%)

Values are displayed as mean and standard deviation or n (%). BMI=body-mass-index, EDV=end-diastolic volume, ESV=end-systolic volume, LBBB=left bundle branch block, LV=left ventricular, LVEF=LV ejection fraction, NYHA=New York Heart Association.

4.2.5.1 Association between VCG and myocardial scar

$Scar_{2SD}$ and $Gray_{2SD}$ inversely correlated with the VCG parameters. From the diffuse fibrosis parameters, there was only an inverse correlation between ECV and QRSd, while there was no association between diffuse fibrosis and QRS_{area} or T_{area} (see Figure 34).

From the VCG parameters, QRS_{area} had the strongest correlation with focal scar, while QRSd showed the lowest correlation. From the LGE parameters, the strongest (inverse) association with QRS_{area} was found for $Scar_{2SD}$.

Figure 34- Scatter plots of CMR scar parameters vs. VCG parameters. Correlation coefficients are based on Spearman correlation analyses

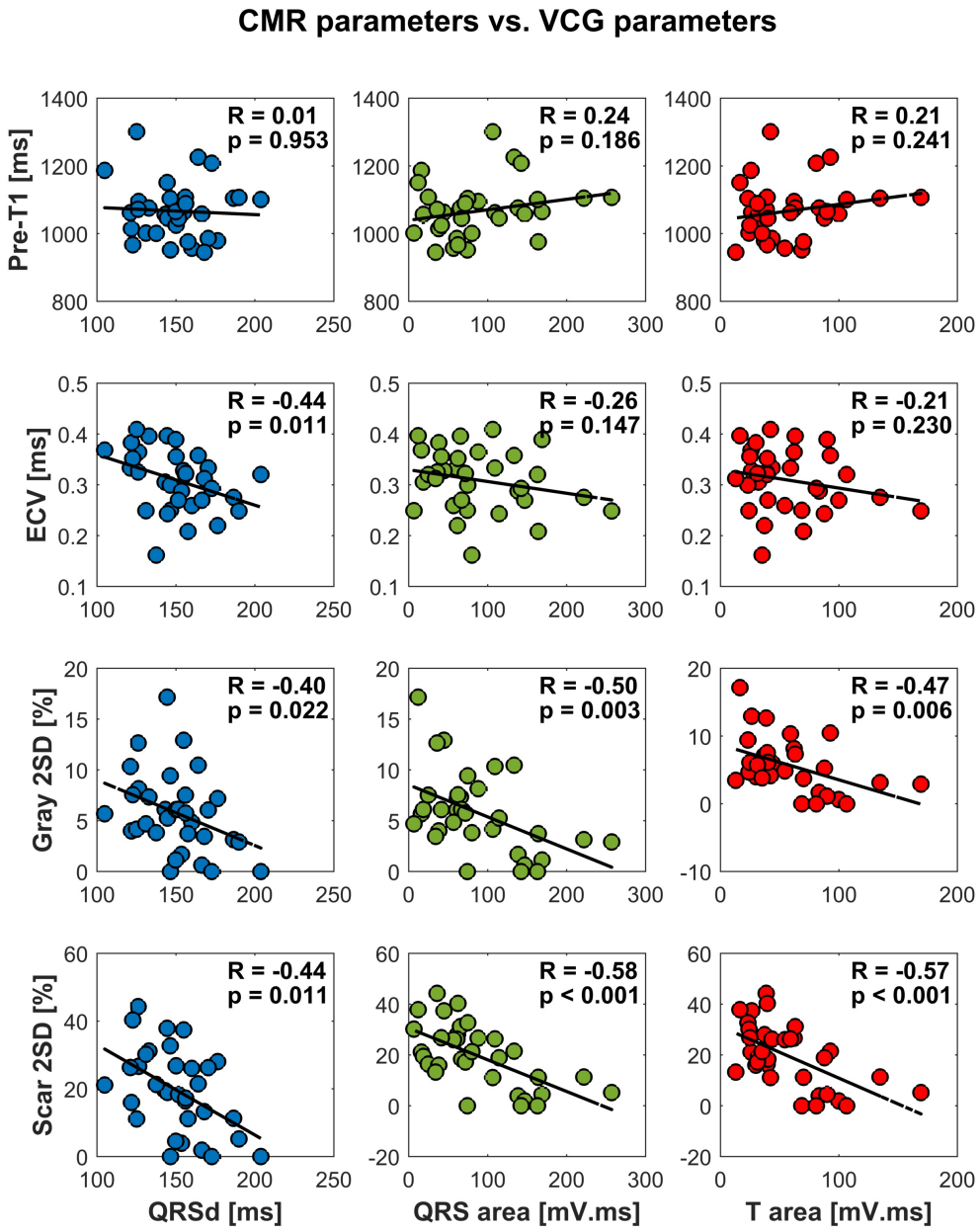

All focal scar CMR parameters correlated inversely with the ECG/ VCG parameter.

QRS_{area} correlated strongly with T_{area} (R: 0.847, p<0.001) and to a lesser extent also with QRSd (R: 0.415, p=0.016). There was a strong correlation between $Scar_{2SD}$ and

$Gray_{2SD}$ (R: 0.869, p<0.001), while $Scar_{2SD}$ did not correlate with pre-T1 or ECV (p=0.505 and 0.136 respectively).

4.2.5.2 CRT response

Nineteen out of 33 patients (58%) showed a reduction in LVESV of ≥15% after six months follow-up and were therefore defined as CRT responders.

$Scar_{2SD}$ and $Gray_{2SD}$ were lower in CRT responders than in non-responders, although only significant for $Gray_{2SD}$ (p<0.011). Pre-T1 and ECV however did not differ between CRT responders and non-responders (p=0.152 and 0.706, respectively). QRS_{area}, but not T_{area}, was significantly higher in responders than in non-responders to CRT (p=0.021) see (Table 12).

Table 12- Parameter value differences between responders and non-responders to CRT

	CRT non-responders (n=14)	CRT responders (n=19)	p-value
T1 mapping (diffuse fibrosis)			
Pre-T1 (ms)	1063 (984-1098)	1065 (1002-1105)	0.706
ECV (%)	0.33 (0.29-0.37)	0.29 (0.24-0.35)	0.152
LGE-CMR (focal scar)			
$Gray_{2SD}$ (%)	7.27 (5.48-10.37)	3.83 (1.69-6.10)	0.011*
$Scar_{2SD}$ (%)	26.16 (18.69-28.84)	13.29 (4.55-26.83)	0.065
VCG parameters			
QRSd (ms)	145 (125-161)	151 (144-168)	0.199
QRS_{area} (mV.ms)	59 (33-78)	106 (62-163)	0.021*
T_{area} (mV.ms)	41 (32-63)	42 (25-90)	0.577

*Responders are defined as reduction of LVESV ≥15%. P-values are based Mann Whitney u-tests. Continuous variables are displayed as median and interquartile ranges. *indicates significance (p-value ≤0.05).*

4.2.5.3 ROC analyses for CMR and VCG parameters identifying CRT response

Pre-T1 and ECV were poor predictors for CRT response, while $Scar_{2SD}$ and $Gray_{2SD}$ were substantially better at predicting CRT response ([AUC: 0.692, p=0.063] and [AUC: 0.759, p=0.012] respectively). QRS_{area}, but not T_{area} or QRSd, significantly predicted CRT response (AUC: 0.737, p=0.022) (see Table 13 and Figure 35).

Table 13- ROC analyses predicting CRT response for CMR and VCG parameters

	AUC	CI	p-value	Threshold	Sensitivity	Specificity
T1 mapping (diffuse fibrosis)						
Pre-T1 (ms)	0.461	0.258-0.663	0.702	<1063	47%	50%
ECV (%)	0.650	0.455-0.846	0.145	<0.32	68%	72%
LGE-CMR (focal scar)						
$Gray_{2SD}$ (%)	0.759	0.586-0.933	0.012*	<5.91	74%	71%
$Scar_{2SD}$ (%)	0.692	0.503-0.881	0.063	<20.29	68%	72%
VCG						
QRSd (ms)	0.635	0.438-0.832	0.190	>148	63%	57%
QRS_{area} (mV.ms)	0.737	0.564-0.910	0.022*	>66	74%	71%
T_{area} (mV.ms)	0.560	0.358-0.762	0.560	>39	63%	50%

*indicates significance (p-value ≤0.05).

Figure 35- ROC analyses predicting CRT response (ΔLVESV ≥15%) for CMR focal scar parameters and VCG parameters

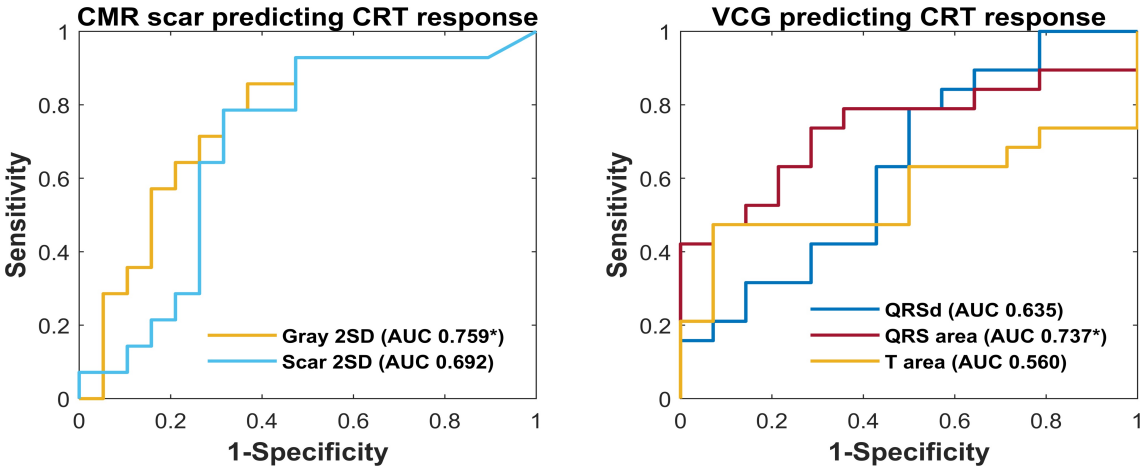

4.2.5.4 Combining VCG and Scar parameters

The study population was dichotomized using the cut-off values for $Scar_{2SD}$, $Gray_{2SD}$ and QRS_{area} derived from the ROC analyses in Table 13. The percentage of CRT responders was significantly higher in patients with low $Gray_{2SD}$ and low $Scar_{2SD}$ versus patients with high focal scar parameters (Figure 36A). The percentage of CRT response was also higher in patients with high QRS_{area} as compared to those with low QRS_{area} (Figure 36B).

Crosstab analyses between QRS_{area} and $Gray_{2SD}$ or $Scar_{2SD}$ showed that the percentage CRT response was highest (92%) in patients with a combination of low $Gray_{2SD}$ (≤5.91% LV mass) or low $Scar_{2SD}$ (≤20.29% LV mass) and high QRS_{area} (>66 mV.ms). The four subgroups in $Scar_{2SD}$+QRS_{area} combinations differed significantly from each other (overall: p<0.001; Figure 36C). For $Gray_{2SD}$+QRS_{area} combinations, although the overall group comparison did not reach a significant level (overall: p-value =0.088), there is a significant difference between the subgroup [low $Gray_{2SD}$+high QRS_{area}] when

compared with the other subgroups; there is no significant differences between the subgroups [low $Gray_{2SD}$+low QRS_{area}] and [high $Gray_{2SD}$+high QRS_{area}].

Figure 36

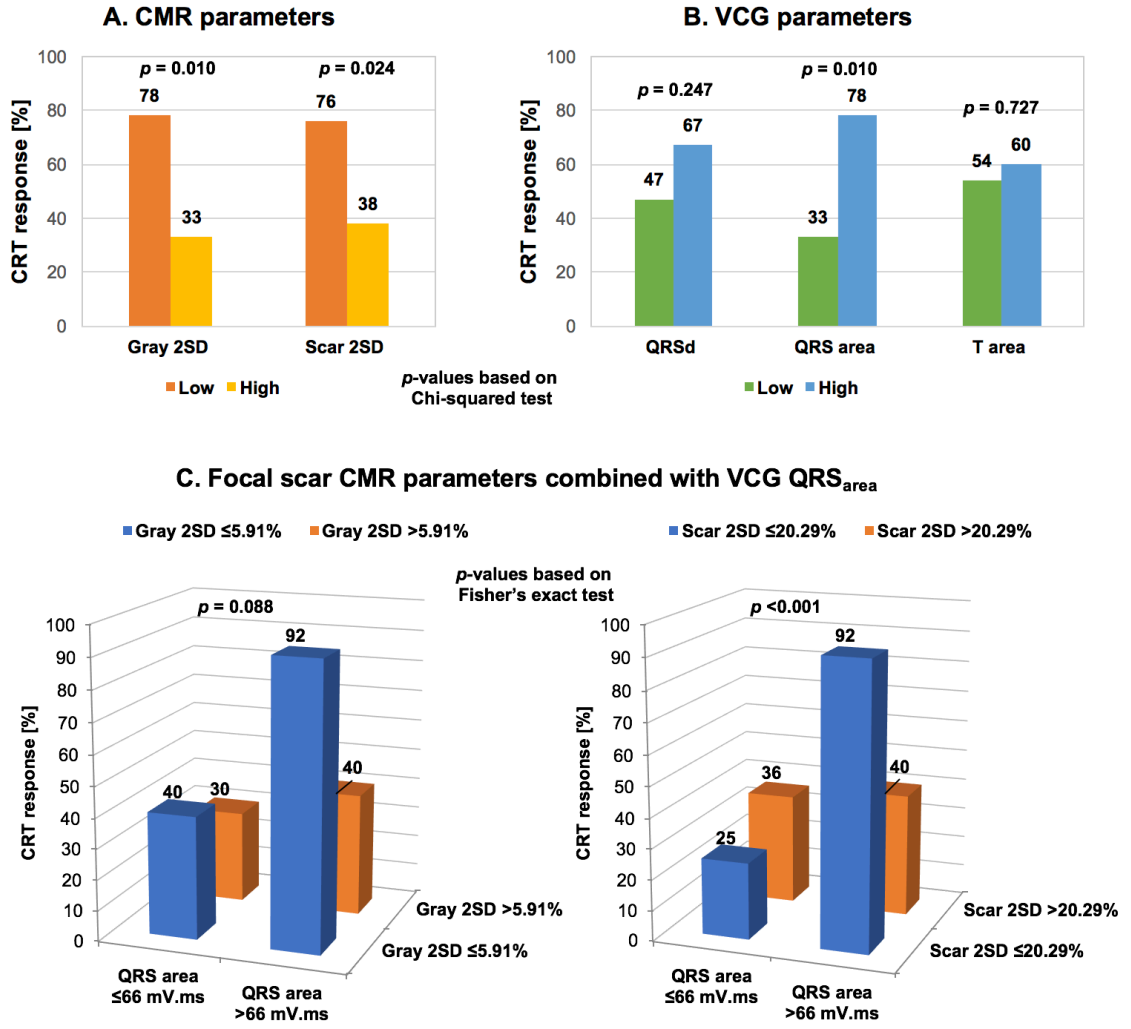

2D bar graphs showing CRT response percentage per focal scar CMR (A) and VCG (B) parameter when dividing the study population using the cut-off value as determined by ROC analyses. P-values in A and B are based on Chi-squared tests.

3D bar graphs demonstrating CRT response percentage when combining QRS_{area} with focal scar CMR parameters (C). P-values in each graph are based on Fisher's exact tests.

4.2.6 Discussion

The present study is the first to investigate the relationship between VCG parameters and CMR defined scar, and between these parameters and CRT response. The principal findings of this study are:

1) $QRS_{area,}$ but not QRSd or T_{area}, significantly correlated inversely with focal scar, suggesting that myocardial scar leads to a smaller QRS_{area}

2) combining QRS_{area} and CMR focal scar assessment improves the prediction of CRT response beyond that by either VCG or scar parameters alone particularly identifying a cohort very likely to respond.

4.2.6.1 The role of VCG in clinical context

The VCG technique was first described almost a century ago. VCG measures the electrical activity of the heart as a vector loop consisting of momentary magnitudes and directions in 3D space for each time point in the heart cycle. Various VCG systems have been introduced, from which the Frank VCG system (employing seven recording electrodes) was the most common VCG system in clinical care in the 1960s together with the current 12-lead ECG system.[83] After a period of discontinuation in clinical practice, interest in the use of VCG regained in the late 1980s, and mathematical matrices were developed to synthesize the VCG from the 12-lead ECG.[165] Advantages of VCG parameters over the 12-lead ECG-derived morphology definitions (like LBBB) is that VCG parameters are objective continuous parameters and therefore more suitable for statistical analyses. QRS_{area} and T_{area} defined as the 3D integral of the QRS- and T-

wave loop respectively, resemble dispersion of depolarization and repolarization, and are the most common VCG parameters recently investigated in CRT.[163,166-168]

4.2.6.2 The association between VCG and CMR scar

The usefulness of VCG for identification of myocardial scar has been investigated by Bizarro et al. almost four decades ago.[169] In this small study, automatically generated VCG parameters from both the QRS- and T- loop were able to identify 85% of the patients with autopsy-confirmed scar. Ever since, the majority of studies have focused on comparing features from the 12-lead ECG with myocardial scar.[170,171] However, the use of these ECG criteria in estimating scar extent is complex and particularly debatable in patients ventricular conduction disturbances.[171]

In the present study, correlation analyses suggested that QRS_{area} decreased with focal scar burden (encompassing dense scar core), and to a lesser extent scar border zone; but VCG parameters were not significantly associated with measures of diffuse fibrosis. This suggests that scar tissue with higher density affects the VCG 3D loop the most.

A low QRS_{area} theoretically resembles less dispersion and subsequently a small amount of unopposed forces during ventricular depolarization. The size of these forces likely depends on the uniformity of slow conduction and the amount of viable myocardium. A lower number of viable myocardial cells, lateralization of connexins, and increased axial resistivity after myocardial infarction may lead to a decrease of total electrical forces during the cardiac cycle and therefore an overall decrease of VCG amplitude, and subsequently low QRS_{area} and T_{area}.

QRS_{area} is not only affected by the severity of focal myocardial scar, but may also be affected by the etiology of heart failure alone. Van Deursen et al. reported lower QRS_{area} in patients with ischemic cardiomyopathy compared to patients with non-ischemic cardiomyopathy.[163]

Interestingly, patients with higher percentages of focal scar had lower QRSd. This may be explained by the fact that our study population consists of patients with ventricular conduction disturbances (a prerequisite for CRT implantation) that intrinsically, even in the absence of scar, already prolongs QRSd.

4.2.6.3 The role of VCG in CRT response prediction

The significant association of a large QRS_{area} with more LV reverse remodeling after CRT is in line with earlier studies demonstrating a significant association of QRS_{area} with CRT response.[163,172] QRS_{area} has been shown to be associated with delayed electrical activation on the LV lateral wall.[172] QRS_{area} represented unopposed ventricular contraction forces. A larger QRSarea therefore reflected a greater degree of ventricular electrical dyssynchrony which is amenable to CRT.[39,163]

The strength of QRS_{area} in predicting CRT response is particularly demonstrated in a recent multicentre prospective study by Maass et al. where numerous clinical, echocardiographic, blood, and electrocardiographic biomarkers were studied and related to LV reverse remodeling.[166] From all these biomarkers, only QRS_{area} and echocardiographic interventricular mechanical delay and apical rocking remained significantly associated with LV reverse remodeling in the multivariate model. Although T_{area} in their data initially showed a strong significant association in the

unadjusted model with LV reverse remodeling (p-value <0.0001), significance was not preserved in the multivariate model.[166] Interestingly, T_{area} proved to predict CRT response better than QRS_{area} in retrospective studies by Engels and Vegh et al. The fact that QRS_{area} outperformed T_{area} in both the Maass and the present study indicates that a potential role for T_{area} in CRT response prediction is not fully understood yet.[85,168]

4.2.6.4 The relevance of myocardial scar regarding CRT response

The association between focal scar burden and poor CRT response has been investigated in numerous studies.[78,94,164] Chalil et al. demonstrated that CRT recipients with a scar size of <33% showed significantly more favorable clinical response to patients with ≥33% scar. Patients with a posterolateral scar, the common site for LV lead placement, also had a higher risk of cardiovascular death and HF hospitalization. Leyva et al. concordantly studied the use of LGE to guide LV lead placement remote from scar tissue in a large cohort of 559 patients. In their data, patients with LGE confirmed scar showed the highest risk of cardiovascular death and lowest echocardiographic CRT response, confirming the importance of pacing remote from scar.[164]

After the introduction of T1 mapping in CMR, a few studies additionally investigated the potential role of diffuse fibrosis in CRT response.[76,173] The association between diffuse fibrosis and focal scar and LV reverse remodeling was studied by Chen et al. prospectively in CRT candidates with ischemic and non-ischemic etiologies of HF. In a multivariate model only focal scar burden, but not diffuse fibrosis, was able to predict LV reverse remodeling significantly. Höke et al investigated the association of diffuse fibrosis with CRT response prediction specifically in the non-ischemic cohort.[173] In

their data both focal scar as well as diffuse fibrosis were associated with LV reverse remodeling after CRT. These findings indicate that diffuse fibrosis may have a potential role in CRT response prediction in patients with non-ischemic cardiomyopathy.

4.2.6.5 Combining VCG with CMR for a better CRT response prediction

The present study demonstrates that combining parameters reflecting both electrical and tissue substrate for CRT may be an accessible approach to further improve CRT response prediction. Almost all (92%) patients with a low extent of focal scar and a large QRS_{area} were CRT responders. This finding is important, since myocardial scar burden and QRS_{area} are inversely related to each other. Apparently, the negative effect of scar on CRT response is stronger than that on QRS_{area} alone. Potential explanations for this observation may be that 1) scar reduces the amount of resynchronization, 2) pacing in scar may even further reduce resynchronization and 3) pacing in scar has been shown to be pro-arrhythmic.[174]

4.2.6.6 Clinical Implications

The present study supports earlier findings that QRS_{area} may improve the selection of CRT candidates and extends this idea by demonstrating that further improvement in selection may be obtained by combining scar characterization using CMR and VCG analysis. The refined positive predictive value using such combined VCG-CMR focal scar index is highly encouraging, in particular in the ischemic cardiomyopathy cohort, in whom the CRT response is commonly low. [75]

4.2.7 Limitations

This study incorporated a relative small number of patients from a single center with the inherent limitation of such study design. Nevertheless, the consecutive patient's cohort reflects a broad real-world experience. The optimal thresholding values for the scar VCG parameters should be taken in the context of the study and a larger population study is needed to validate these optimal thresholding values and different cut-offs may be required in ischemic and non-ischemic cardiomyopathy.

4.2.8 Conclusions

Focal scar CMR parameters and QRS_{area} are independent predictors for CRT response and are inversely associated with each other. The highest percentage of CRT response was observed in patients with low focal scar CMR values and high QRS_{area}, indicating that combined CMR-VCG parameters may improve prediction to CRT response.

Chapter 5 COST-EFFECTIVENESS OF A RISK-STRATIFIED APPROACH TO CARDIAC RESYNCHRONISATION THERAPY DEFIBRILLATORS AT THE TIME OF GENERATOR CHANGE

5.1 Abstract

Objective:

Responders to cardiac resynchronisation therapy whose device has a defibrillator component and who do not receive a therapy in the lifetime of the first generator have a very low incidence of appropriate therapy after box change. We investigated the cost implications of using a risk stratification tool at the time of generator change resulting in these patients being reimplanted with a resynchronisation pacemaker.

Methods:

A decision tree was created using previously published data which had demonstrated an annualised appropriate defibrillator therapy risk of 2.33%. Costs were calculated at National Health Service national tariff rates (2016-2017). EQ-5D utility values were applied to device re-implantations, admissions and mortality data, which were then used to estimate quality-adjusted life-years over 5 years.

Results:

At 5 years, the incremental cost of replacing a resynchronisation defibrillator device with a second resynchronisation defibrillator vs resynchronisation pacemaker was £5,045 per patient. Incremental quality adjusted life-years gained was 0.0165 (defibrillator vs pacemaker), resulting in an incremental cost effectiveness ratio of £305,712 per quality adjusted life-years gained. Probabilistic sensitivity analysis resulted in an incremental cost effectiveness ratio of £313,612 (defibrillator vs

pacemaker). For re-implantation of all patients with a defibrillator rather than a pacemaker to yield an incremental cost effectiveness ratio of less than £30,000 per QALY gained (current NHS cut-off for approval of treatment), the annual arrhythmic event rate would need to be 9.3%. The budget impact of selective replacement was a saving of £2,133,985 per year.

Conclusions:

Implanting low risk patients with a resynchronisation defibrillator with the same device at the time of generator change is not cost-effective by current NHS criteria. Further research is required to understand the impact of these findings on individual patients at the time of generator change.

5.2 Introduction

Cardiac resynchronisation therapy both with and without a defibrillator is a proven and cost effective treatment for symptomatic patients with left ventricular dysfunction and prolonged QRS duration. [[10,175-177]] However, there has been no statistically powered direct comparison of cardiac resynchronisation therapy with a defibrillator (CRTD) and without a defibrillator (CRTP).[[177]] Furthermore, there is minimal evidence to support the continuation of defibrillator therapy in patients with a primary prevention device who have not received appropriate therapy during the lifetime of the initial device. Registry data suggest that the risk of appropriate therapy following generator change may be as high as 25% at 5 years in an unselected cohort of patients implanted with both primary and secondary prevention defibrillators who did not receive appropriate therapy during the initial generator lifetime.[178] However, patients with a primary prevention ICD whose left ventricular (LV) ejection fraction has improved and who have not received an appropriate therapy have been shown to have a much lower risk of

subsequent appropriate therapy (2.8% per year).[179] The risk of appropriate therapy in patients responding to CRT may be further reduced due to LV improvement. In keeping with this we have previously demonstrated a low rate of appropriate therapy following generator replacement (2.33% per annum) in patients who had received primary prevention CRTD implantation with positive remodelling that had not received appropriate therapy during the lifetime of the initial device.[180] This figure is nearly identical to that published in a meta-analysis which estimated a 2.3/100 patient-year rate of appropriate therapy in CRT responders with a remodelled ejection fraction of >45%.[181]

In the United Kingdom, a need to save £22 billion per year by 2020/21 has been identified by NHS England requiring ongoing assessment of both the cost-effectiveness and budget impact of treatment options.[117] We therefore set out to determine the cost-effectiveness and budget impact of replacing an end of life CRTD generator with either CRTD or CRTP in patients who initially received a primary prevention CRTD for heart failure, required an elective generator replacement and had no theoretical ongoing ICD indication (TOII). TOII was defined as patients with a left ventricular ejection fraction >40% who had not received appropriate defibrillation therapy during the initial generator lifetime.

5.3 Methods

A decision tree was constructed to describe the pathway of patients (see Figure 37).

Figure 37- Decision tree used in the economic model

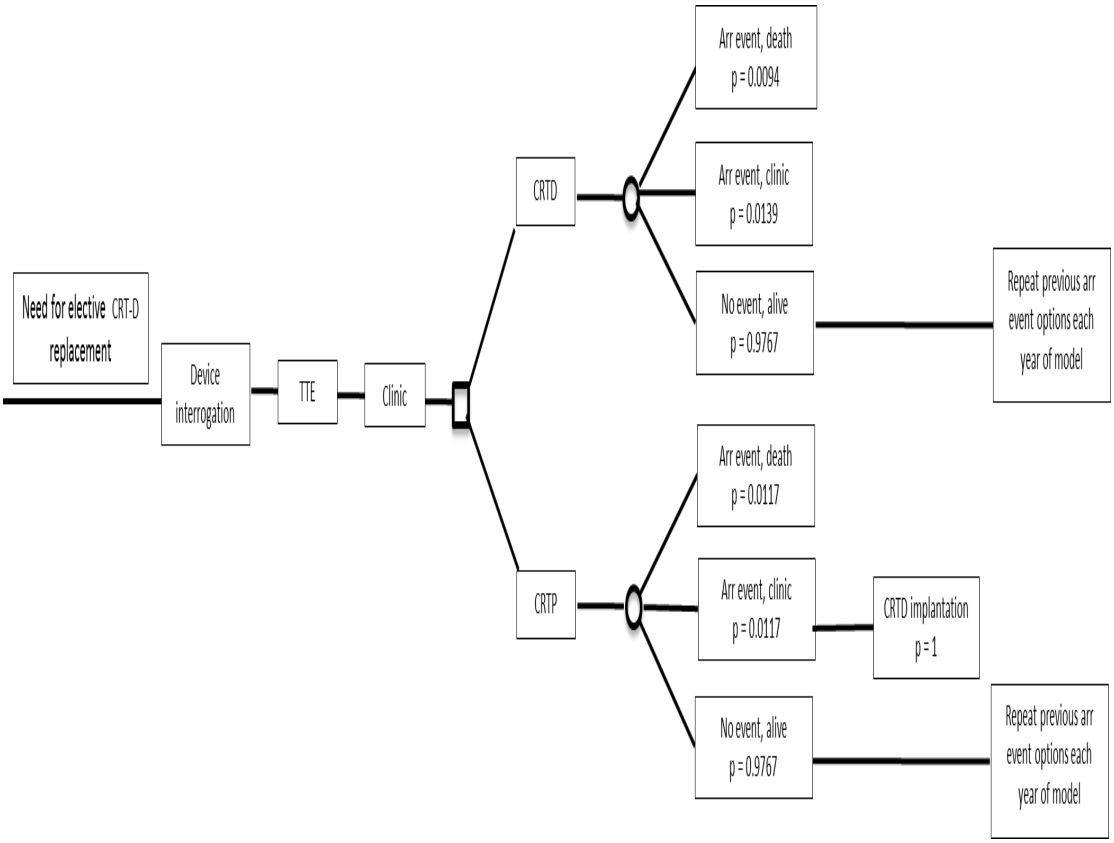

TTE = trans-thoracic echocardiogram, clinic = out-patient clinic visit, Arr event = arrhythmic event occurring after generator replacement. Device interrogation, TTE and the first clinic visit occur in year 1 only, ie prior to elective generator replacement. Arrhythmic events and upgrade of CRTP to CRTD occur annually thereafter and were modelled out to five years.

Device interrogation, trans-thoracic echocardiogram (TTE) and the first clinic visit were modelled to occur in year 1 only, i.e prior to elective generator replacement and for all patients, regardless of the final device replacement choice. Arrhythmic events and upgrade of CRTP to CRTD were modelled to occur annually thereafter and out to five

years. Modelling was not pursued beyond five years as this was considered to be outside the scope of current NHS budget consideration and would introduce the additional complexity of further generator replacement. The base case model was deterministic, i.e data were input as single values. A probabilistic analysis i.e data input as distributions, was also undertaken and is detailed below.

Furthermore, the overall budget impact was assessed to estimate the financial consequences. The overall percentage of CRTD devices replaced in England was estimated from the pacemaker and ICD replacement rates reported in the latest available cardiac device audit.[182] This was then applied to the reported total number of CRTD implantations to estimate the annual number of CRTD implantations that were generator replacement procedures.

5.3.1 Clinical Events

Clinical event rates used in the model are shown on Figure 37. An arrhythmic event rate of 2.33% per year was derived from the data reported by Sebag et al.[180] This was a critical input and is the annualised arrhythmic event rate calculated from the observation of Sebag et al, that 2/39 patients without TOII suffered an arrhythmic event over 26.4 months of follow up after first generator replacement. In patients modelled to be implanted with CRTP at first generator replacement, 50% mortality was assumed to result from an arrhythmic event, although this was varied in sensitivity analysis. Survivors in the CRTP arm were then modelled to require a further out-patient visit and upgrade to a CRTD. Therefore, the base case scenario for patients implanted with CRTP at first generator replacement included an annual probability of death of 0.0117 and an annual probability of out-patient visit followed by upgrade to CRTD of 0.0117.

The alternative scenario of CRTD implantation at first generator replacement was assumed to reduce the rate of arrhythmic death by 19%, (although this was varied in sensitivity analysis).[183] This therefore reduced the annual probability of arrhythmic death for patient receiving CRTD at first generator replacement in the base case to 0.0094 and increased the annual probability of a further out-patient visit to 0.0139, maintaining an overall annual arrhythmic event probability of 0.0233. Patients in this arm of the model had zero probability of upgrade to CRTD as this type of device would have been implanted at the first generator replacement.

5.3.2 Quality-adjusted life years

Expression of outcomes in terms of quality-adjusted life years (QALYs) allows a cost to be applied to compare healthcare interventions in a common currency. The EQ-5D questionnaire is used to determine utility values that can then be converted into QALYs. This approach, using a standard part of NICE's methodology has been successfully adopted in previous cost effective analyses.[183,184] Results are commonly expressed as an incremental cost effectiveness ratio (ICER), which is a division of the additional cost of the treatment option by the incremental QALYs gained by employing that option. An ICER of £20,000 to £30,000 per QALY gained is the range in which cost effectiveness is acceptable in terms of NHS resource use and this range was considered applicable to the current evaluation.

The QALY losses used in the model are shown in Table 14. Mortality and CRTD implantation after an arrhythmic event used to calculate QALY differences between the two generator replacement options. A baseline utility of 0.8708 was used for a patient with CRT. This was derived from the utility of 0.78 for a patient aged 66, plus the utility gain of 0.0908, associated with the use of CRT. The QALY loss due to death was

taken as the fall from 0.8708 to zero. The QALY loss due to an upgrade from CRTP to CRTD was calculated to be 0.0036. Upgrade to CRTD was assumed to incur the same QALY loss as a heart failure admission. The utility for a heart failure admission was calculated, from the work of Swinburn et al and Lewis et al, to be 0.1197.[185] This was taken to persist for 11 days, which is the mean length of stay for a heart failure admission.

Table 14- Event probabilities and utility values used in the economic model

Description	Model input	Standard Error	Distribution	Source
Annual probability of death with CRTP	0.0117	0.0172	Beta	Sebag et al
Annual probability of out-patient attendance following survival of arrhythmic event	0.0117	0.0172	Beta	Sebag et al
Annual probability of upgrade of CRTP to CRTD following survival of arrhythmic event	0.0117	0.0172	Beta	Sebag et al
Proportion of CRTP patients dying as a result of arrhythmic event	0.50	-	Fixed, but varied in sensitivity analysis	Assumption
Relative risk of death for CRTD vs CRTP	0.81	0.09	Beta	Woods et al
Baseline QALY for patient with CRT	0.8707	0.0118	Beta	Kind
QALY loss associated with arrhythmic event and CRTD implantation	0.0036	0.0036	Beta	Swinburn et al, Lewis et al

5.3.3 Costs

National tariff costs for England for the year 2016-17 were applied to device interrogation, trans-thoracic echocardiogram, out-patient visit and CRTP implantation. CRTD replacement and upgrade from a CRTP to CRTD (CRTD complete system implantation) was costed according to the methodology used to inform NICE's 2014 Technology Appraisal – i.e a device cost plus the tariff price. The CRTD device cost was taken from the same NICE appraisal and assumed to be unchanged since that time. Where there were different tariff values for complication/co-morbidity splits, averages weighted by the number of admissions for each were calculated. The base tariff price was multiplied by the market forces factor (local cost factor) for the hospitals implanting CRT devices, and the mean of these values were used in the model. The cost for a CRTD generator and CRTD whole system were not multiplied by market forces factors. Costs used in the model are shown on Table 15

Table 15- Costs used in the economic model

Description	Mean Cost (£)	Std Error	Distribution	Source
Device interrogation	£104	£0.75	Gamma	TFC 320, follow up attendance, single professional
Trans-thoracic echocardiogram	£73	£0.53	Gamma	HRG RA60A, simple echocardiogram, 19 years and over
Out-patient clinic visit	£104	£0.75	Gamma	TFC 320, follow up attendance, single professional
CRTD generator	£2,560	£19	Gamma	HRG EA39Z, pacemaker

change procedure				procedure without generator implant.
CRTD pulse generator	£11,752	-	Fixed	14
CRTD implantation procedure	£6,735	£49	Gamma	HRG EA56Z, implantation of cardiac resynchronisation therapy defibrillator.
CRTD whole system	£12,293	-	Fixed	14
CRTP implantation	£8,233	£60	Gamma	HRG EA07Z, Pace 3 - Biventricular and all congenital pacemaker Procedures - Resynchronisation Therapy
Arrhythmic death	£76	£0.55	Gamma	HRG VB09Z, emergency medicine, category 1 investigation with category 1-2 treatment (average of two tariffs)

These costs are the average of national tariff costs multiplied by the market forces factor (ie local cost factors) for each hospital that implants CRT devices.

5.3.4 Sensitivity analyses

Inputs to the base case model were varied to their upper and lower 95% confidence intervals in order to determine which factors had most impact. In addition, a probabilistic sensitivity analysis (PSA) was also undertaken, in which most data were input not as fixed values, but as distributions. The annual arrhythmic event rate was also varied in a threshold analysis to determine what the annual arrhythmic event rate would need to be in order for a blanket strategy of replacing CRTD with CRTD to be cost effective.

5.4 Results

In the base case analysis at 5 years, the incremental cost of replacing a CRTD device with a second CRTD in a patient with no TOII was £5,045. Incremental QALYs gained was 0.0165, resulting in an ICER of £305,712 per QALY gained. Although elective generator replacement with a second CRTD device improved outcome (resulted in more QALYs), it was notably more costly and the cost per QALY gained was well above range normally considered to be cost-effective (£20,000 per QALY gained).[186] In this cohort of patients, effective strategy. Table 16 is a Tornado plot showing the impact of varying a number of model inputs to their upper and lower values- largely to 95% confidence interval values.

Table 16- Tornado plot showing the impact of separately varying a range of input to their upper and lower 95% confidence intervals

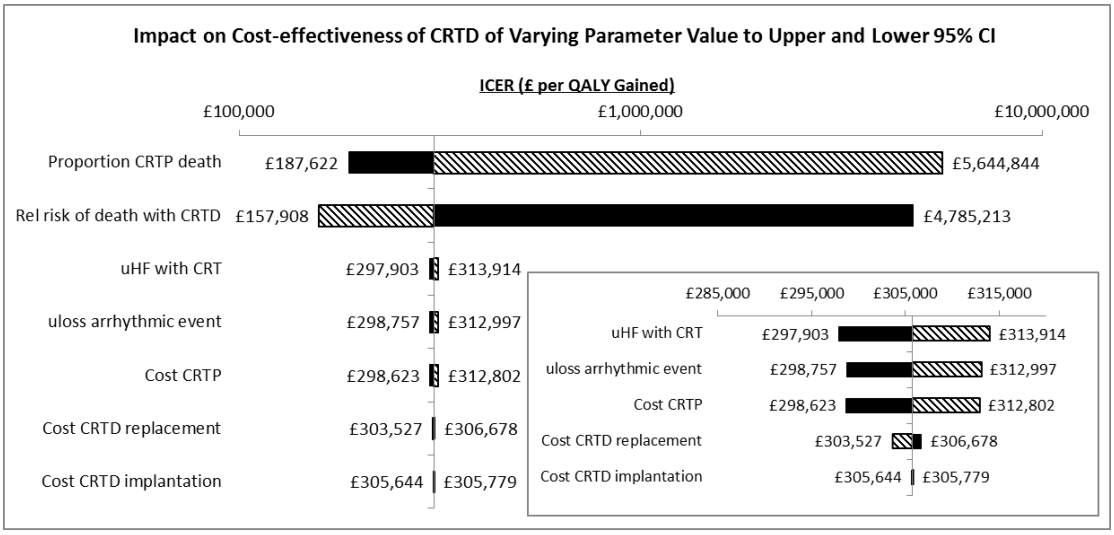

The inset shows detail of the changes with proportion of CRTP death and relative risk of death with CRTD removed. Hatched bars show the impact of using the lower 95% CI, solid bars show the impact of using the upper 95% CI. Data labels on each bars show the ICER resulting from the change in value. A shift to the right of the centre line shows an ICER that denotes less favourable cost effectiveness than the base case.

The proportion of patients dying after an arrhythmic event following generator replacement with CRTP and the relative risk of death for CRTD versus CRTP had the biggest impact on the results. By comparison, the costs of device interrogation, TTE, out-patient visit and death had no impact on the ICER at 5 years and are therefore not shown on the Tornado plot. None of these variations resulted in an ICER that would have made generator replacement with CRTD cost-effective. PSA resulted in an incremental cost of £4,942 and 0.0158 QALYs gained for CRTD versus CRTP, resulting in an ICER of £313,612. PSA also showed that generator replacement with CRTD was cost effective in only 2.7% of simulations at £20,000 per QALY gained and 3.2% of simulations at £30,000 per QALY gained, supporting the view that generator replacement with CRTP is most likely to be cost-effective (see Figure 38).

Figure 38- Cost effectiveness acceptability curve showing probability that generator replacement with CRTD is cost effective

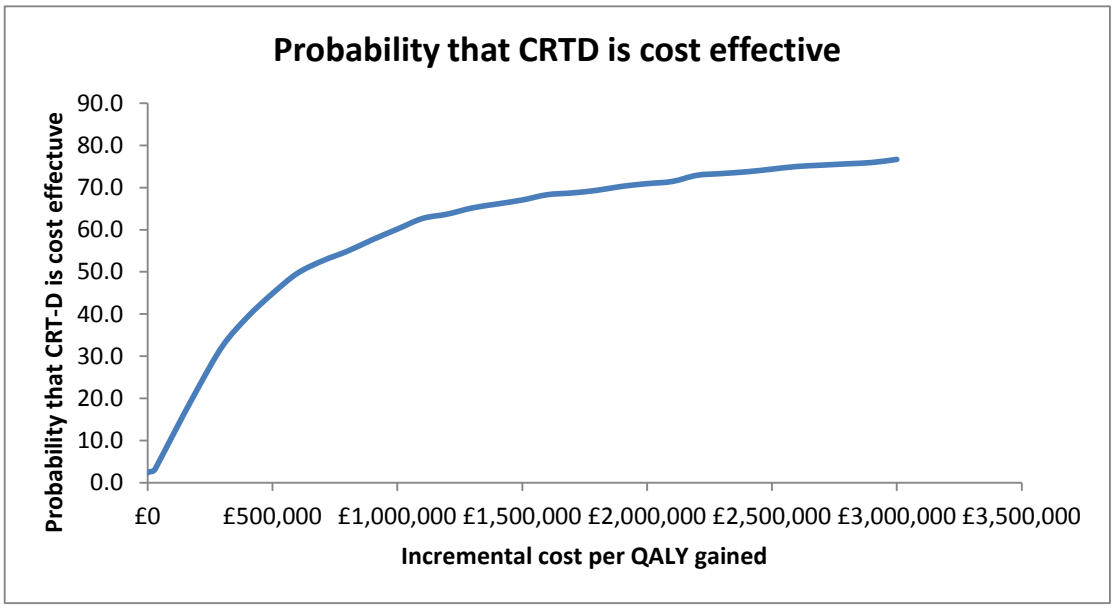

In order for the CRTD to yield an ICER of less than £30,000 per QALY gained, the annual arrhythmic event rate would need to be 9.3% (ICER of £29,613). In order for the CRTD to yield an ICER of less than £20,000 per QALY gained, the annual arrhythmic event rate would need to be 10.4% (ICER of £19,929).

The budget impact of selective replacement of CRTD with CRTP in patients with no TOII was a saving of £2,133,985 per year for England. This is based on an estimate of 1,160 CRTD generator replacements per year (23% of the total CRTD implants), multiplied by the proportion of patients with no TOII multiplied by the incremental cost of a 'CRTD for all' strategy at 5 years.

5.5 Discussion

Using a simple clinical risk stratification tool at the time of generator change clearly demonstrated a significant cost saving far in excess of that seen with a blanket CRTD re-implantation strategy in patients with no theoretical ongoing ICD indication. Whilst an unstratified approach of CRTD generator replacement in all patients might be clinically preferable, it is highly unlikely to be cost-effective in the current economic climate. These findings would suggest that there is a role for such a risk stratification strategy as the health service attempts to increase efficiency in increasingly austere times. By conducting a threshold analysis, we were able to demonstrate that the annual arrhythmic risk would have to rise as high as 10.4% for the blanket strategy currently employed to be cost effective.

Clearly, cost-effectiveness is not the only consideration at the time of generator change, particularly where arrhythmic events may result in death. In the study of Sebag, neither of the patient received therapy had shocks but instead had ATP for slow VT. In order to implement this strategy, cardiologists would need to be accepting of a low rate of mortality in patients that received a CRTP at generator replacement and this would have significant ethical issues which would have to be considered with an individualised patient approach. Lewis et al have recently demonstrated that 83% of patients felt that it was "important" or "very important" to discuss the risks and benefits of continued therapy with their physician.[187] They also found that >50% patients were unaware that ICD replacement was not compulsory and that 74% patients over-estimated the potential benefits of having a defibrillator. Finally the authors noted that patients underestimated the risk of generator replacement including the risks of device infection. There is also evidence that cardiologists tend to deny quality of life issues and the long-term consequences of ICD placement whilst potentially allowing patients to significantly overestimate the benefits of ICD implantation.

Further to the ethical aspects raised, there are potential legal issues to be considered: As with all treatments, we advocate that the risks and benefits of switching to a CRTP should be discussed with patients and consent to the small increased arrhythmic risk should be sought. Switching to a CRTP without patient consent based on a general policy initiative such as NICE guidance may result in some patients seeking legal redress either at the time of generator change or if they have an arrhythmia. This would be a matter of public policy for the Department of Health and would go against our favoured patient-centred, individualised approach to risk stratification.

Beyond our risk stratification tool, it may be feasible to further select patients at reduced risk of appropriate therapy from a defibrillator. The recent DANISH study failed to show a mortality benefit in long-term follow up in non-ischaemic patients with a primary prevention defibrillator despite a significant reduction in sudden arrhythmic deaths.[91] A significant proportion of these patients had CRTD and it is possible that these patients represent a lower risk group than a matched ischaemic cohort and may not require CRTD at box change. In accordance with this, in the study of Sebag, 67% of patients who were eligible for CRTP following risk re-stratification had non-ischaemic cardiomyopathy. Other markers of arrhythmic risk including pre-implant cardiac magnetic resonance imaging indices (e.g. T1 mapping and Grayzone) may also be of assistance in further refining risk stratification.[101]

With shrinking resources and increased healthcare requirements, there is a need for novel approaches to healthcare delivery which means that cost effectiveness issues need to be revisited when significant financial outgoings related to a treatment are anticipated. A treatment that is cost effective in a patient at one time point may cease

to be at another as its potential benefit wanes. Our data here reflects one example of this but similar analyses need to be undertaken in all areas of medicine to ensure the best clinical and affordable decisions are made for all patients.

5.6 Limitations:

We used NHS tariff prices rather than reference costs as tariff prices are those paid service commissioners to hospitals. In multiplying the tariff price by the market forces factor for each hospital, we have arrived at a monetary value that is actually spent by the health service. This approach also allowed a cost distribution to be used in the PSA.

It could be argued that in a blanket strategy of CRTD implantation in all patients, the cost of device interrogation, TTE to determine left ventricular ejection fraction and out-patient visit may not be required. However, these costs were shown to not affect the ICER and it is likely that an out-patient visit would still be likely before CRTD replacement. If these costs were removed, the cost of 'CRTD for all' would reduce by £281 per patient. It would therefore still remain cost-saving to employ a strategy of replacing CRTD with CRTP and upgrading to CRTD when an arrhythmic event occurred in patients with no TOII. We have included these costs in the model in order to determine the complete cost of the risk stratification strategy.

We are unable to include in our analysis any potential psychological harm that may come to patients if they were risk re-stratified to CRTP against their will. As noted above, there is a significant lack of clarity amongst patients over the benefit accrued from ICD insertion and it is contended that this psychological harm may be obviated to

a large degree with proper consultation. Nonetheless it is accepted that for a proportion of patients this strategy would be unacceptable.

Recent NICE guidance has recommended the use of specific CRTD devices due to potential prolonged battery life. This would likely reduce the number of patients surviving to box change. However, it is feasible that those who fulfil our risk stratification criteria for CRTP at 9 years are at an even lower risk of sudden arrhythmic death making the decision to switch to CRTP less contentious and economically even more desirable. Further research is required to investigate this cohort. It should also be noted that it is unlikely that all patients will be offered a single manufacturer's devices as it is common practise to buy devices from several manufacturers to minimise the risk associated with potential product malfunctions.

5.6.1 Practical considerations in switching from CRTD to CRTP

From a practical perspective, many CRTD generators now have a DF4 adaptor. Whilst a DF1-CRTD can be changed to a CRTP with ease, there are currently no adaptors available to plug a DF4 lead into an IS1 port. These patients would require a new right ventricular lead to receive CRTP. There are added risks associated with lead insertion and these would have to be factored into the decision-making process. It should be noted, however, that there are many different adaptors on the market which have been designed to overcome previous issues with device/ lead incompatibility; there is no specific reason why a DF4 to IS1 adaptor could not be manufactured.

Finally, the CRTP generator typically has a significantly smaller volume than a CRTD generator. This is potentially attractive at the time of generator change as patients often

get thinner as they age making a less bulky device preferable. This could potentially result in fewer pocket complications.

5.7 Conclusion

The QALY cost and ICER of replacing CRTD generators with a second CRTD device in patients without TOII at the time of generator change when compared with the use of a simple risk re-stratification tool which results in patients potentially receiving either CRTD or CRTP is far in excess of therapies that would be standardly approved by NICE. However, this re-assessment of the need for a potentially lifesaving treatment is novel, potentially controversial and thus requires an individualised patient–centred approach at this stage.

Chapter 6 SYNTHESIS OF STUDIES, DISCUSSION AND CONCLUSION

6.1 Synthesis and discussion

I have attempted in this thesis and during the period of study to examine different questions relating to complex cardiac implantable electronic devices. The research presented here represents a snapshot of many ongoing projects in which I am still actively involved. Through the invasive haemodynamic studies described in chapter 3 I have investigated elements of the basic physiology that underpins why and how these devices work. In chapter 4, I have sought to determine novel strategies by which patients may be risk-stratified and in future possibly even selected as to whether they are suitable candidates for CRT or ICD devices using both CMR and VCG. These experiments have shed new light on the interaction of the surface electrocardiographic data with the structural changes observed using CMR. Finally, I have examined the need for and, primarily, cost -effectiveness of ongoing provision of defibrillators in low risk groups at the time of generator change.

Through these experiments several new insights have been described.

- Whilst endocardial pacing increases coronary flow minimally, there are large increases in both the forward compression wave and backward expansion wave. However it appears that changes in contractility drive the changes in flow and wave intensity rather than vice versa. The changes in wave intensity and coronary flow are in effect a passive phenomenon rather than the driving force to increased contractility.

- T1 mapping is a powerful marker in the prediction of VA in patients with NCM. Grayzone predicts VA in the ICM population. The specificity of these findings by aetiology is biologically plausible and this is the first description of potential substrate base risk stratification

- Fragmentation of QRS is a measure of scar-core and did not predict arrhythmic risk in our ICD population regardless of aetiology.

- QRSarea as measured by VCG is inversely correlated with scar burden as measured by CMR and both predict response to CRT. This is the first described investigation of the relationship between VCG and CMR indices

- Replacing all CRTD generators on a like for like basis is not cost-effective in the NHS. Use of a simple clinical tool to risk stratify patients *at the time of generator change* could result in significant healthcare savings without significant harm.

6.2 Future research directions

The role of CMR to risk stratify ICD patients needs to be evaluated in a prospective, randomised clinical trial particularly in a NCM cohort using T1 mapping where the cut-offs used in Chapter 4 resulted in a very low risk of VA. The need for this study is further highlighted by the recent DANISH study where at 7 years device therapy failed to improve survival of all-comers (NCM).[91] The study did however show benefit to ICD implantation at approximately 4 years and it may be that CMR helps to identify a higher risk cohort in whom ICD implantation may be of benefit. At the moment such studies

are hindered by the variation in scanners making the use of cut-off values difficult to incorporate into multi-centre studies.

Further research is required into the relationship between VCG metrics (QRS_{area}, $Twave_{area}$) and CMR specifically with reference to the ICD population and VA. I hope to be involved with future projects in this field.

Whilst implanting a CRTP rather than a CRTD may be financially prudent and clinically acceptable, further research is required into the acceptability of these strategies to physicians and patients. I am currently overseeing an MSc project investigating the view of physicians on these decisions.

Finally, there is a need for ongoing research to understand the physiological response to CRT, to determine whether it is possible to better select patients for this treatment or whether it is indeed possible to turn non-responders into responders. The studies presented here suggest that future studies should investigate the role of myocardial scar and other parts of the cascade of heart failure describe above rather than the coronary blood supply per se.

Appendix A. First author publications related to period of study

Changes in contractility determine coronary haemodynamic is dyssnchronous heart failure, not vice versa. **Claridge S,** Briceno N, Chen Z, De Silva K, Modi B, Jackson T, Behar JM, Niederer S, Rinaldi CA, Perera D^2 Accepted for publication International Journal of Cardiology (Heart and Vasculature) 2018

Relationship between vectrocardiographic QRS_{area}, myocardial scar qunantification and response to cardiac resynchronisation therapy. **Claridge S***, Nguyên UC*, Vernooy K, Engels EB, Razavi R, Rinaldi CA, Chen Z, Prinzen FW. J Electrocardiol 2018. doi: 10.1016/j.jelectrocard.2018.01.009.

Predictors and Outcomes of patients requiring repeat transvenous lead extraction of pacemaker and defibrillator leads. **Claridge S,** Johnson J, Sadnan G, Behar JM, Porter B, Sienieiwicz B, Jackson T, Webb J, Gould J, Sohal M, Hamid S, Patel N, Gill J, Rinaldi CA. PACE 2018 doi: 10.1111/pace.13266

The cost of cardiac resynchronization therapy generator replacement? **Claridge S**, Sieniewicz B, Gould J, Rinaldi CA. Heart Rhythm 2017 doi: 10.1016/j.hrthm.2017.12.008

Cost effectiveness of a risk-stratified approach (high vs low) to cardiac resynchronisation therapy defibrillators at the time of generator change. **Claridge S**, Sebag FA, Fearn S, Behar JM, Porter B, Jackson T, Sieniewicz S, Webb J, Chen Z, O'Neill M, Gill J, Leclercq C, Rinaldi CA. Heart 2017. Doi:10.1136/heartjnl-2017-3111749

Substrate dependent risk stratification for implantable cardioverter defibrillator therapies using cardiac magnetic resonance imaging: The importance of T1 mapping in non-ischemic patients. **Claridge S**, Mennuni S, Jackson T, Behar JM, Porter B, Sieniewicz B, Bostock J, O'Neill M, Murgatroyd F, Gill J, Carr-White G, Chiribiri A, Razavi R, Chen Z, Rinaldi CA. J Cardiovasc Electrophysiol. 2017 May 9. doi: 10.1111/jce.13226.

Diagnosis and management of iatrogenic cardiac perforation caused by pacemaker and defibrillator leads. **Claridge S***, Rajkumar C* et al. Europace 2016 Jun 27. pii: euw074.

Effects of Epicardial and Endocardial Cardiac Resynchronization Therapy on Coronary Flow: Insights From Wave Intensity Analysis. **Claridge S**, Chen Z, Jackson T, De Silva K, Behar J, Sohal M, Webb J, Hyde E, Lumley M, Asrress K, Williams R, Bostock J, Ali M, Gill J, O'Neill M, Razavi R, Niederer S, Perera D, Rinaldi CA. J Am Heart Assoc. 2015 Dec 17;4(12). pii: e002626. doi: 10.1161/JAHA.115.002626.

Current concepts relating coronary flow, myocardial perfusion and metabolism in left bundle branch block and cardiac resynchronisation therapy. **Claridge S**, Chen Z, Jackson T, Sammut E, Sohal M, Behar J, Razavi R, Niederer S, Rinaldi CA. Int J Cardiol. 2014 Nov 27;181C:65-72.

Appendix B. Other publications related to period of study

Beat-to-Beat Variability of Ventricular Action Potential Duration Oscillates at Low Frequency During Sympathetic Provocation in Humans. Porter B, van Duijvenboden S, Bishop MJ, Orini M, Claridge S, Gould J, Sieniewicz BJ, Sidhu B, Razavi R, Rinaldi CA, Gill JS, Taggart P. Front Physiol. 2018 Apr 4;9:147. doi: 10.3389/fphys.2018.00147. eCollection 2018.

A cost effectiveness study establishing the impact and accuracy of implementing the NICE guidelines lowering plasma NTproBNP threshold in patients with clinically suspected heart failure at our institution. Webb J, Draper J, Rua T, Yiu Y, Piper S, Teall T, Fovargue L, Bolca E, Jackson T, **Claridge S**, Sieniewicz B, Porter B, McDiarmid A, Rajani R, Kapetanakis S, Rinaldi CA, Razavi R, McDonagh TA, Carr-White G. Int J Cardiol. 2018 Apr 15;257:131-136. doi: 10.1016/j.ijcard.2017.10.126

Myocardial strain computed at multiple spatial scales from tagged magnetic resonance imaging: Estimating cardiac biomarkers for CRT patients. Sinclair M, Peressutti D, Puyol-Antón E, Bai W, Rivolo S, Webb J, **Claridge S**, Jackson T, Nordsletten D, Hadjicharalambous M, Kerfoot E, Rinaldi CA, Rueckert D, King AP. Med Image Anal. 2018 Jan;43:169-185. doi: 10.1016/j.media.2017.10.004. Epub 2017 Oct 31

Updates in Cardiac Resynchronization Therapy for Chronic Heart Failure: Review of Multisite Pacing. Antoniadis AP, Sieniewicz B, Gould J, Porter B, Webb J,

Claridge S, Behar JM, Rinaldi CA. Curr Heart Fail Rep. 2017 Oct;14(5):376-383. doi: 10.1007/s11897-017-0350-z

Autonomic Modulation in Patients with Heart Failure Increases Beat-to-Beat Variability of Ventricular Action Potential Duration. Porter B, Bishop MJ, **Claridge S**, Behar J, Sieniewicz BJ, Webb J, Gould J, O'Neill M, Rinaldi CA, Razavi R, Gill JS, Taggart P.Front Physiol. 2017 May 29;8:328. doi: 10.3389/fphys.2017.00328. eCollection 2017.

Comprehensive use of cardiac computed tomography to guide left ventricular lead placement in cardiac resynchronization therapy. Behar JM, Rajani R, Pourmorteza A, Preston R, Razeghi O, Niederer S, Adhya S, **Claridge S**, Jackson T, Sieniewicz B, Gould J, Carr-White G, Razavi R, McVeigh E, Rinaldi CA.Heart Rhythm. 2017 May 4. pii: S1547-5271(17)30574-X. doi: 10.1016/j.hrthm.2017.04.041

Image Integration to Guide Wireless Endocardial LV Electrode Implantation for CRT. Behar JM, Sieniewicz B, Mountney P, Toth D, Panayiotou M, **Claridge S**, Rhode K, Rinaldi CA. JACC Cardiovasc Imaging. 2017 Apr 12. pii: S1936-878X(17)30143-2. doi: 10.1016/j.jcmg.2017.01.015.

Usefulness of Cardiac Magnetic Resonance Imaging to Measure Left Ventricular Wall Thickness for Determining Risk Scores for Sudden Cardiac Death in Patients With Hypertrophic Cardiomyopathy. Webb J, Villa A, Bekri I, Shome J, Teall T, **Claridge S**, Jackson T, Porter B, Ismail TF, Di Giovine G, Rinaldi CA, Carr-White G, Al-Fakih K, Razavi R, Chiribiri A. Am J Cardiol. 2017 May 1;119(9):1450-1455. doi: 10.1016/j.amjcard.2017.01.021.

Biophysical Modeling to Determine the Optimization of Left Ventricular Pacing Site and AV/VV Delays in the Acute and Chronic Phase of Cardiac Resynchronization Therapy. Lee AW, Crozier A, Hyde ER, Lamata P, Truong M, Sohal M, Jackson T, Behar JM, **Claridge S**, Shetty A, Sammut E, Plank G, Rinaldi CA, Niederer S.J Cardiovasc Electrophysiol. 2017 Feb;28(2):208-215. doi: 10.1111/jce.13134.

The role of multi modality imaging in selecting patients and guiding lead placement for the delivery of cardiac resynchronization therapy. Behar JM, **Claridge S**, Jackson T, Sieniewicz B, Porter B, Webb J, Rajani R, Kapetanakis S, Carr-White G, Rinaldi CA. Expert Rev Cardiovasc Ther. 2017 Feb;15(2):93-107. doi: 10.1080/14779072.2016.1252674. Epub 2016 Nov 7. Review.

Optimized Left Ventricular Endocardial Stimulation Is Superior to Optimized Epicardial Stimulation in Ischemic Patients With Poor Response to Cardiac Resynchronization Therapy: A Combined Magnetic Resonance Imaging, Electroanatomic Contact Mapping and Hemodynamic Study to Target Endocardial Lead Placement. Behar J, Jackson T, Hyde E, **Claridge S** et al. JACC EP 2016; doi: 10.1016/j.jacep.2016.04.00

Cost-Effectiveness Analysis of Quadripolar Versus Bipolar Left Ventricular Leads for Cardiac Resynchronization Defibrillator Therapy in a Large, Multicenter UK Registry. Behar J, Chin H, Fearn S, Ormerod J, Gamble J, Foley PWX, Bostock J, **Claridge S**, Jackson T, Sohal M, Antoniadis A, Razavi R, Betts T, Herring N, Rinaldi C. JACC EP 2016; doi: 10.1016/j.jacep.2016.04.009

Coupling of ventricular action potential duration and local strain patterns during reverse remodelling in responders and non-responders to cardiac resynchronization therapy. Chen Z, Hanson B, Sohal M, Sammut E, Jackson T, Child N, **Claridge S**, Behar J, Niederer S, Gill J, Carr-White G, Razavi R, Aldo Rinaldi C, Taggart P. Heart Rhythm. 2016 Jun 11. pii: S1547-5271(16)30414-3. doi: 10.1016/j.hrthm.2016.06.014

Multisite pacing for Cardiac Resynchronization Therapy: Promises and Pitfalls. Antoniadis AP, Behar JM, **Claridge S**, Jackson T, Sohal M, Rinaldi CA. Curr Cardiol Rep. 2016 Jul;18(7):64.

Improvement of Right Ventricular Hemodynamics with Left Ventriuclar Endocardial pacing during Cardiac Resynchronization Therapy Hyde ER, Behar JM, Crozier A, **Claridge S**, Jackson T, Sohal M, Gill JS, O'Neill MD, Razavi R, Niederer SA, Rinaldi CA. Pacing Clin Electrophysiol. 2016 Jun;39(6):531-41. doi: 10.1111/pace.12854. Epub 2016 May 9

The impact of beat-to-beat variability in optimising the acute hemodynamic response in cardiac resynchronisation therapy. Niederer S, Walker C, Crozier A, Hyde ER, Blazevic B, Behar JM, **Claridge S**, Sohal M, Shetty A, Jackson T, Rinaldi C. Clin Trials Regul Sci Cardiol. 2015 Dec;12:18-22.

Management of heart failure with preserved ejection fraction. Webb J, Jackson T, **Claridge S**, Sammut E, Behar J, Carr-White G Practitioner.2015 Oct;259(1786):21-4, 2-3

Focal but not diffuse myocardial fibrosis burden quantification using cardiac magnetic resonance imaging predicts left ventricular reverse modeling following

cardiac resynchronization therapy Chen Z, Sohal M, Sammut E, Child N, Jackson T, **Claridge S**, Cooklin M, O'Neill M, Wright M, Gill J, Chiribiri A, Schaeffter T, Carr-White G, Razavi R, Rinaldi CA. J Cardiovasc Electrophysiol. 2015 Oct 14. doi: 10.1111/jce.12855.

Mechanistic insights into the benefits of multisite pacing in cardiac resynchronization therapy: The importance of electrical substrate and rate of left ventricular activation. Sohal M, Shetty A, Niederer S, Lee A, Chen Z, Jackson T, Behar JM, **Claridge S**, Bostock J, Hyde E, Razavi R, Prinzen F, Rinaldi CA. Heart Rhythm. 2015 Jul 9. pii: S1547-5271(15)00894-2. doi: 10.1016/j.hrthm.2015.07.012.

Beneficial Effect on Cardiac Resynchronization from Left Ventricular Endocardial Pacing Is Mediated by Early Access to High Conduction Velocity Tissue: An Electrophysiological Simulation Study. Hyde ER, Behar JM, **Claridge S**, Jackson T, Lee AW, Remme EW, Sohal M, Plank G, Razavi R, Rinaldi CA, Niederer SA. Circ Arrhythm Electrophysiol. 2015 Jul 1. pii: CIRCEP.115.002677. [Epub ahead of print]

Narrow QRS systolic heart failure: is there a target for cardiac resynchronization? Jackson T, **Claridge S**, Behar J, Sammut E, Webb J, Carr-White G, Razavi R, Rinaldi CA. Expert Rev Cardiovasc Ther. 2015 Jul;13(7):783-97.

Imaging of extensive caseating intramyocardial calcification secondary to lymphoma. Marciniak A, Marciniak M, Chiribiri A, **Claridge S**, Ramos V, Rajani R. Circ Cardiovasc Imaging. 2015 Apr;8(4)

A comparison of delayed transvenous re-implantation and immediate surgical epicardial approach in pacing dependent patients undergoing extraction of infected permanent pacemakers. Amraoui S, Sohal M, Li A, Williams S, Scully P, Jackson T, **Claridge S**,

Behar J, Ritter P, Barandon L, Ploux S, Bordachar P, Rinaldi CA. Heart Rhythm. 2015 Feb 20. pii: S1547-5271(15)00202-7.

Limitations of chronic delivery of multi-vein left ventricular stimulation for cardiac resynchronization therapy. Behar JM, Bostock J, Ginks M, Jackson T, Sohal M, **Claridge S**, Razavi R, Rinaldi CA. J Interv Card Electrophysiol. 2015 Mar;42(2):135-42

A U-shaped type II contraction pattern in patients with strict left bundle block predicts super response to cardiac resynchronisation therapy. Jackson T, Sohal M, chen Z, child N, Sammut E, Behar J, **Claridge S,** Carr-White G, Razavi R, Rinaldi CA. Heart Rhythm 2014 Oct;11(10):1790-7.

Appendix C. Shortlisting related to period of study

Finalist Royal Society of Medicine 2015- Cardiology President's Medal- Work related to wave intensity analysis

Finalist Young Investigator of the Year Award 2016- Heart Rhythm Congress- Work relating to MRI and ECG parameters to predict appropriate therapy in ICD patients.

1. CARDIOVASCULAR DISEASE STATISTICS 2015. December 2015:1-75.

2. NATIONAL HEART FAILURE AUDIT. August 2016:1-72.

3. SOLVD Investigators, Yusuf S, Pitt B, Davis CE, Hood WB, Cohn JN. Effect of enalapril on survival in patients with reduced left ventricular ejection fractions and congestive heart failure. *N Engl J Med*. 1991;325(5):293-302. doi:10.1056/NEJM199108013250501.

4. Pitt B, Zannad F, Remme WJ, et al. The effect of spironolactone on morbidity and mortality in patients with severe heart failure. Randomized Aldactone Evaluation Study Investigators. *N Engl J Med*. 1999;341(10):709-717. doi:10.1056/NEJM199909023411001.

5. Poole-Wilson PA, Swedberg K, Cleland JGF, et al. Comparison of carvedilol and metoprolol on clinical outcomes in patients with chronic heart failure in the Carvedilol Or Metoprolol European Trial (COMET): randomised controlled trial. *Lancet*. 2003;362(9377):7-13. doi:10.1016/S0140-6736(03)13800-7.

6. Swedberg K, Komajda M, Böhm M, et al. Ivabradine and outcomes in chronic heart failure (SHIFT): a randomised placebo-controlled study. *Lancet*. 2010;376(9744):875-885. doi:10.1016/S0140-6736(10)61198-1.

7. McMurray JJV, Packer M, Desai AS, et al. Angiotensin-neprilysin inhibition versus enalapril in heart failure. *N Engl J Med*. 2014;371(11):993-1004. doi:10.1056/NEJMoa1409077.

8. Cazeau S, Ritter P, Lazarus A, et al. Multisite pacing for end-stage heart failure: early experience. *Pacing Clin Electrophysiol*. 1996;19(11 Pt 2):1748-1757.

9. Daubert JC, Ritter P, Le Breton H, et al. Permanent left ventricular pacing with transvenous leads inserted into the coronary veins. *Pacing Clin Electrophysiol*. 1998;21(1 Pt 2):239-245.

10. Cleland JGF, Daubert J-C, Erdmann E, et al. The Effect of Cardiac Resynchronization on Morbidity and Mortality in Heart Failure. *http://dxdoiorg/101056/NEJMoa050496*. 2009;352(15):1539-1549. doi:10.1056/NEJMoa050496.

11. Tang ASL, Wells GA, Talajic M, et al. Cardiac-resynchronization therapy for mild-to-moderate heart failure. *N Engl J Med*. 2010;363(25):2385-2395. doi:10.1056/NEJMoa1009540.

12. Yu C-M, Bleeker GB, Fung JW-H, et al. Left ventricular reverse remodeling but not clinical improvement predicts long-term survival after cardiac resynchronization therapy. *Circulation*. 2005;112(11):1580-1586. doi:10.1161/CIRCULATIONAHA.105.538272.

13. Pitzalis MV, Iacoviello M, Romito R, et al. Cardiac resynchronization therapy tailored by echocardiographic evaluation of ventricular asynchrony. *J Am Coll Cardiol*. 2002;40(9):1615-1622.

14. Sogaard P, Egeblad H, Kim WY, et al. Tissue Doppler imaging predicts improved systolic performance and reversed left ventricular remodeling during long-term cardiac resynchronization therapy. *J Am Coll Cardiol*. 2002;40(4):723-730.

15. Sogaard P, Egeblad H, Pedersen AK, et al. Sequential versus simultaneous biventricular resynchronization for severe heart failure: evaluation by tissue Doppler imaging. *Circulation*. 2002;106(16):2078-2084.

16. Notabartolo D, Merlino JD, Smith AL, et al. Usefulness of the peak velocity difference

by tissue Doppler imaging technique as an effective predictor of response to cardiac resynchronization therapy. *Am J Cardiol*. 2004;94(6):817-820. doi:10.1016/j.amjcard.2004.05.072.

17. Chung ES, Leon AR, Tavazzi L, et al. Results of the Predictors of Response to CRT (PROSPECT) trial. *Circulation*. 2008;117(20):2608-2616. doi:10.1161/CIRCULATIONAHA.107.743120.

18. Nijjer SS, Pabari PA, Stegemann B, et al. The limit of plausibility for predictors of response: application to biventricular pacing. *JACC Cardiovasc Imaging*. 2012;5(10):1046-1065. doi:10.1016/j.jcmg.2012.07.010.

19. Ukkonen H, Sundell J, Knuuti J. Effects of CRT on myocardial innervation, perfusion and metabolism. *Europace*. 2008;10 Suppl 3(suppl 3):iii114-iii117. doi:10.1093/europace/eun228.

20. Vernooy K, Verbeek XAAM, Peschar M, et al. Left bundle branch block induces ventricular remodelling and functional septal hypoperfusion. *Eur Heart J*. 2005;26(1):91-98. doi:10.1093/eurheartj/ehi008.

21. Vanderheyden M, Bartunek J. Cardiac resynchronization therapy in dyssynchronous heart failure: zooming in on cellular and molecular mechanisms. *Circulation*. 2009;119(9):1192-1194. doi:10.1161/CIRCULATIONAHA.108.841544.

22. Vanderheyden M, Mullens W, Delrue L, et al. Myocardial gene expression in heart failure patients treated with cardiac resynchronization therapy responders versus nonresponders. *J Am Coll Cardiol*. 2008;51(2):129-136. doi:10.1016/j.jacc.2007.07.087.

23. Vernooy K, van Deursen CJM, Strik M, Prinzen FW. Strategies to improve cardiac resynchronization therapy. *Nat Rev Cardiol*. 2014;11(8):481-493. doi:10.1038/nrcardio.2014.67.

24. Abraham WT, Fisher WG, Smith AL, et al. Cardiac Resynchronization in Chronic Heart Failure. *N Engl J Med*. 2002;346(24):1845-1853. doi:10.1056/NEJMoa013168.

25. St John Sutton MG, Plappert T, Abraham WT, et al. Effect of cardiac resynchronization therapy on left ventricular size and function in chronic heart failure. *Circulation*. 2003;107(15):1985-1990. doi:10.1161/01.CIR.0000065226.24159.E9.

26. Long-term prognosis after cardiac resynchronization therapy is related to the extent of left ventricular reverse remodeling at midterm follow-up. 2009;53(6):483-490. doi:10.1016/j.jacc.2008.10.032.

27. Mullens W, Grimm RA, Verga T, et al. Insights from a cardiac resynchronization optimization clinic as part of a heart failure disease management program. *J Am Coll Cardiol*. 2009;53(9):765-773. doi:10.1016/j.jacc.2008.11.024.

28. Shetty AK, Sohal M, Chen Z, et al. A comparison of left ventricular endocardial, multisite, and multipolar epicardial cardiac resynchronization: an acute haemodynamic and electroanatomical study. *Europace*. February 2014:eut420. doi:10.1093/europace/eut420.

29. Morgan JM, Biffi M, Gellér L, et al. ALternate Site Cardiac ResYNChronization (ALSYNC): a prospective and multicentre study of left ventricular endocardial pacing for cardiac resynchronization therapy. *Eur Heart J*. 2016;37(27):2118-2127. doi:10.1093/eurheartj/ehv723.

30. Hyde ER, Behar JM, Claridge S, et al. Beneficial Effect on Cardiac Resynchronization from Left Ventricular Endocardial Pacing Is Mediated by Early Access to High Conduction Velocity Tissue: An Electrophysiological Simulation Study. *Circ Arrhythm Electrophysiol*. July 2015:CIRCEP.115.002677. doi:10.1161/CIRCEP.115.002677.

31. Ginks MR, Duckett SG, Kapetanakis S, et al. Multi-site left ventricular pacing as a potential treatment for patients with postero-lateral scar: insights from cardiac magnetic resonance imaging and invasive haemodynamic assessment. *Europace*. 2012;14(3):373-379. doi:10.1093/europace/eur336.

32. Padeletti L, Pieragnoli P, Ricciardi G, et al. Acute hemodynamic effect of left ventricular endocardial pacing in cardiac resynchronization therapy: assessment by pressure-volume loops. *Circ Arrhythm Electrophysiol*. 2012;5(3):460-467. doi:10.1161/CIRCEP.111.970277.

33. Nelson GS, Berger RD, Fetics BJ, et al. Left ventricular or biventricular pacing improves cardiac function at diminished energy cost in patients with dilated cardiomyopathy and left bundle-branch block. *Circulation*. 2000;102(25):3053-3059.

34. Kyriacou A, Pabari PA, Mayet J, et al. Cardiac resynchronization therapy and AV optimization increase myocardial oxygen consumption, but increase cardiac function more than proportionally. *Int J Cardiol*. October 2013. doi:10.1016/j.ijcard.2013.10.026.

35. Svendsen M, Prinzen FW, Das MK, et al. Bi-ventricular pacing improves pump function only with adequate myocardial perfusion in canine hearts with pseudo-left bundle branch block. *Exp Biol Med (Maywood)*. 2012;237(6):644-651. doi:10.1258/ebm.2012.012023.

36. Higgins JP, Williams G, Nagel JS, Higgins JA. Left bundle-branch block artifact on single photon emission computed tomography with technetium Tc 99m (Tc-99m) agents: mechanisms and a method to decrease false-positive interpretations. *Am Heart J*. 2006;152(4):619-626. doi:10.1016/j.ahj.2006.06.009.

37. Delhaas T, Arts T, Prinzen FW, Reneman RS. Regional fibre stress-fibre strain area as an estimate of regional blood flow and oxygen demand in the canine heart. *J Physiol (Lond)*. 1994;477(Pt 3):481-496. doi:10.1111/(ISSN)1469-7793/homepage/Permissions.html.

38. Vernooy K, Verbeek XAAM, Peschar M, et al. Left bundle branch block induces ventricular remodelling and functional septal hypoperfusion. *Eur Heart J*. 2005;26(1):91-98. doi:10.1093/eurheartj/ehi008.

39. Vernooy K, Cornelussen RNM, Verbeek XAAM, et al. Cardiac resynchronization therapy cures dyssynchronopathy in canine left bundle-branch block hearts. *Eur Heart J*. 2007;28(17):2148-2155. doi:10.1093/eurheartj/ehm207.

40. Lebtahi NE, Stauffer JC, Delaloye AB. Left bundle branch block and coronary artery disease: Accuracy of dipyridamole thallium-201 single-photon emission computed tomography in patients with exercise anteroseptal perfusion defects. *J Nucl Cardiol*. 1997;4(4):266-273. doi:10.1016/S1071-3581(97)90103-3.

41. Ogano M, Iwasaki Y-K, Tanabe J, et al. Cardiac Resynchronization Therapy Restored Ventricular Septal Myocardial Perfusion and Enhanced Ventricular Remodeling in Patients with Non-ischemic Cardiomyopathy Presenting with Left Bundle Branch Block: Ventricular septal redistribution by CRT in LBBB. *Heart Rhythm*. February 2014. doi:10.1016/j.hrthm.2014.02.014.

42. Koepfli P, Wyss CA, Gaemperli O, et al. Left bundle branch block causes relative but not absolute septal underperfusion during exercise. *Eur Heart J*. 2009;30(24):2993-2999. doi:10.1093/eurheartj/ehp372.

43. Adomian GE, Beazell J. Myofibrillar disarray produced in normal hearts by chronic electrical pacing. *Am Heart J*. 1986;112(1):79-83.

44. Tse HF, Lau CP. Long-term effect of right ventricular pacing on myocardial perfusion and function. *J Am Coll Cardiol*. 1997;29(4):744-749.

45. Masci PG, Marinelli M, Piacenti M, et al. Myocardial structural, perfusion, and metabolic correlates of left bundle branch block mechanical derangement in patients with dilated cardiomyopathy: a tagged cardiac magnetic resonance and positron emission tomography study. *Circ Cardiovasc Imaging*. 2010;3(4):482-490. doi:10.1161/CIRCIMAGING.109.934638.

46. Skalidis EI, Kochiadakis GE, Koukouraki SI, Parthenakis FI, Karkavitsas NS, Vardas PE. Phasic coronary flow pattern and flow reserve in patients with left bundle branch block and normal coronary arteries. *J Am Coll Cardiol*. 1999;33(5):1338-1346.

47. Skalidis EI, Kochiadakis GE, Koukouraki SI, et al. Myocardial perfusion in patients with permanent ventricular pacing and normal coronary arteries. *J Am Coll Cardiol*. 2001;37(1):124-129.

48. Nowak B, Stellbrink C, Schaefer WM, et al. Comparison of regional myocardial blood flow and perfusion in dilated cardiomyopathy and left bundle branch block: role of wall thickening. *J Nucl Med*. 2004;45(3):414-418.

49. Neri G, Zanco P, Zanon F, Buchberger R. Effect of biventricular pacing on metabolism and perfusion in patients affected by dilated cardiomyopathy and left bundle branch block: evaluation by positron emission tomography. *Europace*. 2003;5(1):111-115.

50. Nielsen JC, Bøttcher M, Jensen HK, Nielsen TT, Pedersen AK, Mortensen PT. Regional myocardial perfusion during chronic biventricular pacing and after acute change of the pacing mode in patients with congestive heart failure and bundle branch block treated with an atrioventricular sequential biventricular pacemaker. *Eur J Heart Fail*. 2003;5(2):179-186.

51. Nowak B, Stellbrink C, Sinha AM, et al. Effects of cardiac resynchronization therapy on myocardial blood flow measured by oxygen-15 water positron emission tomography in idiopathic-dilated cardiomyopathy and left bundle branch block. *Am J Cardiol*. 2004;93(4):496-499. doi:10.1016/j.amjcard.2003.10.055.

52. Lindner O, Vogt J, Kammeier A, et al. Effect of cardiac resynchronization therapy on global and regional oxygen consumption and myocardial blood flow in patients with non-ischaemic and ischaemic cardiomyopathy. *Eur Heart J*. 2005;26(1):70-76. doi:10.1093/eurheartj/ehi046.

53. Knaapen P, van Campen LMC, de Cock CC, et al. Effects of cardiac resynchronization therapy on myocardial perfusion reserve. *Circulation*. 2004;110(6):646-651. doi:10.1161/01.CIR.0000138108687.19.C1.

54. Valzania C, Gadler F, Winter R, et al. Effects of cardiac resynchronization therapy on coronary blood flow: evaluation by transthoracic Doppler echocardiography. *Eur J Heart Fail*. 2008;10(5):514-520. doi:10.1016/j.ejheart.2008.03.011.

55. Fang F, Chan JY-S, Lee AP-W, et al. Improved coronary artery blood flow following the correction of systolic dyssynchrony with cardiac resynchronization therapy. *Int J Cardiol*. 2013;167(5):2167-2171. doi:10.1016/j.ijcard.2012.05.094.

56. Sundell J, Engblom E, Koistinen J. The effects of cardiac resynchronization therapy on left ventricular function, myocardial energetics, and metabolic reserve in patients with dilated …. *Journal of the …*. 2004.

57. Deftereos S, Giannopoulos G, Kossyvakis C, et al. Differential effect of biventricular and right ventricular DDD pacing on coronary flow reserve in patients with ischemic cardiomyopathy. *J Cardiovasc Electrophysiol*. 2010;21(11):1233-1239. doi:10.1111/j.1540-8167.2010.01827.x.

58. Parker KH, Jones CJH. Forward and Backward Running Waves in the Arteries: Analysis Using the Method of Characteristics. *J Biomech Eng*. 1990;112(3):322-326. doi:10.1115/1.2891191.

59. Koh TW, Pepper JR, DeSouza AC, Parker KH. Analysis of wave reflections in the arterial system using wave intensity: A novel method for predicting the timing and amplitude of reflected waves. *Heart Vessels*. 1998;13(3):103-113. doi:10.1007/BF01747827.

60. Parker KH. An introduction to wave intensity analysis. *Med Biol Eng Comput*. 2009;47(2):175-188. doi:10.1007/s11517-009-0439-y.

61. Davies JE, Whinnett ZI, Francis DP, et al. Use of simultaneous pressure and velocity measurements to estimate arterial wave speed at a single site in humans. *Am J Physiol Heart Circ Physiol*. 2006;290(2):H878-H885. doi:10.1152/ajpheart.00751.2005.

62. Davies JE, Whinnett ZI, Francis DP, et al. Evidence of a dominant backward-propagating “suction” wave responsible for diastolic coronary filling in humans, attenuated in left ventricular hypertrophy. *Circulation*. 2006;113(14):1768-1778. doi:10.1161/CIRCULATIONAHA.105.603050.

63. Sun Y-H, Anderson TJ, Parker KH, Tyberg JV. Effects of left ventricular contractility and coronary vascular resistance on coronary dynamics. *Am J Physiol Heart Circ Physiol*. 2004;286(4):H1590-H1595. doi:10.1152/ajpheart.01100.2001.

64. Sun YH, Anderson TJ, Parker KH, Tyberg JV. Wave-intensity analysis: a new approach to coronary hemodynamics. *J Appl Physiol*. 2000;89(4):1636-1644.

65. Davies JE. Evidence of a Dominant Backward-Propagating “Suction” Wave Responsible for Diastolic Coronary Filling in Humans, Attenuated in Left Ventricular Hypertrophy. *Circulation*. 2006;113(14):1768-1778. doi:10.1161/CIRCULATIONAHA.105.603050.

66. Sen S, Petraco R, Mayet J, Davies J. Wave intensity analysis in the human coronary circulation in health and disease. *Curr Cardiol Rev*. 2014;10(1):17-23. doi:10.2174/1573403X10999140226121300.

67. Raphael CE, Cooper R, Parker KH, et al. Mechanisms of Myocardial Ischemia in Hypertrophic Cardiomyopathy: Insights From Wave Intensity Analysis and Magnetic Resonance. *J Am Coll Cardiol*. 2016;68(15):1651-1660. doi:10.1016/j.jacc.2016.07.751.

68. Lumley M, Williams R, Asrress KN, et al. Coronary Physiology During Exercise and Vasodilation in the Healthy Heart and in Severe Aortic Stenosis. *J Am Coll Cardiol*. 2016;68(7):688-697. doi:10.1016/j.jacc.2016.05.071.

69. De Silva K, Foster P, Guilcher A, et al. Coronary wave energy: a novel predictor of functional recovery after myocardial infarction. *Circ Cardiovasc Interv*. 2013;6(2):166-175. doi:10.1161/CIRCINTERVENTIONS.112.973081.

70. Davies JE, Sen S, Broyd C, et al. Arterial pulse wave dynamics after percutaneous aortic valve replacement: fall in coronary diastolic suction with increasing heart rate as a basis for angina symptoms in aortic stenosis. *Circulation*. 2011;124(14):1565-1572. doi:10.1161/CIRCULATIONAHA.110.011916.

71. Kyriacou A, Whinnett ZI, Sen S, et al. Improvement in Coronary Blood Flow Velocity With Acute Biventricular Pacing Is Predominantly Due to an Increase in a Diastolic Backward-Travelling Decompression (Suction) Wave. *Circulation*. 2012;126(11):1334-1344. doi:10.1161/CIRCULATIONAHA.111.075606.

72. Kyriacou A, Whinnett ZI, Sen S, et al. Improvement in coronary blood flow velocity with acute biventricular pacing is predominantly due to an increase in a diastolic backward-travelling decompression (suction) wave. *Circulation*. 2012;126(11):1334-1344. doi:10.1161/CIRCULATIONAHA.111.075606.

73. Kim RJ, Fieno DS, Parrish TB, et al. Relationship of MRI delayed contrast

enhancement to irreversible injury, infarct age, and contractile function. *Circulation*. 1999;100(19):1992-2002.

74. Kramer CM, Barkhausen J, Flamm SD, Kim RJ, Nagel E, Society for Cardiovascular Magnetic Resonance Board of Trustees Task Force on Standardized Protocols. Standardized cardiovascular magnetic resonance (CMR) protocols 2013 update. *J Cardiovasc Magn Reson*. 2013;15(1):91. doi:10.1186/1532-429X-15-91.

75. Barsheshet A, Goldenberg I, Moss AJ, et al. Response to preventive cardiac resynchronization therapy in patients with ischaemic and nonischaemic cardiomyopathy in MADIT-CRT. *Eur Heart J*. 2011;32(13):1622-1630. doi:10.1093/eurheartj/ehq407.

76. Chen Z, Sohal M, Sammut E, et al. Focal But Not Diffuse Myocardial Fibrosis Burden Quantification Using Cardiac Magnetic Resonance Imaging Predicts Left Ventricular Reverse Modeling Following Cardiac Resynchronization Therapy. *J Cardiovasc Electrophysiol*. 2016;27(2):203-209. doi:10.1111/jce.12855.

77. Leyva F, Taylor RJ, Foley PWX, et al. Left ventricular midwall fibrosis as a predictor of mortality and morbidity after cardiac resynchronization therapy in patients with nonischemic cardiomyopathy. *J Am Coll Cardiol*. 2012;60(17):1659-1667. doi:10.1016/j.jacc.2012.05.054.

78. Chalil S, Stegemann B, Muhyaldeen SA, et al. Effect of posterolateral left ventricular scar on mortality and morbidity following cardiac resynchronization therapy. *Pacing Clin Electrophysiol*. 2007;30(10):1201-1209. doi:10.1111/j.1540-8159.2007.00841.x.

79. Khan FZ, Virdee MS, Palmer CR, et al. Targeted left ventricular lead placement to guide cardiac resynchronization therapy: the TARGET study: a randomized, controlled trial. *J Am Coll Cardiol*. 2012;59(17):1509-1518. doi:10.1016/j.jacc.2011.12.030.

80. Flett AS, Hayward MP, Ashworth MT, et al. Equilibrium contrast cardiovascular magnetic resonance for the measurement of diffuse myocardial fibrosis: preliminary validation in humans. *Circulation*. 2010;122(2):138-144. doi:10.1161/CIRCULATIONAHA.109.930636.

81. Messroghli DR, Plein S, Higgins DM, et al. Human myocardium: single-breath-hold MR T1 mapping with high spatial resolution--reproducibility study. *Radiology*. 2006;238(3):1004-1012. doi:10.1148/radiol.2382041903.

82. Moon JC, Messroghli DR, Kellman P, et al. Myocardial T1 mapping and extracellular volume quantification: a Society for Cardiovascular Magnetic Resonance (SCMR) and CMR Working Group of the European Society of Cardiology consensus statement. *J Cardiovasc Magn Reson*. 2013;15(1):92. doi:10.1186/1532-429X-15-92.

83. FRANK E. An accurate, clinically practical system for spatial vectorcardiography. *Circulation*. 1956;13(5):737-749.

84. Engels EB, Alshehri S, van Deursen CJM, et al. The synthesized vectorcardiogram resembles the measured vectorcardiogram in patients with dyssynchronous heart failure. *J Electrocardiol*. 2015;48(4):586-592. doi:10.1016/j.jelectrocard.2015.04.001.

85. Engels EB, Végh EM, van Deursen CJM, Vernooy K, Singh JP, Prinzen FW. T-wave area predicts response to cardiac resynchronization therapy in patients with left bundle branch block. *J Cardiovasc Electrophysiol*. 2015;26(2):176-183. doi:10.1111/jce.12549.

86. Antiarrhythmics versus Implantable Defibrillators (AVID) Investigators. A comparison of antiarrhythmic-drug therapy with implantable defibrillators in patients resuscitated from near-fatal ventricular arrhythmias. *N Engl J Med*. 1997;337(22):1576-1583. doi:10.1056/NEJM199711273372202.

87. Connolly SJ, Gent M, Roberts RS, et al. Canadian implantable defibrillator study (CIDS) : a randomized trial of the implantable cardioverter defibrillator against amiodarone. *Circulation*. 2000;101(11):1297-1302.

88. Prophylactic implantation of a defibrillator in patients with myocardial infarction and reduced ejection fraction. *N Engl J Med*. 2002;346(12):877-883. doi:10.1056/NEJMoa013474.

89. Bardy GH, Lee KL, Mark DB, et al. Amiodarone or an implantable cardioverter-defibrillator for congestive heart failure. *N Engl J Med*. 2005;352(3):225-237. doi:10.1056/NEJMoa043399.

90. Kadish A, Dyer A, Daubert JP, et al. Prophylactic defibrillator implantation in patients with nonischemic dilated cardiomyopathy. *N Engl J Med*. 2004;350(21):2151-2158. doi:10.1056/NEJMoa033088.

91. Køber L, Thune JJ, Nielsen JC, et al. Defibrillator Implantation in Patients with Nonischemic Systolic Heart Failure. *N Engl J Med*. 2016;375(13):1221-1230. doi:10.1056/NEJMoa1608029.

92. Implantable cardioverter de brillators and cardiac resynchronisation therapy for arrhythmias and heart failure. March 2018:1-68.

93. Boyé P, Abdel-Aty H, Zacharzowsky U, et al. Prediction of life-threatening arrhythmic events in patients with chronic myocardial infarction by contrast-enhanced CMR. *JACC Cardiovasc Imaging*. 2011;4(8):871-879. doi:10.1016/j.jcmg.2011.04.014.

94. Chalil S, Foley PWX, Muyhaldeen SA, et al. Late gadolinium enhancement-cardiovascular magnetic resonance as a predictor of response to cardiac resynchronization therapy in patients with ischaemic cardiomyopathy. *Europace*. 2007;9(11):1031-1037. doi:10.1093/europace/eum133.

95. Scott PA, Rosengarten JA, Curzen NP, Morgan JM. Late gadolinium enhancement cardiac magnetic resonance imaging for the prediction of ventricular tachyarrhythmic events: a meta-analysis. *Eur J Heart Fail*. 2013;15(9):1019-1027. doi:10.1093/eurjhf/hft053.

96. Krijnen PAJ, Nijmeijer R, Meijer CJLM, Visser CA, Hack CE, Niessen HWM. Apoptosis in myocardial ischaemia and infarction. *J Clin Pathol*. 2002;55(11):801-811.

97. de Bakker JM, van Capelle FJ, Janse MJ, et al. Reentry as a cause of ventricular tachycardia in patients with chronic ischemic heart disease: electrophysiologic and anatomic correlation. *Circulation*. 1988;77(3):589-606.

98. Yan AT, Shayne AJ, Brown KA, et al. Characterization of the peri-infarct zone by contrast-enhanced cardiac magnetic resonance imaging is a powerful predictor of post-myocardial infarction mortality. *Circulation*. 2006;114(1):32-39. doi:10.1161/CIRCULATIONAHA.106.613414.

99. Roes SD, Borleffs CJW, van der Geest RJ, et al. Infarct tissue heterogeneity assessed with contrast-enhanced MRI predicts spontaneous ventricular arrhythmia in patients with ischemic cardiomyopathy and implantable cardioverter-defibrillator. *Circ Cardiovasc Imaging*. 2009;2(3):183-190. doi:10.1161/CIRCIMAGING.108.826529.

100. Schmidt A, Azevedo CF, Cheng A, et al. Infarct tissue heterogeneity by magnetic resonance imaging identifies enhanced cardiac arrhythmia susceptibility in patients with left ventricular dysfunction. *Circulation*. 2007;115(15):2006-2014. doi:10.1161/CIRCULATIONAHA.106.653568.

101. Chen Z, Sohal M, Voigt T, et al. Myocardial tissue characterization by cardiac magnetic resonance imaging using T1 mapping predicts ventricular arrhythmia in ischemic and non-ischemic cardiomyopathy patients with implantable cardioverter-defibrillators.

Heart Rhythm. 2015;12(4):792-801. doi:10.1016/j.hrthm.2014.12.020.

102. Puntmann VO, Carr-White G, Jabbour A, et al. T1-Mapping and Outcome in Nonischemic Cardiomyopathy: All-Cause Mortality and Heart Failure. *JACC Cardiovasc Imaging*. 2016;9(1):40-50. doi:10.1016/j.jcmg.2015.12.001.

103. Gulati A, Jabbour A, Ismail TF, et al. Association of fibrosis with mortality and sudden cardiac death in patients with nonischemic dilated cardiomyopathy. *JAMA*. 2013;309(9):896-908. doi:10.1001/jama.2013.1363.

104. European Heart Rhythm Association (EHRA), European Society of Cardiology (ESC), Heart Rhythm Society, et al. 2012 EHRA/HRS expert consensus statement on cardiac resynchronization therapy in heart failure: implant and follow-up recommendations and management. In: Vol 14. 2012:1236-1286. doi:10.1093/europace/eus222.

105. Simson MB, Untereker WJ, Spielman SR, et al. Relation between late potentials on the body surface and directly recorded fragmented electrograms in patients with ventricular tachycardia. *Am J Cardiol*. 1983;51(1):105-112.

106. Pietrasik G, Goldenberg I, Zdzienicka J, Moss AJ, Zareba W. Prognostic significance of fragmented QRS complex for predicting the risk of recurrent cardiac events in patients with Q-wave myocardial infarction. *Am J Cardiol*. 2007;100(4):583-586. doi:10.1016/j.amjcard.2007.03.063.

107. Das MK, Michael MA, Suradi H, et al. Usefulness of fragmented QRS on a 12-lead electrocardiogram in acute coronary syndrome for predicting mortality. *Am J Cardiol*. 2009;104(12):1631-1637. doi:10.1016/j.amjcard.2009.07.046.

108. Das MK, Khan B, Jacob S, Kumar A, Mahenthiran J. Significance of a fragmented QRS complex versus a Q wave in patients with coronary artery disease. *Circulation*. 2006;113(21):2495-2501. doi:10.1161/CIRCULATIONAHA.105.595892.

109. Das MK, Maskoun W, Shen C, et al. Fragmented QRS on twelve-lead electrocardiogram predicts arrhythmic events in patients with ischemic and nonischemic cardiomyopathy. *Heart Rhythm*. 2010;7(1):74-80. doi:10.1016/j.hrthm.2009.09.065.

110. Cheema A, Khalid A, Wimmer A, et al. Fragmented QRS and mortality risk in patients with left ventricular dysfunction. *Circ Arrhythm Electrophysiol*. 2010;3(4):339-344. doi:10.1161/CIRCEP.110.940478.

111. Pei J, Li N, Gao Y, et al. The J wave and fragmented QRS complexes in inferior leads associated with sudden cardiac death in patients with chronic heart failure. *Europace*. 2012;14(8):1180-1187. doi:10.1093/europace/eur437.

112. Forleo GB, Rocca Della DG, Papavasileiou LP, et al. Predictive value of fragmented QRS in primary prevention implantable cardioverter defibrillator recipients with left ventricular dysfunction. *Journal of Cardiovascular Medicine*. 2011;12(11):779-784. doi:10.2459/JCM.0b013e32834ae458.

113. Rosengarten JA, Scott PA, Morgan JM. Fragmented QRS for the prediction of sudden cardiac death: a meta-analysis. *Europace*. 2015;17(6):969-977. doi:10.1093/europace/euu279.

114. Greenwood JP, Maredia N, Younger JF, et al. Cardiovascular magnetic resonance and single-photon emission computed tomography for diagnosis of coronary heart disease (CE-MARC): a prospective trial. *Lancet*. 2012;379(9814):453-460. doi:10.1016/S0140-6736(11)61335-4.

115. Ahn M-S, Kim J-B, Joung B, Lee M-H, Kim S-S. Prognostic implications of fragmented QRS and its relationship with delayed contrast-enhanced cardiovascular magnetic resonance imaging in patients with non-ischemic dilated cardiomyopathy. *Int J Cardiol*.

2013;167(4):1417-1422. doi:10.1016/j.ijcard.2012.04.064.

116. Ahn M-S, Kim J-B, Yoo B-S, et al. Fragmented QRS complexes are not hallmarks of myocardial injury as detected by cardiac magnetic resonance imaging in patients with acute myocardial infarction. *Int J Cardiol*. 2013;168(3):2008-2013. doi:10.1016/j.ijcard.2012.12.086.

117. Hunter S. NHS England Funding and Resource 2017-19: supporting “Next Steps for the NHS Five Year Forward View.” April 2017:1-8.

118. Anderson JL, Heidenreich PA, Barnett PG, et al. ACC/AHA statement on cost/value methodology in clinical practice guidelines and performance measures: a report of the American College of Cardiology/American Heart Association Task Force on Performance Measures and Task Force on Practice Guidelines. *Circulation*. 2014;129(22):2329-2345. doi:10.1161/CIR.0000000000000042.

119. Das MK, Suradi H, Maskoun W, et al. Fragmented wide QRS on a 12-lead ECG: a sign of myocardial scar and poor prognosis. *Circ Arrhythm Electrophysiol*. 2008;1(4):258-268. doi:10.1161/CIRCEP.107.763284.

120. Kors JA, van Herpen G, Sittig AC, van Bemmel JH. Reconstruction of the Frank vectorcardiogram from standard electrocardiographic leads: diagnostic comparison of different methods. *Eur Heart J*. 1990;11(12):1083-1092.

121. Bracke FA, Houthuizen P, Rahel BM, van Gelder BM. Left ventricular endocardial pacing improves the clinical efficacy in a non-responder to cardiac resynchronization therapy: role of acute haemodynamic testing. *Europace*. 2010;12(7):1032-1034. doi:10.1093/europace/euq043.

122. Rinaldi CA, Leclercq C, Kranig W, et al. Improvement in acute contractility and hemodynamics with multipoint pacing via a left ventricular quadripolar pacing lead. *J Interv Card Electrophysiol*. 2014;40(1):75-80. doi:10.1007/s10840-014-9891-1.

123. Pappone C, Ćalović Ž, Vicedomini G, et al. Multipoint left ventricular pacing improves acute hemodynamic response assessed with pressure-volume loops in cardiac resynchronization therapy patients. *Heart Rhythm*. 2014;11(3):394-401. doi:10.1016/j.hrthm.2013.11.023.

124. Niederer SA, Lamata P, Plank G, et al. Analyses of the redistribution of work following cardiac resynchronisation therapy in a patient specific model. *PLoS ONE*. 2012;7(8):e43504. doi:10.1371/journal.pone.0043504.

125. Djordjevic Dikic A, Nikcevic G, Raspopovic S, et al. Prognostic role of coronary flow reserve for left ventricular functional improvement after cardiac resynchronization therapy in patients with dilated cardiomyopathy. *Eur Heart J Cardiovasc Imaging*. July 2014:jeu136. doi:10.1093/ehjci/jeu136.

126. Ginks MR, Shetty AK, Lambiase PD, et al. Benefits of endocardial and multisite pacing are dependent on the type of left ventricular electric activation pattern and presence of ischemic heart disease: insights from electroanatomic mapping. *Circ Arrhythm Electrophysiol*. 2012;5(5):889-897. doi:10.1161/CIRCEP.111.967505.

127. Bowditch HP. On the peculiarities of excitability which the fibres of cardiac muscle show1, 2. 1871.

128. Savitzky A, Golay MJE. Smoothing and Differentiation of Data by Simplified Least Squares Procedures. *Anal Chem*. 1964;36(8):1627-1639. doi:10.1021/ac60214a047.

129. Itoh M, Shinke T, Yoshida A, Kozuki A, Takei A. Reduction in coronary microvascular resistance through cardiac resynchronization and its impact on chronic reverse remodelling of left ventricle in patients with non-ischaemic cardiomyopathy | EP Europace. …. 2015.

130. Kaźmierczak J, Peregud-Pogorzelska M, Gorący J, Wojtarowicz A, Kiedrowicz R, Kornacewicz-Jach Z. Effect of cardiac resynchronisation therapy on coronary blood flow in patients with non-ischaemic dilated cardiomyopathy. *Kardiol Pol*. 2014;72(6):511-518. doi:10.5603/KP.a2014.0019.

131. Lehrke S, Lossnitzer D, Schöb M, et al. Use of cardiovascular magnetic resonance for risk stratification in chronic heart failure: prognostic value of late gadolinium enhancement in patients with non-ischaemic dilated cardiomyopathy. *Heart*. 2011;97(9):727-732. doi:10.1136/hrt.2010.205542.

132. Tsagalou EP, Anastasiou-Nana M, Agapitos E, et al. Depressed coronary flow reserve is associated with decreased myocardial capillary density in patients with heart failure due to idiopathic dilated cardiomyopathy. *J Am Coll Cardiol*. 2008;52(17):1391-1398. doi:10.1016/j.jacc.2008.05.064.

133. Treasure CB, Vita JA, Cox DA, et al. Endothelium-dependent dilation of the coronary microvasculature is impaired in dilated cardiomyopathy. *Circulation*. 1990;81(3):772-779.

134. Nitenberg A, Foult JM, Blanchet F, Zouioueche S. Multifactorial determinants of reduced coronary flow reserve after dipyridamole in dilated cardiomyopathy. *Am J Cardiol*. 1985;55(6):748-754.

135. Steendijk P, Tulner SA, Bax JJ, et al. Hemodynamic effects of long-term cardiac resynchronization therapy: analysis by pressure-volume loops. *Circulation*. 2006;113(10):1295-1304. doi:10.1161/CIRCULATIONAHA.105.540435.

136. van Deursen C, van Geldorp IE, Rademakers LM, et al. Left ventricular endocardial pacing improves resynchronization therapy in canine left bundle-branch hearts. *Circ Arrhythm Electrophysiol*. 2009;2(5):580-587. doi:10.1161/CIRCEP.108.846022.

137. Nijjer SS, Pabari PA, Stegemann B. The limit of plausibility for predictors of response: application to biventricular pacing. *JACC: …*. 2012.

138. Broyd CJ, Nijjer S, Sen S, et al. Estimation of coronary wave intensity analysis using non-invasive techniques and its application to exercise physiology. *Am J Physiol Heart Circ Physiol*. December 2015:ajpheart.00575.2015. doi:10.1152/ajpheart.00575.2015.

139. Zanon F, Gasparini M, Morgan JM, et al. ORAL ABSTRACT SESSION: PREDICTION OF RESPONSE TO CRT AND PATIENT OUTCOMES1526Biventricular, left ventricular only and multipoint pacing in CRT patients: an acute hemodynamic comparison1527Optimizing the LV pacing site by means of electrical delay and LVdp/dtmax may predict the clinical outcome in CRT patients: results of one year follow-up1528Validation of a simple risk stratification tool for patients implanted with cardiac resynchronization therapy: the valid-crt risk score1529Safety and outcome of left ventricular endocardial pacing: the 12 months results of the alternate site cardiac resynchronization (ALSYNC) study1530Cardiac re-synchronization therapy for infants with left bundle branch block caused by various etiologies1531Positive response to cardiac resynchronization therapy reduces arrhythmic events after elective generator change in patients with primary prevention CRT-D1532Association of apical rocking with long-term major adverse cardiac events in patients undergoing cardiac resynchronization therapy1533Prognostic value of epicardial strain amplitude at CRT left ventricular pacing site1534Biventricular pacing increases left anterior descending artery flow by increasing the dominant backward-travelling decompression (suction) wave in patients with left bundle branch block1535Impact of collagen turnover markers on echocardiographic response and mortality after CRT-D implantation in TRUST-CRT study population. *EP Europace*. 2015;17(suppl 3):iii229-iii231. doi:10.1093/europace/euv179.

140. Westerhof N, Boer C, Lamberts RR, Sipkema P. Cross-Talk Between Cardiac Muscle and Coronary Vasculature. *Physiol Rev*. 2006;86(4):1263-1308. doi:10.1152/physrev.00029.2005.

141. Sun YH, Anderson TJ, Parker KH. Effects of left ventricular contractility and coronary vascular resistance on coronary dynamics. *American Journal of …*. 2004.

142. Fang F, Chan JY-S, Lee AP-W, et al. Improved coronary artery blood flow following the correction of systolic dyssynchrony with cardiac resynchronization therapy. *Int J Cardiol*. 2013;167(5):2167-2171. doi:10.1016/j.ijcard.2012.05.094.

143. Lamberts RR, Van Rijen MHP, Sipkema P, Fransen P, Sys SU, Westerhof N. Coronary perfusion and muscle lengthening increase cardiac contraction: different stretch-triggered mechanisms. *Am J Physiol Heart Circ Physiol*. 2002;283(4):H1515-H1522. doi:10.1152/ajpheart.00113.2002.

144. Fok H, Guilcher A, Li Y, et al. Augmentation pressure is influenced by ventricular contractility/relaxation dynamics: novel mechanism of reduction of pulse pressure by nitrates. *Hypertension*. 2014;63(5):1050-1055. doi:10.1161/HYPERTENSIONAHA.113.02955.

145. Skalidis EI, Kochiadakis GE, Igoumenidis NE, Vardakis KE, Vardas PE. Phasic coronary blood flow velocity pattern and flow reserve in the atrium: regulation of left atrial myocardial perfusion. *J Am Coll Cardiol*. 2003;41(4):674-680.

146. Duckett SG, Ginks M, Shetty AK, et al. Invasive acute hemodynamic response to guide left ventricular lead implantation predicts chronic remodeling in patients undergoing cardiac resynchronization therapy. *J Am Coll Cardiol*. 2011;58(11):1128-1136. doi:10.1016/j.jacc.2011.04.042.

147. Rolandi MC, De Silva K, Lumley M, et al. Wave speed in human coronary arteries is not influenced by microvascular vasodilation: implications for wave intensity analysis. *Basic Res Cardiol*. 2014;109(2):405-411. doi:10.1007/s00395-014-0405-1.

148. Tracy CM, Epstein AE, Darbar D, et al. 2012 ACCF/AHA/HRS focused update of the 2008 guidelines for device-based therapy of cardiac rhythm abnormalities: a report of the American College of Cardiology Foundation/American Heart Association Task Force on Practice Guidelines and the Heart Rhythm Society. [corrected]. *Circulation*. 2012;126(14):1784-1800. doi:10.1161/CIR.0b013e3182618569.

149. Kuck K-H, Schaumann A, Eckardt L, et al. Catheter ablation of stable ventricular tachycardia before defibrillator implantation in patients with coronary heart disease (VTACH): a multicentre randomised controlled trial. *The Lancet*. 2010;375(9708):31-40.

150. Reddy VY, REYNOLDS MR, Neuzil P, et al. Prophylactic Catheter Ablation for the Prevention of Defibrillator Therapy. *http://dxdoiorg/101056/NEJMoa065457*. 2009;357(26):2657-2665. doi:10.1056/NEJMoa065457.

151. Poole JE, Johnson GW, Hellkamp AS, et al. Prognostic importance of defibrillator shocks in patients with heart failure. *N Engl J Med*. 2008;359(10):1009-1017. doi:10.1056/NEJMoa071098.

152. Chimura M, Kiuchi K, Okajima K, et al. Distribution of ventricular fibrosis associated with life threatening ventricular tachyarrhythmias in patients with nonishcemic dilated cardiomyopathy. *J Cardiovasc Electrophysiol*. 2015;26(11):1239-1246. doi:10.1111/jce.12767.

153. Akar FG, Tomaselli GF. Conduction abnormalities in nonischemic dilated cardiomyopathy: basic mechanisms and arrhythmic consequences. *Trends Cardiovasc Med*. 2005;15(7):259-264. doi:10.1016/j.tcm.2005.08.002.

154. Rogers T, Dabir D, Mahmoud I, Voigt T. Standardization of T1 measurements with MOLLI in differentiation between health and disease–the ConSept study. *J Cardiovasc Magn …*. 2013.

155. Goebel J, Seifert I, Nensa F, et al. Can Native T1 Mapping Differentiate between Healthy and Diffuse Diseased Myocardium in Clinical Routine Cardiac MR Imaging? Bauer WR, ed. *PLoS ONE*. 2016;11(5):e0155591. doi:10.1371/journal.pone.0155591.

156. Ibanez L, Schroeder W, Ng L, Cates J. MIDAS - The ITK Software Guide. 2003.

157. Puntmann VO, Voigt T, Chen Z, et al. Native T1 mapping in differentiation of normal myocardium from diffuse disease in hypertrophic and dilated cardiomyopathy. *JACC Cardiovasc Imaging*. 2013;6(4):475-484. doi:10.1016/j.jcmg.2012.08.019.

158. TUNG R, JOSEPHSON ME, REDDY V, REYNOLDS MR. Influence of Clinical and Procedural Predictors on Ventricular Tachycardia Ablation Outcomes: An Analysis From the Substrate Mapping and Ablation in Sinus Rhythm to Halt Ventricular Tachycardia Trial (SMASH-VT). *J Cardiovasc Electrophysiol*. 2010;21(7):799-803. doi:10.1111/j.1540-8167.2009.01705.x.

159. Fukuzawa K, Yoshida A, Kubo S, et al. Endocardial substrate mapping for monomorphic ventricular tachycardia ablation in ischemic and non-ischemic cardiomyopathy. *Kobe J Med Sci*. 2008;54(2):E122-E135.

160. Ruwald A-C, Schuger C, Moss AJ, et al. Mortality Reduction In Relation To ICD Programming In MADIT-RIT. *Circ Arrhythm Electrophysiol*. 2014;7(5):CIRCEP.114.001623-CIRCEP.114.001792. doi:10.1161/CIRCEP.114.001623.

161. Auricchio A, Prinzen FW. Non-responders to cardiac resynchronization therapy: the magnitude of the problem and the issues. *Circ J*. 2011;75(3):521-527.

162. Maass AH, Vernooy K, Wijers SC, et al. Refining success of cardiac resynchronization therapy using a simple score predicting the amount of reverse ventricular remodelling: results from the Markers and Response to CRT (MARC) study. *Europace*. February 2017. doi:10.1093/europace/euw445.

163. van Deursen CJM, Vernooy K, Dudink E, et al. Vectorcardiographic QRS area as a novel predictor of response to cardiac resynchronization therapy. *J Electrocardiol*. 2015;48(1):45-52. doi:10.1016/j.jelectrocard.2014.10.003.

164. Leyva F, Foley PWX, Chalil S, et al. Cardiac resynchronization therapy guided by late gadolinium-enhancement cardiovascular magnetic resonance. *J Cardiovasc Magn Reson*. 2011;13(1):29. doi:10.1186/1532-429X-13-29.

165. Kors JA. Lead transformations and the dipole approximation: Practical applications. *J Electrocardiol*. 2015;48(6):1040-1044. doi:10.1016/j.jelectrocard.2015.08.015.

166. Maass AH, Vernooy K, Cramer MJ, et al. Refining success of cardiac resynchronization therapy using a simple score predicting the amount of reverse ventricular remodelling: results from the MARC study - authors reply. *Europace*. June 2017. doi:10.1093/europace/eux169.

167. Mafi Rad M, Blaauw Y, Dinh T, et al. Different regions of latest electrical activation during left bundle-branch block and right ventricular pacing in cardiac resynchronization therapy patients determined by coronary venous electro-anatomic mapping. *Eur J Heart Fail*. 2014;16(11):1214-1222. doi:10.1002/ejhf.178.

168. Végh EM, Engels EB, van Deursen CJM, et al. T-wave area as biomarker of clinical response to cardiac resynchronization therapy. *Europace*. 2016;18(7):1077-1085. doi:10.1093/europace/euv259.

169. Bizarro RO, O'Brien PC, Titus JL, Smith RE. Vectorcardiographic identification of myocardial scar: a discriminative study with automatically processed vectorcardiographic information. *J Electrocardiol*. 1978;11(3):273-276.

170. Strauss DG, Selvester RH, Lima JAC, et al. ECG quantification of myocardial scar in cardiomyopathy patients with or without conduction defects: correlation with cardiac magnetic resonance and arrhythmogenesis. *Circ Arrhythm Electrophysiol*. 2008;1(5):327-336. doi:10.1161/CIRCEP.108.798660.

171. Poels TT, Kats S, Veenstra L, van Ommen V, Maessen JG, Prinzen FW. Reservations about the Selvester QRS score in left bundle branch block - Experience in patients with transcatheter aortic valve implantation. *J Electrocardiol*. 2017;50(2):261-267. doi:10.1016/j.jelectrocard.2017.01.002.

172. Mafi Rad M, Wijntjens GWM, Engels EB, et al. Vectorcardiographic QRS area identifies delayed left ventricular lateral wall activation determined by electroanatomic mapping in candidates for cardiac resynchronization therapy. *Heart Rhythm*. 2016;13(1):217-225. doi:10.1016/j.hrthm.2015.07.033.

173. Höke U, Khidir MJH, van der Geest RJ, et al. Relation of Myocardial Contrast-Enhanced T1 Mapping by Cardiac Magnetic Resonance to Left Ventricular Reverse Remodeling After Cardiac Resynchronization Therapy in Patients With Nonischemic Cardiomyopathy. *Am J Cardiol*. 2017;119(9):1456-1462. doi:10.1016/j.amjcard.2017.01.023.

174. Roque C, Trevisi N, Silberbauer J, et al. Electrical storm induced by cardiac resynchronization therapy is determined by pacing on epicardial scar and can be successfully managed by catheter ablation. *Circ Arrhythm Electrophysiol*. 2014;7(6):1064-1069. doi:10.1161/CIRCEP.114.001796.

175. Boriani G, Biffi M, Martignani C, et al. Is cardiac resynchronization therapy cost-effective? *Europace*. 2009;11 Suppl 5(Supplement 5):v93-v97. doi:10.1093/europace/eup274.

176. Brignole M, Auricchio A, Baron-Esquivias G, et al. 2013 ESC Guidelines on cardiac pacing and cardiac resynchronization therapy: the Task Force on cardiac pacing and resynchronization therapy of the European Society of Cardiology (ESC). Developed in collaboration with the European Heart Rhythm Association (EHRA). *Eur Heart J*. 2013;34(29):2281-2329. doi:10.1093/eurheartj/eht150.

177. Bristow MR, Saxon LA, Boehmer J, et al. Cardiac-resynchronization therapy with or without an implantable defibrillator in advanced chronic heart failure. *N Engl J Med*. 2004;350(21):2140-2150. doi:10.1056/NEJMoa032423.

178. Merchant FM, Jones P, Wehrenberg S, Lloyd MS, Saxon LA. Incidence of defibrillator shocks after elective generator exchange following uneventful first battery life. *J Am Heart Assoc*. 2014;3(6):e001289-e001289. doi:10.1161/JAHA.114.001289.

179. Kini V, Soufi MK, Deo R, et al. Appropriateness of primary prevention implantable cardioverter-defibrillators at the time of generator replacement: are indications still met? *J Am Coll Cardiol*. 2014;63(22):2388-2394. doi:10.1016/j.jacc.2014.03.025.

180. Sebag FA, Lellouche N, Chen Z, et al. Positive response to cardiac resynchronization therapy reduces arrhythmic events after elective generator change in patients with primary prevention CRT-D. *J Cardiovasc Electrophysiol*. 2014;25(12):1368-1375. doi:10.1111/jce.12496.

181. Chatterjee NA, Roka A, Lubitz SA, et al. Reduced appropriate implantable cardioverter-defibrillator therapy after cardiac resynchronization therapy-induced left ventricular function recovery: a meta-analysis and systematic review. *Eur Heart J*. 2015;36(41):2780-2789. doi:10.1093/eurheartj/ehv373.

182. NATIONAL AUDIT OF CARDIAC RHYTHM MANAGEMENT. February 2017:1-28.

183. Woods B, Hawkins N, Mealing S, et al. Individual patient data network meta-analysis of mortality effects of implantable cardiac devices. *Heart*. 2015;101(22):1800-1806.

doi:10.1136/heartjnl-2015-307634.

184. Behar JM, Chin HMS, Fearn S, et al. Cost-Effectiveness Analysis of Quadripolar Versus Bipolar Left Ventricular Leads for Cardiac Resynchronization Defibrillator Therapy in a Large, Multicenter UK Registry. *JACC Clin Electrophysiol*. 2017;3(2):107-116. doi:10.1016/j.jacep.2016.04.009.

185. Lewis EF, Li Y, Pfeffer MA, et al. Impact of cardiovascular events on change in quality of life and utilities in patients after myocardial infarction: a VALIANT study (valsartan in acute myocardial infarction). *JACC Heart Fail*. 2014;2(2):159-165. doi:10.1016/j.jchf.2013.12.003.

186. Implantable cardioverter de brillators and cardiac resynchronisation therapy for arrhythmias and heart failure. March 2018:1-68.

187. Lewis KB, Nery PB, Birnie DH. Decision making at the time of ICD generator change: patients' perspectives. *JAMA Intern Med*. 2014;174(9):1508-1511. doi:10.1001/jamainternmed.2014.3435.